TAMPEREEN TEKNILLINEN YLIOPISTO
TAMPERE UNIVERSITY OF TECHNOLOGY
*Julkaisu 613 • Publication 613*

Jarno Niemelä

# Aspects of Radio Network Topology Planning in Cellular WCDMA

Tampere 2006

Tampereen teknillinen yliopisto. Julkaisu 613
Tampere University of Technology. Publication 613

Jarno Niemelä

# Aspects of Radio Network Topology Planning in Cellular WCDMA

Thesis for the degree of Doctor of Technology to be presented with due permission for public examination and criticism in Tietotalo Building, Auditorium TB109, at Tampere University of Technology, on the 29th of September 2006, at 12 noon.

Tampereen teknillinen yliopisto - Tampere University of Technology
Tampere 2006

ISBN 952-15-1645-3 (printed)
ISBN 952-15-1730-1 (PDF)
ISSN 1459-2045

# Abstract

Even through there are several studies in the literature regarding the topology of CDMA-based networks, there is a clear need for a solid analysis including extensive simulations and radio interface measurements of different radio network topologies and their impact on WCDMA radio network coverage and capacity. This thesis covers a thorough analysis of WCDMA radio network topology and its impact on the whole WCDMA radio network planning process. The scope is not just limited to a traditional planning approach, but also additional network elements such as repeater and services as location techniques are considered as a part of WCDMA radio network topology planning. In addition, methods for verifying the quality of the deployed radio network topology are presented. The information given to readers in this thesis should be most applicable for network operators (planners), as they should be able to plan networks which provide a high system capacity with a limited amount of radio equipment and efficient utilization of radio resources.

The content of this thesis has been divided into three parts. The first part concerns the assessment of different site and antenna configurations on the network coverage, system capacity, and expected functionality of WCDMA network. Fundamentally, the target of this part is to provide planning guidelines for optimization of the WCDMA radio network topology. Moreover, it assesses the impact of site locations, sectoring, and different antenna configurations on optimum radio network topology through the definition of coverage overlapping index. In addition, this part will further cover analysis of the impact of site locations and sector overlapping on the network performance. The most extensive research is performed regarding antenna downtilt that provides as an output valuable information of the selection of antenna downtilt angle for different cell types. Finally, some planning aspects are provided for site evolution from 3-sectored to 6-sectored sites.

The second part of the thesis introduces a method for evaluating the quality of topology planning through radio interface measurements. In addition, it offers an example of the functionality and performance of WCDMA radio network planning tool. The third part of the thesis addresses the impact of supplementary radio network element or functionalities on topology planning. Firstly, the impact of repeater deployment is studied in capacity-limited networks through simulations and radio interface measurements. Secondly, the effect of a mobile positioning method called cell ID+RTT is studied with respect to the topology planning process.

# Preface

The research work performed for this thesis was carried out during the years 2003-2005 at the Institute of Communications Engineering, Tampere University of Technology, Tampere, Finland. I would like to thank all the current and earlier personnel of the Institute of Communications Engineering, and especially the Digital Transmission Group, for providing the most inspiring and pleasant working environment.

First of all, I would like to express my deepest gratitude to my supervisor Prof. Jukka Lempiäinen for providing the opportunity to join his group, his invaluable guidance, continuous support, and friendship during the research work leading to this thesis. I am also grateful to the thesis reviewers, Professor Sven-Gustav Hägmann from Helsinki University of Technology, Helsinki, Finland, and Associate Professor Per-Erik Östling, from Aalborg University, Aalborg, Denmark, for providing excellent comments during reviewing process of the manuscript.

I would like to dedicate special thanks to my colleagues in the Radio Network Group with whom I had the pleasure to work with: M. Sc. Jakub Borkowski, Tech. Stud. Tero Isotalo, M. Sc. Panu Lähdekorpi, and M. Sc. Jaroslaw Lacki. Thanks guys for memorable events and discussions that I was able to share with you. In addition to above mentioned persons, I would like to thank the following companies and persons: From European Communications Engineering (ECE) B. Sc. Kimmo Oinonen for extremely valuable support with the planning tool, M. Sc. Jarkko Itkonen for the most interesting technical discussions and his valuable comments, and M. Sc (EE), M. Sc. (Econ) Matti Manninen for hints regarding simulation paramaters; Nokia Networks for providing Nokia NetAct Planner for research purposes; Elisa Communications Oyj, especially M. Sc. Vesa Orava, for enabling measurements in their network, for providing the repeater and antennas for repeater measurements, and also of the relevant feedback; Nemo Technologies, especially M. Sc. Kai Ojala, for providing measurement equipments and technical support; FM Kartta Oy for providing digital maps and technical support, and finally the city of Tampere for enabling repeater deployment in their premises. In addition, I thank also Mr. John Shepherd from the Language Center, Tampere University of Technology, for his effort on proofreading the thesis in a tight schedule. Finally, I am also grateful for Dr. Tech. Ari Viholainen for sharing the most excellent template for this thesis, and also for Dr. Tech. Mikko Valkama for several practical hints during my studies.

The research work was financially supported by the Graduate School in Electronics, Telecommunications, and Automation (GETA), the National Technology Agency of Finland (TEKES), the Nokia Foundation, and the Foundation for Advancement of Technology (TES), all of which are gratefully acknowledged. I would also like to

thank Tarja Erälaukko and Sari Kinnari secretaries of our laboratory, and the head of our laboratory, Prof. Markku Renfors, for their help with practical and everyday matters.

I wish to express my warmest thanks to my parents Pauli and Kirsti Niemelä for their parenting, guidance, and love throughout the early days of my life and also during my work. Finally, I am extremely grateful for my wife Eeva-Maria for her love and support during my work, and especially of her patience of having occasionally 100% BLER over the air interface during evenings, and to my daughter Nea and my son Niklas for providing non-technical talks and actions for daddy.

Tampere, Finland
September 2006.

*Jarno Niemelä*

# Table of Contents

# List of Publications

This thesis is a compilation of the following publications:

[P1] J. Niemelä, T. Isotalo, and J. Lempiäinen, "Optimum Antenna Downtilt Angles for Macrocellular WCDMA Network," in *EURASIP Journal on Wireless Communications and Networking*, Num. 5, Dec. 2005, pp. 816–827.

[P2] J. Niemelä and J. Lempiäinen, "Impact of Base Station Locations and Antenna Orientations on UMTS Radio Network Capacity and Coverage Evolution," in *Proc. IEEE 6th International Symposium on Wireless Personal Multimedia and Communications*, Oct. 2003, vol. 2, pp. 82–86.

[P3] J. Niemelä and J. Lempiäinen, "Impact of the Base Station Antenna Beamwidth on Capacity in WCDMA Cellular Networks," in *Proc. IEEE 57th Semiannual Vehicular Technology Conference*, Apr. 2003, vol. 1, pp. 80–84.

[P4] J. Niemelä, J. Borkowski, and J. Lempiäinen, "Verification Measurements of Mechanical Downtilt in WCDMA," in *Proc. IEE 6th International Conference on 3G and Beyond*, Nov. 2005, pp. 325–329.

[P5] J. Niemelä, T. Isotalo, J. Borkowski, and J. Lempiäinen, "Sensitivity of Optimum Downtilt Angle for Geographical Traffic Load Distribution in WCDMA," in *Proc. IEEE 62nd Semiannual Vehicular Technology Conference*, Sept. 2005, vol. 2, pp. 1202–1206.

[P6] J. Niemelä and J. Lempiäinen, "Mitigation of Pilot Pollution through Base Station Antenna Configurationin WCDMA," in *Proc. IEEE 60th Semiannual Vehicular Technology Conference*, Sept. 2004, vol. 6, pp. 4270–4274.

[P7] J. Niemelä, J. Borkowski, and J. Lempiäinen, "Using Idle Mode $E_c/N_0$ Measurements for Network Plan Verification," in *Proc. IEEE International Symposium on Wireless Personal Multimedia and Communications*, Sept. 2005, vol. 2, pp. 1276–1280.

[P8] J. Niemelä, J. Borkowski, and J. Lempiäinen, "Performance of static WCDMA simulator," in *Proc. IEEE International Symposium on Wireless Personal Multimedia and Communications*, Sept. 2005, vol. 2, pp. 1266–1270.

[P9] J. Niemelä, P. Lähdekorpi, J. Borkowski, and J. Lempiäinen, "Assessment of repeaters for WCDMA UL and DL performance in capacity-limited environment," in *Proc. 14th IST Mobile Summit*, June 2005.

[P10] J. Borkowski, J. Niemelä, and J. Lempiäinen, "Applicability of repeaters for hotspots in UMTS," in *Proc. 14th IST Mobile Summit*, June 2005.

[P11] J. Borkowski, J. Niemelä, and J. Lempiäinen, "Performance of Cell ID+RTT Hybrid Positioning Method for UMTS Radio Networks," in *Proc. 5th European Wireless Conference*, Feb. 2004, pp. 487–492.

[P12] J. Borkowski, J. Niemelä, and J. Lempiäinen, "Enhanced Performance of Cell ID+RTT by Implementing Forced Soft Handover Algorithm," in *Proc. IEEE 60th Semiannual Vehicular Technology Conference*, Sept. 2004, vol. 5, pp. 3545–3549.

In addition, some new analysis regarding coverage overlap has been included in Chapter 3 based on the simulations provided in [P1]. On top of this, the number of simulation scenarios in [P3] was considerably increased, and correspondingly, the results analysis in Chapter 3 has been extended.

# List of Abbreviations

| | |
|---|---|
| 2D | 2-Dimensional |
| 3D | 3-Dimensional |
| 3G | Third Generation |
| 3GPP | The Third Generation Partnership Project |
| AC | Admission Control |
| AGPS | Assisted Global Positioning System |
| AOA | Angle of Arrival |
| AS | Active Set |
| BER | Bit Error Rate |
| BLER | Block Error Rate |
| BPL | Building Penetration Loss |
| BS | Base Station |
| CAEDT | Continuously Adjustable Electrical Downtilt |
| CAPEX | Capital Expenditure |
| CCCH | Common Control Channel |
| CDF | Cumulative Distribution Function |
| cf. | confer |
| CDMA | Code Division Multiple Access |
| Cell ID | Cell Identification |
| COI | Coverage Overlapping Index |
| CVS | Cumulative Virtual Banking |
| CW | Continuous Wave |
| DAS | Distributed Antenna System |
| DCH | Dedicated Channel |
| DPCCH | Dedicated Physical Control Channel |
| DPCH | Dedicated Physical Channel |
| DL | Downlink |
| EDT | Electrical Downtilt |
| E-CGI | Enhanced Cell Global Identification |
| e.g. | exempli gratia (for example) |
| etc. | etcetera |
| FDMA | Frequency Division Multiple Access |
| FSHO | Forced Soft Handover |
| GPS | Global Positioning System |
| GSM | Global System for Mobile communications |
| HAPs | High Altitude Platforms |

| | |
|---|---|
| HSDF | Hotspot Density Factor |
| HSDPA | High Speed Downlink Packet Access |
| IC | Interference Cancellation |
| i.e. | id est (this is) |
| IM | Interference Margin |
| IPDL | Idle Period Downlink |
| KPI | Key Performance Indicator |
| LOS | Line of Sight |
| MDT | Mechanical Downtilt |
| MIMO | Multiple Input Multiple Output |
| Node B | 3GPP term for base station |
| ODA | Optimum Downtilt Angle |
| OFDMA | Orthogonal Frequency Division Multiple Access |
| OPEX | Operational Expenditure |
| OTDOA | Observed Time Difference of Arrival |
| P-CPICH | Primary Common Pilot Channel |
| PE-IPDL | Positioning Elements Idle Period Downlink |
| QoS | Quality of Service |
| RET | Remote Electrical Tilt |
| RF | Radio Frequency |
| RNC | Radio Network Controller |
| RNP | Radio Network Planning |
| RRM | Radio Resource Management |
| RSCP | Received Signal Code Power |
| RSSI | Received Signal Strength Indicator |
| RTT | Round Trip Time |
| S-CPICH | Secondary Common Pilot Channel |
| SfHO | Softer Handover |
| SHO | Soft Handover |
| SOI | Sector Overlapping Index |
| SIR | Signal to Interference Ratio |
| STD | Standard Deviation |
| TA | Timing Advance |
| TA-IPDL | Time Alignment Idle Period Downlink |
| TCH | Traffic Channel |
| TX | Transmit |
| UL | Uplink |
| UMTS | Universal Mobile Telecommunications System |
| UTRA FDD | UMTS Terrestrial Radio Access Frequency Division Duplex |
| WCDMA | Wideband Code Division Multiple Access |

# List of Symbols

| | |
|---|---|
| $C$ | Chip rate |
| $COI$ | Coverage overlapping index |
| $C/I$ | Carrier to interference ratio |
| $d_{dom}$ | Length of dominance area |
| $E\{\cdot\}$ | Statistical expectation |
| $E_b/N_0$ | Energy per bit over noise spectral density |
| $E_c/N_0$ | Energy per chip over noise spectral density |
| $G_{bs}$ | Base station antenna gain |
| $G_{donor}$ | Donor antenna gain |
| $G_{rep}$ | Repeater gain |
| $G_{serving}$ | Serving antenna gain |
| $G_t$ | Repeater gain parameter |
| $h_{bs}$ | Base station antenna height |
| $i$ | Other-to-own-cell interference (general) |
| $i_{DL}$ | Other-to-own-cell interference (downlink) |
| $i_{UL}$ | Other-to-own-cell interference (uplink) |
| $i_{other}$ | Other cell interference |
| $i_{own}$ | Own cell interference |
| $I_{tot}$ | Total received interference (excluding noise) |
| $IM$ | Interference margin |
| $L$ | Link loss (general) |
| $L_k$ | Link loss in downlink |
| $L_j$ | Link loss in uplink |
| $N$ | Total number of users per snapshot |
| $P_n$ | Noise power |
| $P_{P-CPICH}$ | Transmit power P-CPICH |
| $P_{CCCH}$ | Transmit power for common control channels (excluding P-CPICH) |
| $P_{TCH}$ | Transmit power per traffic channel |
| $P_{TCH}^{tot}$ | Total transmit power of all traffic channels |
| $P_{Tx}$ | Transmit power |
| $P_{Tx}^{tot}$ | Total transmit power |
| $P_{Rx}^{MS}$ | Total received wideband power at mobile station |
| $SHO_{ADD}$ | Addition window for SHO |
| $SIR$ | Signal to interference ratio |
| $SOI$ | Sector overlapping index |
| $R$ | User bit rate |

| | |
|---|---|
| $Y$ | Number of snapshots |
| $W$ | System chip rate |
| | |
| $\alpha$ | Orthogonality factor |
| $\eta_{DL}$ | Load factor (downlink) |
| $\eta_{UL}$ | Load factor (uplink) |
| $\theta^{ver}_{-3\ dB}$ | Half power ($-3$ dB) antenna vertical beamwidth |
| $\nu$ | Activity factor |
| $\mu$ | Mean value |
| $\sigma^2$ | Variance |
| $\sigma$ | Standard deviation (general) |
| $\sigma_{SF}$ | Standard deviation of slow fading |

# CHAPTER 1

# Introduction

## 1.1 Background and Motivation

THE target of any radio network operator is to minimize the capital expenditure (CAPEX) of the equipment required for an operational radio network. In turn, a lesser amount of radio network equipment typically results in lower operational expenditure (OPEX). From the technical point of view, the radio interface planning process of a cellular mobile communication system targets providing the required network coverage, system capacity, and sufficient quality of service (QoS) with minimum economical constraints.

The radio network coverage is mostly defined by the number of utilized sites to cover a certain geographical area, site and antenna configuration, and propagation environment. These factors also partly define the achievable system capacity of a cellular radio network. However, a high system capacity can be achieved only by utilizing the given radio spectrum and deployed radio network efficiently. On the other hand, QoS relates to the quality that the end user experiences while using the radio network, and it can be measured as the satisfaction of the user (e.g., the rate of drop calls).

In Europe and Asia, the current phase in cellular mobile communication systems focuses on the operation and optimization of third generation (3G) systems known as the Universal Mobile Telecommunication System (UMTS). Currently, there are over 100 operational UMTS networks all over the world [1]. Back in 1998, Wideband Code Division Multiple Access (WCDMA) was selected as an air interface multiple access technique for UMTS. Due to WCDMA radio access technology, the radio network planning (RNP) process and planning principles were changed [2–7]. In a WCDMA system, the flow of the planning process follows one of the Global System for Mobile communications (GSM) networks (or FDMA [(frequency division multiple access)] based cellular radio network). However, the detailed radio network planning methods adopted from GSM are no longer valid. For instance, during the planning process of GSM networks, it is possible to clearly divide coverage and capacity planning phases into individual parts. In a cellular WCDMA -based network, users use the same radio resources (i.e. the same frequency band) simultaneously, and the division of different users is performed by unique code sequences. Due to the non-ideal properties of these code sequences, the interference level in the network increases as a function of network load (i.e. number of simultaneous users). In other words, a varying number of users in a sector (or cell) leads to a phenomenon

called *cell breathing*. In practice this means that coverage of a single cell is not constant. Due to this phenomenon, interference has to be taken into account already in the coverage planning phase [2,3,8,9]. Moreover, this means that the system capacity is interference-limited in cellular WCDMA networks. Throughout this thesis, the combined coverage and capacity planning phase is called the *topology planning phase*, where the primary target is to define the radio network layout and configuration.

In general, the interference in a network can be divided into own cell and other cell interference. The main parameter to be optimized during the WCDMA radio network topology planning is other cell (inter cell) interference. The level of other cell interference reflects in the isolation of a cell: the lower the level of other cell interference, the more isolated is the cell. Commonly, the level of other cell interference is measured using the ratio between other cell and own cell interference. This parameter is called other-to-own-cell interference ratio ($i$). In the uplink direction, this parameter is base station sector dependent, whereas in the downlink, it depends on the location of mobiles. All radio network topology related elements—site locations, sectoring, antenna beamwidth, height, and downtilt—have an impact on cell isolation. Moreover, these elements also partly define the radio network coverage and system capacity. Therefore, the topology of WCDMA networks should be designed in such a manner that cells should be as isolated from each other as possible, but still tolerate the time-dependent changes of the radio coverage (i.e. slow fading). By doing this, better network coverage (fewer variations due to cell breathing) and better system capacity (higher number of users in an interference-limited network) can be provided. However, as in any cellular network, the topology planning (or coverage and capacity planning separately) represents only a part of the whole radio network planning process. In WCDMA, this means that proper topology planning provides prerequisites for better functionality for radio resource management (RRM) functions.

Evaluation of the attained quality of the radio network topology is a relatively challenging task. In general, the quality can be estimated either using radio interface measurements or system level simulations. Extracting the most relevant measurement results and the selection of the most important indicators from a set of measurement data is inherently challenging because the measurement results might easily include certain performance factors of non-topology related functionalities. Hence, simple and rapidly executable methods for indicating the quality of deployed network's topology are clearly needed. A more sophisticated method would be to simulate the performance of the radio network topology by means of attainable system capacity. This would remove the need for massive and time-consuming field measurement campaigns. However, this approach places strict requirements for the radio network planning tool and on the selection of its input data and parameters.

Due to more complex radio interface access technique, any additional element or service in the radio interface will have an impact on the available radio resources or interference levels, and hence they will also affect the system capacity. Already in GSM, repeaters have been used to cover coverage holes or locations that otherwise would be hard to cover. In WCDMA, repeaters will affect the interference levels in the network, and hence their impact on the topology planning phase has to be understood. In addition, as the more complex radio interface access technique also

enables new services, the impact of location techniques has to be estimated during the topology planning phase, because the radio network topology has a huge impact on the attainable signal levels in the network that are typically used for position estimation with radio network based location techniques.

## 1.2 Scope of the Thesis

The scope of the thesis is to provide aspects mainly for the topology planning of CDMA cellular radio networks. The reference network (system) throughout the whole thesis is UTRA FDD (UMTS terrestrial radio access frequency division duplex), where the air interface multiple access scheme is based on WCDMA. Even though most of the simulation and measurement results are system-specific, under certain circumstances they can be applied to all CDMA-based networks. Moreover, some the results could also be applied to other types of cellular networks. On top of this, the analysis is mainly concentrated on macrocellular suburban and light urban environments.

The structure of the thesis is divided into three parts: basic elements of radio network topology, verification of the quality of the topology, and supplementary concepts of radio network. The first part will concentrate on the impact of different radio network topologies on the network coverage and system capacity. In the literature, there are a small number of similar studies regarding radio network topology. However, an extensive analysis and a sufficient level of understanding of the dynamics of the capacity as a function of different radio network topology related elements is still lacking. The second part of the thesis will concentrate on the verification methods of the quality of the radio network topology. Firstly, a method that utilizes radio interface measurements for providing an estimate of other-to-own-cell interference of a cell or part of a network is provided and its performance is assessed. Secondly, the reliability of a static radio network simulator that could be used in the radio network planning process is evaluated for urban environment. The third part of the thesis introduces two supplementary radio network concepts and their impact on radio network topology planning. These concepts are repeaters and a network-based mobile positioning technique called cell ID (identification)+ RTT (round trip time). Throughout the repeater analysis, the deployment of repeaters is considered for capacity-limited environments, rather than for coverage-limited environments. Firstly, the assessment of a repeater network is performed with system level simulations, and secondly, the downlink performance is assessed by means of radio interface measurements. Finally, the performance of network-based mobile positioning technique (cell ID+RTT) is evaluated for different radio network topologies.

The thesis is organized as follows: Chapter 1 provides the motivation, scope of the thesis, and gathers the main results of the thesis. Chapter 2 introduces the relevant background information regarding the WCDMA radio network planning process and different assessment methods of radio network topology. In addition, the basic methodology of the static simulator that is used in most of the simulations in this thesis is provided as well. Chapter 3 provides an extensive set of simulation results and analysis of different radio network topologies on the network coverage and

system capacity, and partly on QoS. Different network topologies cover modifications in sectoring, site locations, antenna heights, antenna beamwidths, and antenna downtilt angles. Moreover, the impact of radio network topology on the level of pilot pollution is also studied. The chapter ends with some proposals for site evolution from 3-sectored sites to 6-sectored ones. Chapter 4 introduces two aspects of radio network topology assessment; radio interface measurements and simulations. First, a mapping method of the quality of a cell or a part of a network is developed, and secondly, a reliability study of a static radio network planning tool is provided in an urban WCDMA network. The first part of Chapter 5 provides simulation and measurement results of repeater deployment in a WCDMA network. The second part of the chapter considers the impact of radio network topology on the overall accuracy of network-based cell ID+RTT mobile positioning method with and without forced soft handover (FSHO) extension. Chapter 6 concludes the most significant results of the thesis and discusses about the future work related to radio network topology. Finally, Chapter 7 provides an overview of the publication results and the author's contribution to each publication.

## 1.3 Main Results of the Thesis

The target of the work performed for this thesis was to provide a comprehensive and new analysis of the radio network topology planning for WCDMA networks, and to present the impact of different radio network topologies not only by using system simulations but also radio interface measurements. In addition, the target was to cover certain topology planning aspects for a repeater implementation and for a network-based mobile positioning technique called cell ID+RTT. Hence, as such, the results of this thesis do not provide any novel radio network topology concepts or simulation methodologies, but rely on standard network layouts and simulations to provide the outcomes. However, two novel ideas are presented: the other one is related to the coverage and sector overlap modeling with a single parameter, and the other one to evaluating the quality of the radio network topology by using measurements. Up to date, any publication has not addressed coverage and sector overlap modeling, which is crucial especially for WCDMA networks. This thesis introduces the definitions of coverage overlap index ($COI$) and sector overlap index ($SOI$), and an evaluation of an optimum $COI$ and $SOI$ is presented based on extensive system simulations. Moreover, any verification technique of the quality of WCDMA radio plan has not been presented in the open literature, and hence the introduction of this quality verification method for radio network topology can be treated as a novel.

The rest of the results in this thesis are related to provisioning of new analysis of the WCDMA network coverage and system capacity, and also guidelines for radio network planning process. The most important ones are listed below.

- Showing that a small deviation in the site location or in the antenna direction is not harmful in a macrocellular WCDMA network. This relaxes the site acquisition during the radio network planning process.
- Providing optimum antenna downtilt angles, and as result, an empirical equa-

tion for macrocellular WCDMA network as a function of effective base station antenna height, average site spacing and antenna vertical beamwidth. Moreover, showing that the performance of electrical downtilt outperforms slightly the mechanical downtilt, and that sectoring does not remarkably affect the optimum downtilt angle.

- Verification of the impact of mechanical antenna downtilt on the downlink capacity by using radio interface measurements. The downlink capacity gain of 20% was observed that corresponds to the one observed using simulations.
- Showing that the geographical user distribution over the cell area does not as such change the optimum downtilt angle, which indicates that CAEDT should not be implemented only to response to changes of user locations.
- Illustrating the impact of different 6-sectored antenna configurations on the amount of pilot pollution through system simulations, and more practically by using radio interface measurements.
- Providing guidelines for site evolution from a 3-sectored site to a 6-sectored site regarding the improvements in the absolute coverage and capacity.
- Evaluating the reliability of a static radio network planning tool using the COST-231-Hata and the ray tracing propagation model, and providing a comparison with radio interface measurements in an urban WCDMA network. The results show that in an urban area the COST-231 overestimates clearly the attainable downlink capacity (up to 70%), whereas ray tracing model provides more realistic capacity estimates.
- An evaluation of the impact of analog WCDMA repeaters on the network coverage and capacity using simulations and measurements. The results illustrate that analog repeaters can be used to boost the downlink capacity. However, the uplink has to be planned carefully in terms of the repeater amplification.
- Addressing the impact of radio network topology on the accuracy of the basic cell ID+RTT mobile positioning technique, and showing the impact of the radio network topology on the expected availability of the forced SHO algorithm.

# CHAPTER 2

# Role and Methods of Radio Network Topology Planning

THIS chapter provides an overview of the WCDMA radio interface system planning process and emphasizes the importance of radio network topology planning from system capacity point of view. Moreover, it introduces the most relevant analysis methods for assessing the quality of radio network topology. In addition, the required information for understanding the results of system simulations is provided by means of the introduction of a typical radio network planning tool and its simulation methodology for performance assessment.

## 2.1 Radio Network Planning Process

The radio network planning process consists of dimensioning, detailed planning, and optimization. These main planning phases of the radio network planning process can be identified related to any cellular network regardless of the multiple access scheme or detailed implementation. However, detailed phases typically differ depending on the multiple access scheme of the radio interface and on the parameters required for radio resource management functions.

### 2.1.1 Dimensioning

In the dimensioning phase (also called initial or nominal planning), a rough estimate of the network layout and elements is derived. It provides the first and the most rapid evaluation of the number of network elements, as well as the associate capacity of those elements. As a result of dimensioning, the most critical parameter for a detailed planning phase is the average base station antenna height, which must be defined in order to be able to define the characteristics of the radio propagation channel and optimized planning guidelines (such as antenna tilting) for that environment. The definitions of the dimensioning methods differ slightly in the literature, but the common feature is that dimensioning uses hypothetical data. Nevertheless, the dimensioning phase can already address the capacity requirements of different cells by using, e.g. standard load equations. [2, 3, 9, 10]

### 2.1.2 Detailed Planning

In WCDMA networks, the detailed planning phase consists of configuration planning, topology planning, code planning, and parameter planning.

#### Configuration Planning

In configuration planning, the base station and base station antenna line equipment is defined, and the maximum allowed path loss is calculated in the uplink (UL) and downlink (DL) directions. In power budget calculations, gains (e.g. antenna gain and amplifiers), losses (e.g. cables and filters), and margins (e.g. slow fading, interference, fast fading) are added to transmit and reception power levels. The result of configuration planning is [2]:

- a detailed base station configuration
- a list of antenna line elements for different network evolution phases
- the maximum uplink and downlink path loss information for coverage predictions

#### Topology Planning

The final configuration of the radio network elements and layout is defined during the topology planning phase, which covers simultaneous planning of coverage and capacity [2]. The elements for topology planning can be roughly divided into *base station site configuration* and *base station antenna configuration*. However, the difference between these two elements is partly volatile. The base station site configuration contains definitions for site locations, sector directions, and number of sectors, whereas the base station antenna configuration covers mostly definitions of antenna height and antenna configuration (as radiation characteristics and downtilt). After defining all these parameters (and naturally after deploying the network), the initial stage of the network has been achieved, and the network is ready for operational use (from a network configuration point of view).

As the interference conditions vary according to amount and location of traffic, modeling of the dynamic changes requires radio network system level simulations in order to assess its performance. These system level simulations must be carried out for a certain cluster of cells so that all uplink and downlink changes of other-cell interference are included. System level simulations are based, for example, on static Monte Carlo type of simulations, where a certain number of mobile terminals are located over a coverage area, but the motion of mobiles is not modeled. The results of static simulations include coverage, capacity, and interference-related information such as the transmit power of base stations, maximum number of users in each cell, and other-cell-to-own-cell interference. These results finally give an estimate of whether base station sites are located and configured correctly, and what is the estimated throughput per site. Sections 2.2 and 2.3 provide a more detailed view of the static simulations required for topology planning. [2, 11]

#### Code and Parameter Planning

After the topology planning phase, only code and parameter planning are needed before the network can be launched. In code planning, scrambling codes are allocated for different cells in order to separate cells in the downlink direction. Scrambling code planning is relatively straightforward because there should be enough codes for a WCDMA network. Moreover, the scrambling code planning can be easily performed in a planning tool. [2,3,12]

In the parameter planning phase, initial values for different radio resource management tasks and functionalities are allocated. These parameters can include, e.g. signalling together with handover and power control related parameters, which are all furthermore related to idle, connection establishment, and connected modes. In the parameter planning phase, all parameters are grouped to these different categories, and pre-optimized default values are given when the network or a cell is launched. [2]

### 2.1.3 Optimization

The WCDMA radio network is entirely designed after system level simulations in topology planning, and code and parameter definitions. The following planning phases are verification, monitoring, and optimization. In the verification phase, which is performed prior to commercial launch, different key performance indicators (KPI) related to coverage and functionality are evaluated. This covers evaluation of, e.g. call success rates and soft handover success rates. Fundamentally in the verification phase, coverage and dominance areas are verified and analyzed due to their strong impact on radio network capacity. Verification of the radio network is mainly carried out with the use of a radio interface field measurement tool. Monitoring is continuously performed during the commercial operation of the network by collecting KPI values related to, e.g. call success rates and drop call rates. More detailed monitoring (troubleshooting) can be based on signaling messages between the base station and mobile station measured by a radio interface field measurement tool or by a QoS analyzing tool, for example, from the Iub interface. [2,3]

Finally, optimization contains different kinds of planning-related actions to solve problems found in the verification and monitoring phases. Optimization involves continuous trouble shooting; it could also be called re-planning because all planning phases and their results must be checked before any modifications can be made to the actual plan. The optimization process includes radio interface field measurements and QoS measurements to understand network bottlenecks at the cell, site, and radio network controller (RNC) levels. [2,3,9]

## 2.2 Assessment Methods of Topology

In GSM radio networks, frequency planning traditionally defines the quality of the radio network plan, especially in an interference-limited environment [8]. However, in WCDMA, most of the quality of the radio network plan is defined by the topology, and the resulting interference conditions. On the other hand, the functionality

of the whole network is mostly defined by RRM functions and their parameter selections. The quality of WCDMA topology can be assessed with system level (i.e. network level) analysis, assuming that the propagation environment (digital map, propagation model) and traffic distribution can be reliably modeled. In practice, this means that assessment can be conducted either with *analytical analysis*, *system level simulations* or *radio interface measurements*.

### Analytical Modeling

Analytical investigations are based on mathematical models. This type of studies have the advantages of having a lower cost and requiring less effort than other methods. For example, a coverage and interference assessment can be performed using analytical models [13,14]. In addition, for example an analytical approach with load equation can be used to evaluate the downlink capacity [15]. Even though the approach of analytical models is comparatively simple, more detailed and reliable analysis is problematic due to the high complexity of the WCDMA system.

### System Level Simulations

Another method is to use computer-based simulations of the cellular network. In general, they can be divided into three categories: *static*, *dynamic* and *quasi-dynamic*. Static simulators are characterized by excluding the time dimension, and the results are obtained by extracting sufficient statistics of statistically independent snapshots of the system performance (Monte Carlo approach). Hence, they are suitable for radio network topology assessments if they take reliably into account the detailed radio propagation environment. [2,16]

In contrast, dynamic network simulators (e.g. [17]) include the time dimension, which, on the contrary, adds further complexity. However, dynamic simulations are very appropriate for investigating time dependent mechanisms or dynamic algorithms. RRM functionalities, such as the power control and handover control, can be properly analyzed. Hence, they can be used, e.g. for benchmarking new RRM function or for certain parameter optimization problems.

A middle-way between static and dynamic simulations is the so-called quasi-dynamic simulators (e.g. [18]), which only include a single time dependent process, while the rest of time dependent processes are modeled as static. This solution represents a trade-off between the accuracy of fully dynamic simulations and the simplicity of static simulations. They are suitable also for the assessment of RRM functions as shown in [19].

### Radio Interface Measurements

A practical alternative for topology assessment is to conduct radio interface measurements in a trial or operational network. These radio interface measurements are typically related to verification and monitoring phases. For a specific network configuration, this method can provide the most accurate assessment of the system performance and of the QoS to be experienced by users. However, the results might

be network specific (i.e. depending on the network configuration and environment), and hence may therefore differ from network to network. This also makes the generalization of the results problematic as they might be strongly case dependent. A comprehensive presentation of the radio interface measurements related to UMTS network is presented in [2].

## 2.3 A Static Radio Network Planning Tool

Static simulations offer the most promising way for radio network planning and topology assessment. As a result of simulations, a static planning tool provides an estimate of the average network behavior by using a given network configuration, parameters, and traffic layer (including service requirements and distribution). For this purpose a static planning tool seems to be sufficient, as the whole radio network planning is typically based on average values (e.g. slow fading margins, etc.) [8].

For an operator, the utilization of a radio network planning tool in WCDMA planning process is economically and technically extremely beneficial. In the initial network deployment process, the use of planning tools results in a network consisting of a sufficient number of sites to provide the required QoS for users. Moreover, planning tools can be used to minimize the costs and efforts of the operator, and also to fasten the whole planning processes. Furthermore, a radio network planning tool can provide assistance for the planner during network optimization and evolution when new sites are possibly dimensioned. Naturally, the accuracy of the simulations depends on the quality of the digital map, propagation model, and traffic estimates.

This section provides an essential introduction of the static planning tool [20] that has been used for most of the simulations presented later on in this thesis. However, the emphasis here is limited to coverage and capacity related analysis. A full description of [20] can be found from [2] and [21]. Descriptions of other similar WCDMA radio network planning tools can be found from [3] and [16]. In addition, this section introduces the theoretical background of methods used for estimating the system capacity with the WCDMA radio network simulator. The analysis is performed independently for uplink and downlink directions, as system load behaves differently in these directions [3]. The quality requirements of a radio link are expressed in terms of SIR (signal to interference ratio) requirement. Moreover, the impact of the other-cell interference on the SIR requirement is emphasized.

### 2.3.1 Relation of SIR and Other Cell Interference

In a cellular WCDMA system, the same carrier frequency is used in all cells, and users are separated by unique code sequences. The capacity of a WCDMA system is thus typically interference-limited rather than blocking-limited, since all mobiles and base stations interfere with each other in uplink and downlink directions [2, 9]. The network (or cell) capacity is defined by interference (or load equation) that, on the other hand, sets limits for the maximum number of users in a cell or for the maximum cell throughput. Through this thesis, the system capacity is defined as the maximum number of users that can be supported simultaneously with a pre-defined

service probability target, or correspondingly with a certain downlink or uplink load target.

### Uplink Capacity

The parameter SIR (signal to interference ratio) is used to measure the quality of a connection. In practice, the SIR requirement that results in a certain bit error rate (BER) (for example 0.01) depends at least on the used service and user characteristics (propagation environment, user speed, etc.). During the simulations, the signal quality received at the base station for the *j*th user must satisfy the following condition (e.g. [9,16]):

$$\begin{aligned} SIR_j &= \frac{W}{R_j}\frac{P_{TX,j}}{P_{RX}^{BS}L_j - P_{TX,j}} \\ &= \frac{W}{R_j}\frac{P_{TX,j}/L_j}{i_{other} + i_{own} - P_{TX,j}/L_j + P_n} \end{aligned} \tag{2.1}$$

where *W* is the system chip rate, $R_j$ is the user bit rate of the *j*th mobile[1], $P_{TX,j}$ is the transmit (TX) power of the *j*th mobile, $P_{RX}^{BS}$ is the total received wideband power (including other-cell interference ($i_{other}$), own-cell interference ($i_{own}$), and thermal noise power $P_n$) at the base station, and $L_j$ is the uplink path loss from the *j*th mobile to the base station.

As seen from (2.1), SIR can be controlled by changing the TX power ($P_{TX,j}$), and hence during simulations, a certain SIR requirement is achieved iteratively by changing the mobile's transmit power. During a Monte Carlo simulation process, the powers of each connection are adjusted based of the service-dependent and user profile dependent (e.g. different speeds) parameters. As the interference from other users affects the SIR, the process has to be iterative given certain convergence criteria. Thus, the maximum uplink capacity is defined by the interference-based uplink load factor, $\eta_{UL}$, which is given as interference rise above the thermal noise power[2] (e.g., [16]):

$$\begin{aligned} \eta_{UL} &= \frac{P_{RX}^{BS} - P_n}{P_{RX}^{BS}} \\ &= \frac{i_{own} + i_{other}}{i_{own} + i_{other} + P_n} \end{aligned} \tag{2.2}$$

As the equation of SIR is not a closed-form solution, a direct connection between SIR and $\eta_{UL}$ cannot be presented. However, the uplink capacity can be defined by the load factor. Moreover, $\eta_{UL}$ is used to define a WCDMA radio network planning

[1] $W/R_j$ is the service processing gain and excludes possible gain from channel coding. Moreover, $R_j$ is the user net bit rate of a particular service.

[2] Note that $\eta_{UL}$ can be also given based on the throughput (e.g. [9]). However, interference based load factor is considered here as it can be used in the simulations.

parameter called interference margin[3] ($IM$) that takes into account the changes in the network coverage due to cell breathing:

$$IM = -10\log_{10}(1-\eta_{UL}) \tag{2.3}$$

In the configuration planning phase, the maximum uplink noise rise is typically targeted between 1.5 dB-6 dB (i.e. $\eta_{UL}$ 30-75%) [2, 3, 9]. From a topology planning point of view, the target is to provide as good isolation between cells as possible. The ratio of $i_{other}$ and $i_{own}$ is defined as other-to-own cell interference *i*, and it reflects in the isolation of the considered base station sector (or cell) as it measures the interference received from mobiles from other cells. This ratio can be reduced by, e.g. optimizing the antenna radiation pattern is such a manner that the received other-cell interference is minimized. However, this has to be done such that the coverage in the own cell is still maintained (i.e. $P_{TX,j}$ should be enough from the cell edge according to power budget calculations). Hence, by reducing *i*, with the same interference margin target, the number of supported users can be higher, which turns out to increase system capacity in the uplink.

**Downlink Capacity**

The cell capacity of the downlink (DL) in the WCDMA system behaves differently compared to the uplink. This is caused by the fact that all mobiles share the same transmit power of a base station sector [15]. Furthermore, simultaneous transmission allows the usage of orthogonal codes. However, the code orthogonality ($\alpha$)[4] is partly destroyed by multipath propagation, which depends at least on the propagation environment and mobile speed [9]. In order to satisfy the SIR requirement of the *k*th mobile of the downlink, the following criteria have to be fulfilled:

$$SIR_k = \frac{W}{R_k}\frac{P_{TCH,k}}{P_{RX}^{MS}L_k - \alpha P_{TX}^{tot} - (1-\alpha)P_{TCH,k}} \tag{2.4}$$

In (2.4), $P_{TCH,k}$ is the TX power of the downlink traffic channel (TCH) for the *k*th connection, $L_k$ is the downlink path loss, and $P_{TX}^{tot}$ is the total TX power of a base station sector mobile is connected to, and $P_{RX}^{MS}$ is the total received wideband power at the mobile station expressed as:

$$P_{RX}^{MS} = I_{tot} - \alpha i_{own} + P_n \tag{2.5}$$

where $I_{tot}$ is the total received interference power, $i_{own}$ is the interference power received from the own cell, and $P_n$ is the noise power. The variable $P_{TX}^{tot}$ includes the TX power of primary common pilot channel (P-CPICH), other common control channels (CCCH), and also all traffic channels. Placing (2.5) into (2.4) yields after some modifications:

[3] Interference margin is also called noise rise.

[4] In the context of this thesis, $\alpha$ is a cell-based parameter.

$$SIR_k = \frac{W}{R_k} \frac{P_{TCH,k}/L_k}{i_{other} - \alpha i_{own} - (1-\alpha)P_{TCH,k}/L_k + P_n} \tag{2.6}$$

As seen from (2.6), the resulting SIR is directly decreased by interference power from other sectors. As in the uplink scenario, the presented equation for SIR is not a closed-form solution, and hence the estimation of the correct transmit power requires iteration, since the SIR at each mobile depends on the power allocated to the other mobiles [16]. This equation is exactly the same as those used with the system level simulations presented, e.g. in [3, 22, 23].

In the context of this thesis, the total transmit power $P^{tot}_{TCH,m}$ for the TCH of the $m$th base station sector is the sum of all $K$ connections (including soft and softer handover connections):

$$P^{tot}_{TCH,m} = \sum_{k=1}^{K} P_{TCH,k} \tag{2.7}$$

and the downlink load factor, $\eta_{DL}$, is defined with the aid of the average transmit power of TCHs of base stations for a cluster of cells:

$$\eta_{DL} = \frac{\sum_{m=1}^{M} P^{tot}_{TCH,m}}{M P^{max}_{TCH,m}} \tag{2.8}$$

where $M$ is the number of sectors in the cluster. The downlink capacity is maximized when the minimum $\eta_{DL}$ is achieved with the same number of served users $K$.

### 2.3.2 Simulation Methodology

In a static planning tool, the actual performance estimation is normally divided into two parts: namely *coverage predictions* and *performance analysis* (Monte Carlo analysis).

#### Coverage Analysis

The fundamental part of the performance of the simulator comes from the coverage predictions. In the coverage calculations, path loss matrixes are created based on propagation models, network and site configuration (e.g. antenna radiation patterns and downtilt), and digital maps of the planning area[5]. Propagation is predicted for each pixel on the digital map according to a certain model, and a pixel corresponds to the resolution of the digital map. Hence, in addition to a reliable coverage prediction model, also the resolution of a digital map should be good enough.

Most of the radio network planning tools offer the possibility to use empirical, physical, and deterministic propagation models. However, in practice, the utilized

[5]Digital maps are commonly utilized to predict radio wave propagations in natural and built-up environments. To achieve reliable prediction results, and to be able to plan a radio network successfully, up-to-date and accurate geographical information is needed [8, 24].

**Table 2.1** An example of morphological (land use) correction factors for extended COST-231-Hata model for different clutter types.

| Morphotype | Correction factor [dB] |
|---|---|
| Open | $-17$ |
| Water | $-24$ |
| Forest | $-10$ |
| Building height $<$ 8 m | $-4$ |
| Building height $>$ 8 m | $-3$ |
| Building height $>$ 15 m | $0$ |
| Building height $>$ 23 m | $3$ |

propagation model has to be tuned for the simulation (or planning) area based on field measurements [8]. For example, tuning of the COST-231-Hata propagation model can be done by utilizing area correction factors for different clutter types and by weighting the calculation of area correction factors between the transmission and reception ends. Table 2.1 shows an example of morphological (or area) correction factors. In addition to area correction factors, the propagation slope can also be adjusted. A comprehensive analysis of propagation model tuning is provided in [8].

**Performance Analysis**

In the performance analysis part, predicted path losses are utilized for solving the required transmit power needs iteratively in the uplink and downlink based on (2.1) and (2.4). In cellular radio network planning, it is necessary to make simplified assumptions concerning, e.g. multipath radio propagation channel. However, different detailed link level phenomenon such as fast fading, soft handover (SHO) gain or required fast fading margin can be taken into account in a look-up-table manner.

In the capacity analysis during Monte Carlo process, a large number of randomized snapshots are performed in order to simulate service establishments in the network. At the beginning of each snapshot, base stations' and mobile stations' powers are typically initialized to the level of thermal noise power. Thereafter, the path losses matrices are adjusted with mobile-dependent standard deviations of slow fading. After this initialization, the transmit powers for each link between base station and mobile station are calculated *iteratively* in such a manner that SIR requirements for all connections are satisfied according to (2.1) and (2.4) for uplink and downlink, respectively. During a snapshot, a mobile performs a connection establishment to a sector, which provides the best $E_c/N_0$ on the P-CPICH:

$$\left(\frac{E_c}{N_0}\right)_k = \frac{P_{P-CPICH}}{P_{RX} L_k} \tag{2.9}$$

**Table 2.2** An example of typical cell- and RRM -related simulation parameters for a static planning tool.

| Parameter | Unit | Value |
|---|---|---|
| BS TX $P_{max}$ | [dBm] | 43 |
| Max. BS TX per connection | [dBm] | 38 |
| BS noise figure | [dB] | 5 |
| P-CPICH TX power | [dBm] | 33 |
| CCCH TX power | [dBm] | 33 |
| SIR requirement UL / DL | [dB] | 5/8 |
| SHO window | [dB] | 4 |
| Outdoor / indoor STD for shadow fading | [dB] | 8/12 |
| Building penetration loss | [dB] | 15 |
| UL target noise rise limit | [dB] | 6 |
| DL code orthogonality | | 0.6 |
| Maximum active set size | | 3 |

where $P_{P-CPICH}$ is the power of P-CPICH of the corresponding sector and $P_{RX}$ is the total received wideband power. A mobile is put to outage during a snapshot, if the SIR requirement is not reached in either UL or DL, or the required $E_c/N_0$ is not achieved in the downlink. Also, the uplink noise rise of a cell should not exceed the given limit during connection establishments[6]. The ratio between successful connection attempts and attempted connections during all snapshots is defined as *service probability*. After a successful connection establishment, all other sectors are examined to see whether they satisfy the requirement to be in the active set (AS) of the mobile. If multiple $E_c/N_0$ measurements from different sectors are within the SHO window, a SHO connection is established. After each snapshot, statistics are gathered and a new snapshot is started. For every network configuration, several independent snapshots have to be performed. Finally, the number of required snapshots depends heavily on the size of the simulation area and map resolution.

Even though RRM functions cannot be modeled the with static planning tool, certain RRM-related parameters can, however, be defined. For example, admission control can be implemented by setting uplink noise rise limit, maximum power for single link in the downlink, and maximum power for the whole base station sector. Moreover, SHO can be modeled as explained above. Table 2.2 provides an example of simulation parameters for Monte Carlo -based static simulations.

[6]Cell noise rise is defined in (2.2).

# CHAPTER 3

# Basic Elements of Topology Planning

THE target of radio network topology planning is to provide a configuration that offers the required coverage for different services, and simultaneously maximizes the system capacity. This chapter addresses the impact of:

- coverage overlap (antenna height and site spacing)[1]
- selection of site location
- sectoring and antenna beamwidth
- antenna downtilt

on the WCDMA network coverage and system capacity. Moreover, the impact of the aforementioned elements is addressed on pilot pollution that reflects partly on the expected functionality of the network, and on site evolution from a 3-sectored site to a 6-sectored site.

The chapter begins with consideration of coverage overlap, which is an extremely general term as it is mainly defined by site location (i.e. average site spacings) and antenna configuration (antenna height, downtilt, etc.). Moreover, the radio propagation (urban, suburban, etc.), planning environment (macro, micro, etc.), and also link budget affect the resulting coverage overlap. The chapter continues with an example of selection of site location. The other type of coverage overlap, namely sector overlap is addressed by means of selection of sectoring and antenna horizontal beamwidth. Thereafter, the importance of antenna downtilt is emphasized through simulation campaign as well as measurement results. On top of this, results regarding the impact of proper radio network topology planning on the quality of the radio network are provided. Finally, proposals for site evolution strategy are given when 3-sectored sites are updated to 6-sectored sites.

## 3.1 Coverage Overlap

In any cellular network, coverage overlap is required in order to combat the harmful impact of slow fading of the signal (slow fading margin required), and moreover, to

[1] Antenna downtilt can be perceived as a part of coverage overlap. Hence, its impact on coverage overlapping is also studied in Section 3.1.

be able to provide, e.g. indoor coverage with an outdoor network (building penetration loss). Therefore, in cellular networks, most of the other-cell interference is produced by the coverage overlap requirements. However, an unambiguous definition of coverage overlap is rather difficult, and has not been addressed in the literature.

In general, coverage overlap is affected by the link budget, antenna configuration, average site spacing, and propagation environment. The first three elements are strictly topology related factors, and the fourth one is defined by the planning environment, which also defines the propagation slope [8]. The impact of the maximum allowable path loss on the coverage overlap is obvious; a higher allowable path loss enables better coverage and can thus increase the coverage overlap. The maximum allowable path loss is naturally affected by the base station antenna gain (connection to antenna horizontal and vertical beamwidth). Secondly, a higher antenna position decreases the propagation slope, and therefore increases the cell coverage and resulting coverage overlap. Moreover, a higher antenna position increases the probability of line-of-sight (LOS) connections. Thirdly, the closer the base station sites are to each other, the larger is the resulting coverage overlap. Finally, the propagation environment has an impact on propagation slope, and thereby affects the amount of coverage overlap.

To summarize these points, a small coverage overlap might reduce the network performance through too low network coverage, whereas too high coverage overlap reduces the network performance, increases other-cell interference level, and finally reduces system capacity [25]. This is actually the starting point for radio network topology planning, which requires optimized coverage overlap. Hence, the impact of it has to be understood on system capacity when site selections are made in the topology planning phase. The target of this section is to achieve optimum coverage overlap that maximizes the system capacity. A similar approach from roll-out optimized network configuration point of view is taken in [26].

### Site Spacing

Site spacing (i.e. average distance between sites) is defined either by the coverage or capacity requirements for a planning area. Coverage requirements define the site spacings typically in rural areas, where the capacity does not constrain the system performance and observable QoS. On the other hand, capacity requirements (expected customer density) define site spacings in capacity-limited environment. However, the coverage requirements for indoor users also affect the site density of an urban planning area. If high indoor coverage probabilities (80-90%) are required, the average site density grows, which automatically results in large coverage overlap areas. This easily increases the risk of observing higher other-cell interference levels as well. Hence, optimization of antenna height and, e.g. antenna downtilt is strongly required.

### Antenna Height

The selection of antenna height is typically performed according to the planning environment [8]. In a microcellular planning environment, antennas are systemat-

ically deployed under the average roof top level for capacity purposes. For an urban macrocellular network layer, antenna heights follow the average roof top levels. Correspondingly in suburban areas, the propagation occurs most of the time clearly above roof-top level due to relatively higher antenna position with respect to average roof top levels. On the other hand, the propagation loss in rural areas is dominated by the undulation of the terrain. This means that the propagation slope varies from 20 dB/dec (free space) up to 45 dB/dec (dense urban) depending on the propagation environment [8,27,28].

From a radio network topology optimization point of view, the selection of the antenna height also depends on the site location. A choice of a low antenna installation height increases the number of required sites in a planning area (cf. microcells). Moreover, a lower antenna position in an urban area reduces service coverage probabilities in the network, and might decrease QoS. On the other hand, sectors become more isolated from each other, which results in lower other-cell interference levels [3]. If a higher antenna position is selected, coverage probabilities can be enhanced. However, signals are propagated for longer distances (known as over shooting), which exposes the network to higher other-cell interference levels. Furthermore, higher antenna position may increase SHO areas at the cell edges and result in higher overhead for SHO connections.

### 3.1.1 Coverage Overlap Index

In the following, the impact of coverage overlap is presented on the system capacity with extensive set of system level simulations. Moreover, an optimum empirical value for coverage overlap is evaluated with *coverage overlap index* (*COI*). All relevant simulation parameters and description of the simulation environment can be found from [P1].

The coverage overlap index (*COI*) is defined here as

$$COI = 1 - \frac{\textit{length of dominance area}}{\textit{length of actual coverage area}} \tag{3.1}$$

where *length of dominance area* is the length of the geographical area where the cell is intended to be the most probable server[2]. The *length of actual coverage area* is the cell range defined by the maximum allowable path loss towards the horizontal plane of an antenna and can be calculated with an adequate propagation model. In the context of multi-service WCDMA network, the maximum allowable path loss is defined by the service with the highest path loss (typically, speech/voice). If $COI \rightarrow 0$, the cells in a network would not have sufficient overlap, and the network would most probably be unable to provide a continuous network coverage (without planning margins such as slow fading margin). However, the other-cell interference level would definitely be low as well. Hence, in practice, $COI$ has to be higher than zero in order to tolerate slow fading and to achieve indoor coverage.

In order to provide an idea of the range of *COI*, let us consider an example with link budget values presented in [2]. The isotropic path loss (i.e. without any margins)

[2]The length of the dominance area can be easily extracted from system simulation cell-by-cell basis.

equals 157.1 dB in the downlink. This can be mapped into a cell range of 3.16 km by using the Okumura-Hata propagation model with 35 dB/dec propagation slope, 25 m antenna height, and 2100 MHz frequency. However, by taking into account standard deviation of slow fading ($\sigma_{SF} = 7\ dB$), SHO gain (3 dB), and outdoor location probability requirement (95%), the resulting maximum allowable path loss would be 149.8 dB, and the corresponding cell range 1.95 km. If the network were deployed based on outdoor coverage, the resulting *COI* would be, by the definition, $COI = 1 - (1.95/3.16) = 0.383$. On the contrary, if 90% indoor location probability were required ($\sigma_{SF} = 9\ dB$ and building penetration loss (BPL) = 15 dB), the indoor path loss would be 135.6 dB, and the cell range only 0.77 km. Finally, the *COI* would equal to $COI = 1 - (0.77/3.16) = 0.756$. Note that this example does not include the impact of antenna downtilt that effectively decreases the path loss towards antenna boresight, and hence reduces the *actual coverage area*. Nevertheless, due to planning margins, coverage overlap always exists, which on the contrary, increases other-to-own-cell interference in WCDMA. Therefore, a certain level of other-to-own-cell interference has to be accepted (e.g. $i$=0.5 [3]).

Technically, the utilization of *COI* has two different approaches. In an academic approach, a possible network together with site and antenna configuration could be selected freely, and hence optimization of *COI* should also be based on all these parameters. This kind of scenario could arise in a case where planned site density was smaller than the density candidate site locations, which is a rather hypothetical assumption. In a more practical approach, site locations (and correspondingly site spacings) would be fixed (or pre-defined), and, moreover, antenna heights could not be significantly changed. In this kind of scenario, the optimization of *COI* would be based almost purely on optimizing the antenna configuration (mostly downtilt).

### 3.1.2 Empirical Optimum $COI$

In the following, an optimum *COI* is empirically evaluated based on the simulations presented in [P1]. Parameters in the evaluation are:

- maximum allowable isotropic path loss in DL (157.55 dB, 160.55 dB, 163.55 dB)[3]
- simulated site spacings (1.5 km, 2.0 km, 2.5 km)
- simulated antenna heights (25 m, 35 m, 45 m)
- different antenna types ($65°/6°$, $65°/12°$, $33°/6°$)[4]
- optimum downtilt angles for each scenario

Altogether, three different antenna radiation patterns are considered: namely, 3-sectored sites with $65°/6°$, 3-sectored sites with $65°/12°$, and 6-sectored sites with $33°/6°$. For the evaluation of $COI$, antenna electrical downtilt is taken into account simply by decreasing the maximum path loss in the direction of horizontal plane of the antenna. Moreover, the Okumura-Hata propagation model was used

[3]Maximum allowable isotropic path loss differs only due to different antenna gain.
[4]$xy°/z°$ denotes the half-power beamwidth in the horizontal (xy) / vertical plane (z).

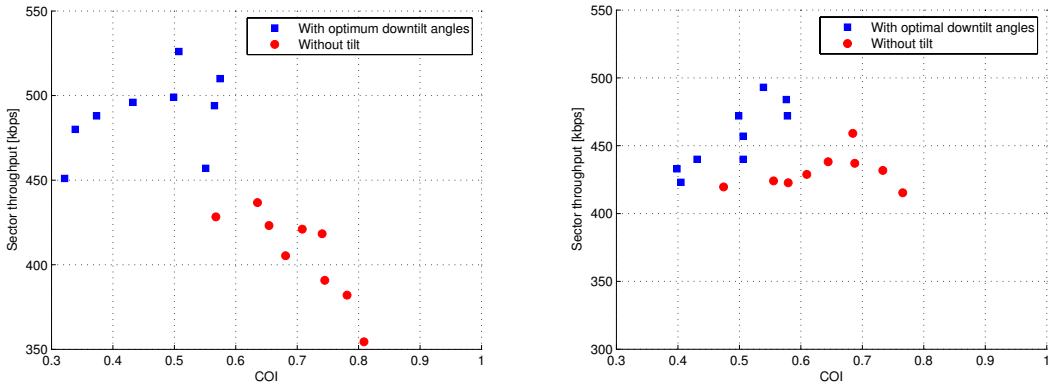


(a) $65°/6°$. (b) $65°/12°$.

**Figure 3.1** Average sector throughput as a function of $COI$ for 3-sectored sites.

at 2100 MHz frequency in such a manner that propagation slope was a function of antenna height. The average area correction factor ($-14$ dB) was evaluated based on the exact land use in the simulation area. Furthermore, as the network was based on the hexagonal grid with nominal antenna directions, the length of the dominance areas for 3-sectored sites were $2/3$ of the site spacing and for 6-sectored sites $1/2$ of the site spacing. Figs. 3.1 and 3.2 gather the average sector throughput as a function of *COI* for different network, site, and antenna configurations. The average sector throughput is derived based on the average BS TX power of 39 dBm of all cells[5].

Fig. 3.1(a) shows the sector throughput as a function of *COI* for 3-sectored network with $65°/6°$. The squared dots are for optimum downtilt scenarios and circular dots are for non-tilted scenarios. Most of the scattering between samples is caused by the utilization of a digital map (the propagation environment was not the same with all site spacing) and practical antenna radiation patterns.

The results indicate that maximum sector throughput can be achieved with $COI \approx 0.5$ (Fig. 3.1(a)), and it can be achieved only by downtilting. The configuration that provides the highest throughput is 1.5 km site spacing with 45 m antenna height[6]. Nevertheless, the tendency of the results is that the system capacity can be maximized with higher antenna position and shorter site spacing. Without any downtilt, the resulting $COI$ is naturally higher, and correspondingly the capacity is lower. The results with and without downtilt cannot be directly compared due to the fact that the definition of $COI$ does not address, e.g. the enhanced coverage near the base station due to antenna downtilt.

With different antenna type (larger vertical beamwidth and smaller antenna gain), the changes in the throughput as a function of $COI$ are not dramatic[7] (Fig. 3.1(b)). Moreover, optimum *COI* is obviously close to 0.5. Finally, Fig. 3.2 shows the corre-

[5] see [P1] for more information regarding simulation parameters together with evaluations of optimum downtilt angles and sector throughputs.

[6] See exact capacity values from Table 3.5

[7] A network of a wider vertical beamwidths is more robust for the variations of the network or antenna configuration, see [P1].

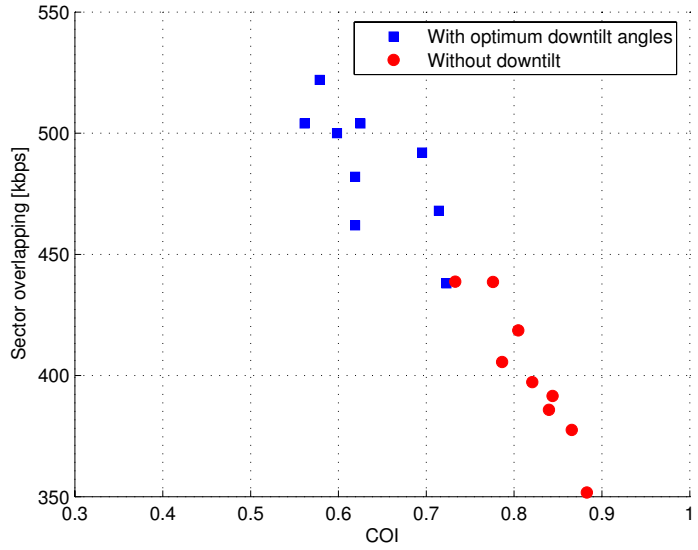


**Figure 3.2** Average sector throughput as a function of $COI$ for 6-sectored network; $33°/6°$.

sponding relation of *COI* and sector throughput for 6-sectored sites. However, the selected site spacings and antenna heights are not able to achieve $COI < 0.5$. Nevertheless, the trend of the results indicates that optimum *COI* would be again around 0.5.

### Conclusions

An empirical approach for estimating an optimum coverage overlap index was presented. The approach targets providing an optimum network configuration in terms of coverage overlap, which is based on site spacing, antenna height, and antenna downtilt. The maximum sector throughput was achieved typically with $COI \approx 0.5$, which can be achieved only through antenna downtilt. Hence, the impact of antenna downtilt should be clearly considered together with site spacing (site locations) and antenna height. Moreover, the optimization process of $COI$ should be based in practice on automatic optimization due to different dominance areas and antenna heights.

As seen from Fig. 3.1, the used definition of $COI$ in (3.1) cannot explicitly explain the impact of downtilt, as for example with $COI = 0.55$ in Fig. 3.1(a), the sector throughput varies between 430 kbps–510 kbps. One reason for this is the fact that the resulting system capacity with higher antenna position is better. However, part of this variation is caused by the utilization of a digital map (different propagation environment with different site spacings).

From an academic point of view, the results indicate that the optimization of the network topology should be as follows: maximize the antenna height and use

correspondingly larger downtilt angles. This kind of network configuration would maximize the system capacity. Hence, deployment of extremely high antenna positions as, for example, in the case of high altitude platforms (HAPs) (e.g. [29, 30]), would seem to provide an interesting deployment strategy purely from radio network topology point of view.

From a more practical point of view, the site density for a planning area must be minimized according to coverage or capacity requirements in order to minimize the network deployment costs and the required number of base stations. For capacity-limited network, deployment of new sites is allowed only if coverage overlap can be maintained at a reasonable level. Otherwise, the system capacity will degrade. Furthermore, as the optimization of site locations and antenna heights might be rather difficult due to practical site acquisition problems (e.g. low number of candidate site locations and aesthetic problems with extremely high antenna positions), the optimization of $COI$ should be based on a proper selection of antenna downtilt (and type) and also on intelligent placing of antennas in order to provide isolation towards other cells.

There are still several open issues to be solved in order to provide an explicit definition and optimum value for coverage overlap. This coverage overlap would finally define a set of optimum parameters that should be used to maximize the WCDMA network system capacity.

## 3.2 A Study of Site Locations and Sector Directions

The site location selection is performed during the topology planning phase. However, the requirements for site density are defined either by coverage or capacity requirements, and moreover, are provided from configuration planning (or from initial topology planning [2]). In practice, the amount of candidate site locations is rather limited, and hence an operator is not always able to use wanted site locations. A set of candidate site locations is reduced, e.g. due to topographical irregularities of the terrain, or authority constraints or government regulations that could prevent an operator for deploying a base station to an optimal place from their network performance point of view. Furthermore, in urban environments, where base stations are often located on the top of buildings, the physical space required for hardware of the planned site solution may not be enough. A rather extensive and practical view of possible problems during site location selection and site acquisition is provided in [10].

Another point of view for WCDMA site locations is the opportunity to reuse the site locations of an existing cellular network (e.g. GSM). This is economically a beneficial approach due to co-locating and co-siting opportunity, if only the costs are considered [3]. However, from an optimum performance point of view, site locations of the existing network could be different from the ones planned for a new network. From the network coverage point of view, existing GSM location could be selected also for WCDMA with certain limitations in coverage [2, 3, 31]. To summarize, the selection process of WCDMA site location has several aspects and also several constraints, and hence, the solutions might be somewhat non-optimal from a technical

point of view.

Another limitation that might occur during site acquisition is the selection of sector direction (or antenna direction). Due to external problems the antenna directions might not have been directed as planned. Moreover, because of obstacles close to the base station site location, or due to errors, e.g. in the base station antenna implementation, the antenna directions may change, and thus affect the network performance. Hence, the effect of antenna direction deviation on the network performance should also be considered.

This section provides simulation results and analysis of two different irregular configurations: namely, irregular site location and irregular sector directions. First, a comparison between hexagonal grid planning and irregular network configuration is presented in order to find out the impact of non-hexagonal site locations on the network performance. Secondly, the impact of irregular antenna directions on the WCDMA network performance is addressed.

### 3.2.1 Irregular Site Locations

In a homogenous and totally flat environment, a hexagonal grid planning with equal site spacings would be the most efficient strategy to deploy a cellular network, and assuming further that the traffic distribution were homogeneous [27]. Even in a generally flat environment, local terrain and clutter cause dramatic spatial variations in the received power [27,32]. This phenomenon is observed as slow fading, in which the mean level of the received signal tends to have a log-normal distribution [27, 33]. In addition, the regularity of traffic distribution is broken by different building distributions. Hence, in practice, a hexagonal network is not an optimum network layout for a cellular network.

The displacement of base station locations from the ideal hexagonal grid has been found to have a negligible impact on carrier-to-interference (C/I) values in cellular systems through simulations in a homogenous environment and with uniform traffic distribution [32, 34–36]. Moreover, in [32] it was shown that especially a CDMA network is rather robust for moderate base station location changes with respect to an ideal hexagonal grid. The results are of great importance due to the fact that small deviations do not affect cellular system performance. Hence, during the site selection process, most importance could be put on economical constraints. In contrast, in [37], which concentrated especially on UMTS system, the base station location was concluded to have a notable impact on downlink and uplink performance with a relatively large cell range.

Another set of simulation results regarding irregular base station site locations was considered in [P2]. However, the target was to study the impact of a small deviation in the base station site location on the top of a digital map on WCDMA system performance. Irregular network configurations (also called non-hexagonal) were formed by introducing a random deviation (i.e. an error vector) for each hexagonal site location. The maximum allowed deviation of the site location was 1/4 of the site spacing, and hence, e.g. with 1.5 km site spacing, the maximum deviation was 375 m. Fig. 3.3 illustrates part of a network with hexagonal and non-hexagonal site locations. Altogether, five different non-hexagonal grids were formed and sim-


**Figure 3.3** Non-hexagonal site locations together with the hexagonal reference locations with 1.5 km site spacing. The ring around each hexagonal site location illustrates the maximum allowable deviation. [P2]

ulated.

The simulation results in Table 3.1 show selected performance indicators for hexagonal and non-hexagonal network layouts of 1.5 km and 3.0 km site spacings. The results are rather pessimistic as no optimization of antenna configuration was performed after randomization of the network layout. With 1.5 km site spacing, the non-hexagonality is hardly seen in any of the performance indicators, and actually the average service probability is slightly larger for non-hexagonal grids. This small increase comes from an improvement of network coverage[8]. However, the network of 3.0 km site spacing is more coverage-limited, and hence the irregularity starts to affect the network performance. As a result, the average service probability is 2 percent smaller. However, randomization of site locations does not change the network capacity as indicated by the results. In this scenario, also the increase of SHO prob-

[8]Utilization of a digital map creates certain coverage-limited location with the hexagonal grid, and randomization of the site locations provided some coverage enhancements that could be seen as increased service probability.

**Table 3.1** Example simulation results with 1.5 km and 3.0 km site spacings. The performance indicators for the non-hexagonal grids are averaged over all five non-hexagonal network layouts, and the values in parenthesis are their standard deviations. DL capacity value is estimated based on average TX power of 39 dBm of all base station sectors. [P2]

| Parameter | | Reference grid | | Non-hexagonal grids | |
|---|---|---|---|---|---|
| | | 1.5 km | 3.0 km | 1.5 km | 3.0 km |
| Service probability | [%] | 98.1 | 96.2 | 98.3 (0.68) | 94.0 (1.08) |
| SHO probability | [%] | 24.9 | 17.2 | 25.0 (0.56) | 18.0 (0.5) |
| SfHO probability | [%] | 3.9 | 4.6 | 3.9 (0.19) | 4.9 (0.1) |
| UL $i$ | | 0.79 | 0.58 | 0.80 (0.02) | 0.60 (0.02) |
| DL capacity | [kbps/sector] | 360 | 360 | 359 (2) | 359 (3) |

ability is slightly larger. As was shown in [P2], a higher indoor location probability does not affect the inter-related simulation results of a non-hexagonal grid. Moreover, the deviation does not have an impact on the system capacity with selected maximum location deviation and site spacings.

**Conclusions**

A small random deviation of site location (less than 1/4 of the site spacing) from the hexagonal grid has a negligible impact on the system performance in a real propagation environment (i.e. when the information of the digital map is taken into account), and when high indoor coverage thresholds are required (1.5 km site spacing). The robustness of the WCDMA network remained, even if different traffic profiles were utilized [P2]. However, if high indoor coverage probabilities are not required, i.e. the cells do not overlap significantly, a random deviation in base station location becomes more and more crucial as with 3.0 km site spacing. Hence, in urban and suburban environments with higher coverage overlap due to required indoor coverage, the requirements for site location selection can be loosened, since the non-hexagonality does not lower network performance. This could be valuable information for a greenfield operator that possibly does not have any preferences for certain site locations due to existing cellular network. Thus, in the case of a greenfield operator, site locations could be selected by using a hexagonal grid layout as a reference. For each site, antenna configuration has to be optimized according to the new site location, and hence the results of selected deviation could be pessimistic. In conclusion, more attention should be paid to optimizing the antenna configuration rather than the site location as it poses more problems also in practice.

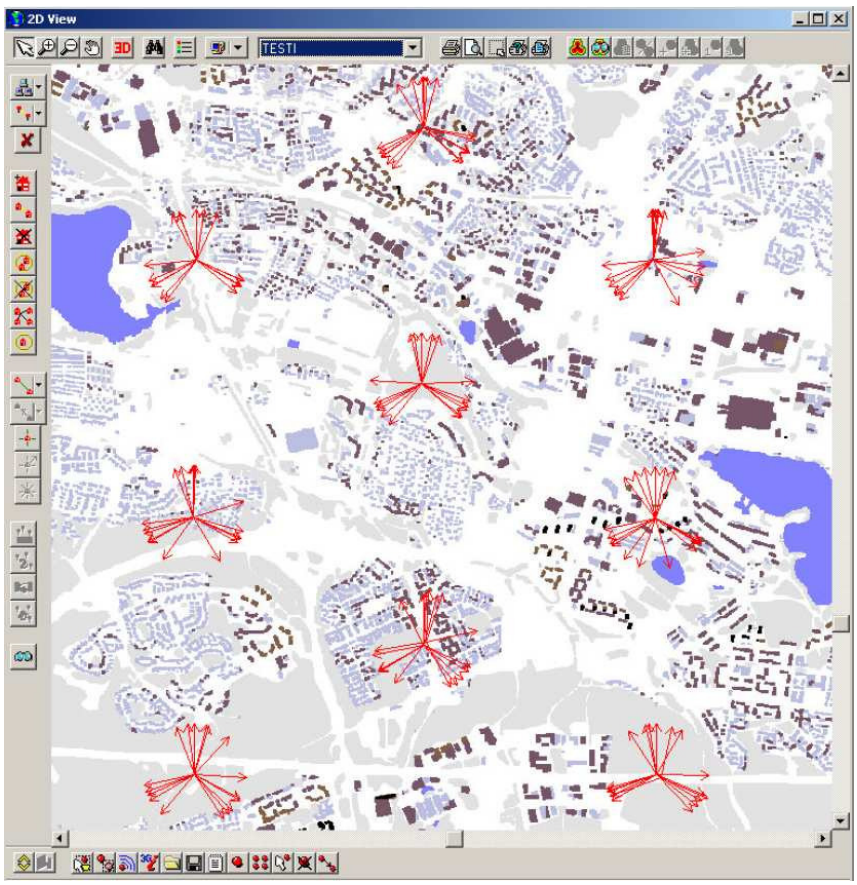


**Figure 3.4** Illustrations of irregular antenna directions. [P2]

### 3.2.2 Irregular Sector Directions

The target of this subsection is to study the impact of errors in the nominal antenna direction on the network performance. Information on the exact sector orientation is crucial, e.g. in planning tools. Therefore, the simulation results with irregular sector directions were compared with the nominal sector directions (i.e. $0°$, $120°$, and $240°$) of the hexagonal grid in order to solve the impact on system performance [P2].

To provide random antenna directions, to each base station antenna direction an error was added according to normal distribution. Fig. 3.4 shows an example of a part of the network with irregular antenna directions at the base stations. The resulting average error from the nominal antenna direction was $9.1°$ in the first scenario and $18.2°$ in the second one. Altogether, five different networks with irregular antenna directions were simulated.

Table 3.2 provides a set of simulation results with 1.5 km site spacing for nominal antenna directions. Due to increased irregularity of the antenna directions, the network performance with irregular sector directions is slightly reduced with respect to nominal sector directions. However, with an average deviation smaller than

**Table 3.2** Example simulation results of 1.5 km site spacing. Random directions 1 is with $9.1^\circ$ and random directions 2 is with $18.2^\circ$ average error in the antenna direction. [P2]

| Parameter | | Nominal directions | Random directions 1 | Random directions 2 |
|---|---|---|---|---|
| Service probability | [%] | 98.1 | 98.0 (0.3) | 98.0 (0.27) |
| SHO probability | [%] | 24.9 | 25.1 (0.18) | 25.0 (0.5) |
| SfHO probability | [%] | 3.9 | 4.1 (0.12) | 4.9 (0.37) |
| UL $i$ | | 0.79 | 0.80 (0.01) | 0.81 (0.01) |
| DL capacity | [kbps/sector] | 360 | 357 (3) | 355 (3) |

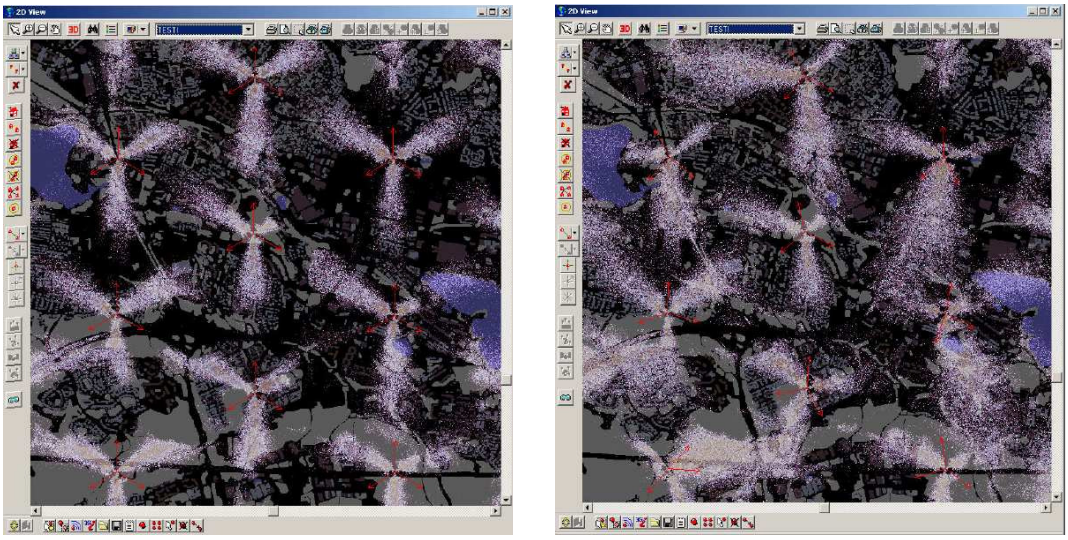

(a) Nominal antenna directions. (b) Randomized antenna directions.

**Figure 3.5** Visualization of SfHO probability from part of the network with (a) nominal antenna directions and (b) random antenna direction (with larger deviation). Black color indicates 0% SfHO probability and lighter color higher probability.

$20^\circ$, there is not much degradation in the system performance, if sector overlap[9] is around 0.5 (3-sectored sites with $65^\circ$ antennas). According to the simulation results in Table 3.2, the maximum system capacity degradation is less than 2 percent. As expected, the most visible impact of direction deviation is seen on the SfHO probability (see also Fig. 3.5).

**Conclusions**

The simulation results indicate that WCDMA network performance is robust for random antenna direction deviation under different traffic scenarios. The effect of antenna direction deviation was found to have almost negligible impact on the WCDMA network performance in a 3-sectored case of $65^\circ$ horizontal beamwidth antennas. However, these antennas are quite suitable for 3-sectored sites, and thus the deviation in the antenna direction could be more crucial, if wider antenna beamwidth or higher order sectoring is utilized.

## 3.3 Sectoring and Antenna Beamwidth

Sectoring is generally identified as a convenient method to increase network coverage and system capacity in a cellular network [38–46]. However, especially in WCDMA, the selection of the antenna beamwidth plays an important and crucial role in sectoring [47–51], [P3]. The coverage enhancement with sectoring is based on the improvement of the power budget[10], and also on the fact that more antennas are implemented at the base station site. The capacity enhancement can be logically observed due to the increasing number of sectors. Ideally, doubling the number of sectors of a base station site would mean doubling the offered capacity of a particular site. However, an ideal *sectoring efficiency*[11] can not be normally achieved due to non-optimal antenna radiation patterns. The capacity gain of a 3-sectored site compared to a 1-sectored site is around 2.5-2.7 [43–46], and 1.7-1.8 between a 6-sectored site and a 3-sectored site [47–50, 53], [P3]. However, in [P1] it was shown that a capacity gain of close to two could be achieved by using correct downtilt angles.

In WCDMA networks, 3-sectored sites probably offer a practical solution in the beginning of the network evolution. However, along with increasing capacity demands, higher order sectoring (such as 6-sectored sites) could be deployed in order to provide better network coverage and system capacity [54]. However, there are several practical limitations in the deployment of 6-sectored sites such as the increasing need of cabling and RF amplifiers [3]. Moreover, the need of capacity has to exceed a certain threshold before the deployment of a 6-sectored site or upgrading of an existing 3-sectored site to a 6-sectored site becomes economically viable.

The simulation results for WCDMA networks have indicated that with a so-called cloverleaf 3-sectored configuration, the optimum antenna beamwidth varies

[9] See Section 3.3 for definition of sector overlap.

[10] Utilization of horizontally narrow antenna beamwidth usually increases the gain of an antenna compared to a wider one [52].

[11] Sectoring efficiency refers to sectoring gain in system capacity.

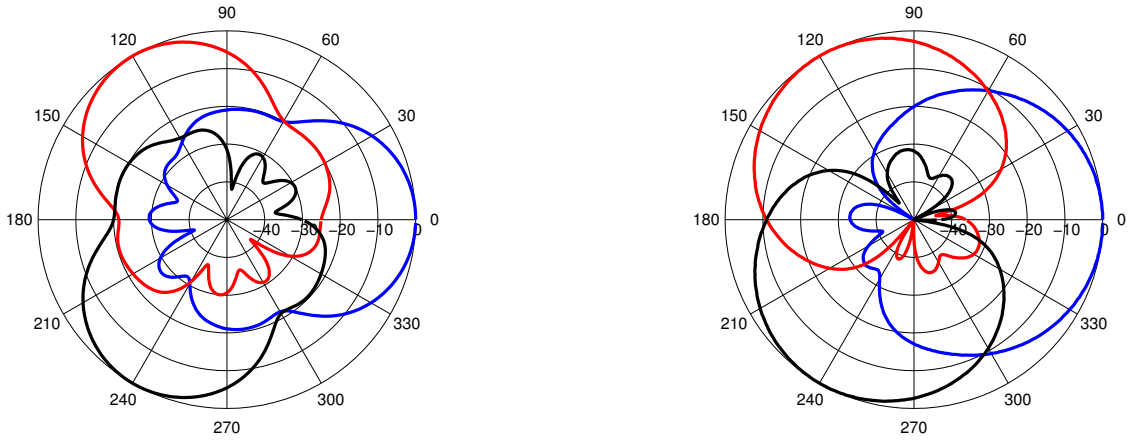


(a) 45°. (b) 65°.

**Figure 3.6** Illustration of radiation patterns for a 3-sectored base station site with (a) 45° and (b) 65° antennas.

between 35° and 65° [47–51], [P3]. However, with a so-called wide-beam 3-sectored configuration [34], the optimum antenna beamwidth is close to 80° [47]. On the other hand, for 6-sectored sites narrower antenna beamwidth is required (from 33° to 40°) [47–49], [P3]. Naturally, the importance of the selection of correct antenna beamwidth increases with higher order sectoring.

In this chapter, the impact of antenna beamwidth (or more generally, sector overlap) on the WCDMA system capacity is addressed with different degree of coverage overlap. The presented results here are extended from the ones published in [P3]. Fundamentally, they differ only in the sense that in the results presented here, 19 base station hexagonal grid configuration was used instead of 10 base station configuration.

### 3.3.1 Sector Overlap Index

The sector overlap index ($SOI$) is defined by the area that is covered by the half-power beamwidth of all sector antennas belonging to a site:

$$SOI = \frac{\textit{angle covered by } \theta_{-3dB}}{360^\circ} \tag{3.2}$$

where *angle covered by* $\theta_{-3dB}$ is the fractional angle of 360° covered by $\theta_{-3dB}$ antenna horizontal beamwidths. Fig. 3.6 provides an example how different antenna horizontal beamwidths 'occupy' a whole circular area if the site is deployed in a 3-sectored manner with 45° antennas or 65° antennas. As seen from Fig. 3.6, the 'switching point' between sectors is at the level of 20 dB and 10 dB with respect to antenna gain in the main beam direction, respectively. As an example, the corresponding $SOI$ for these configurations is 0.375 and 0.54.

**Table 3.3** The number of served users per site with 95% service probability target in different 3-sectored and 6-sectored configurations.

| Site spacing / antenna height | Beamwidth | | | | | |
|---|---|---|---|---|---|---|
| | 3-sectored | | | 6-sectored | | |
| | $45^\circ$ | $65^\circ$ | $90^\circ$ | $33^\circ$ | $45^\circ$ | $65^\circ$ |
| 1.5 km/25 m | 161 | 164 | 155 | 312 | 290 | 225 |
| 1.5 km/45 m | 125 | 115 | 107 | 225 | 210 | 165 |
| 2.0 km/25 m | 160 | 165 | 156 | 320 | 305 | 240 |
| 2.0 km/45 m | 155 | 155 | 140 | 300 | 245 | 218 |
| 2.5 km/25 m | 155 | 160 | 150 | 310 | 280 | 225 |
| 2.5 km/45 m | 155 | 155 | 145 | 305 | 260 | 223 |

### 3.3.2 Optimum Antenna Beamwidths

Table 3.3 presents the achievable system capacities (served users per site) with a 95% service probability target for different configurations. For the 3-sectored configurations, the observed capacity values are moderately equal within the range of simulated antenna beamwidths. In most of the cases, the $65^\circ$ antenna results in the highest capacity, but only with a marginal difference to the $45^\circ$ beamwidth. Actually, for higher degree of coverage overlap, the capacity with $45^\circ$ beamwidth is the same (or even higher) than the system capacity with $65^\circ$ beamwidth. Hence, the results indicate that the importance of the selection of antenna beamwidth becomes more crucial if coverage overlap is increased. Moreover, the results indicate that coverage overlap and sector overlap have to be optimized simultaneously.

The system capacity values for different network configurations can be compared in terms of sector overlap. Fig. 3.7 yields that with 25 m antenna height, $SOI$ between 0.5 and 0.6 results in the optimum system capacity. However, with 45 m antenna heights (equal to higher $COI$), the optimum $SOI < 0.5$. Moreover, with 1.5 km and 45 m configuration, the optimum does not even exist within the range of simulated antenna beamwidths. Hence, it seems that if the $COI$ is for some reason higher, the optimum sector overlap is smaller. Note, however, that these results do not yet include the impact of downtilting.

For the 6-sectored configurations, the selection of antenna beamwidth is more crucial in the whole range of selected antenna beamwidths (Table 3.3). The $33^\circ$ antenna results in the highest capacity values irrespective of the network configuration. Whereas in the 3-sectored configurations, the achieved capacity enhancements vary from 6% to 17% between the best and the worst antenna beamwidth, the corresponding capacity enhancements of 35% or higher are observed with the 6-sectored configuration. Clearly, the selection of antenna beamwidth becomes more vital among higher order sectoring. In terms of $SOI$, it seems that the optimum beamwidth for

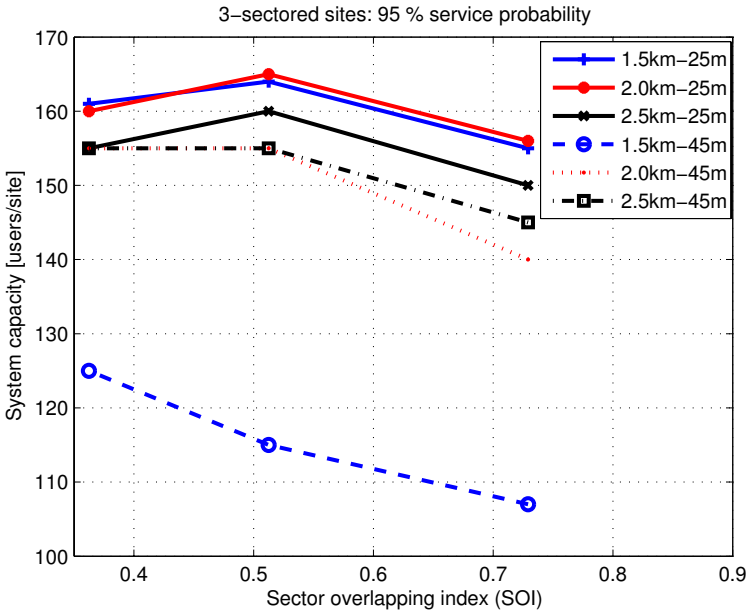


**Figure 3.7** Sector overlap for 3-sectored sites with $65°/6°$ antennas.

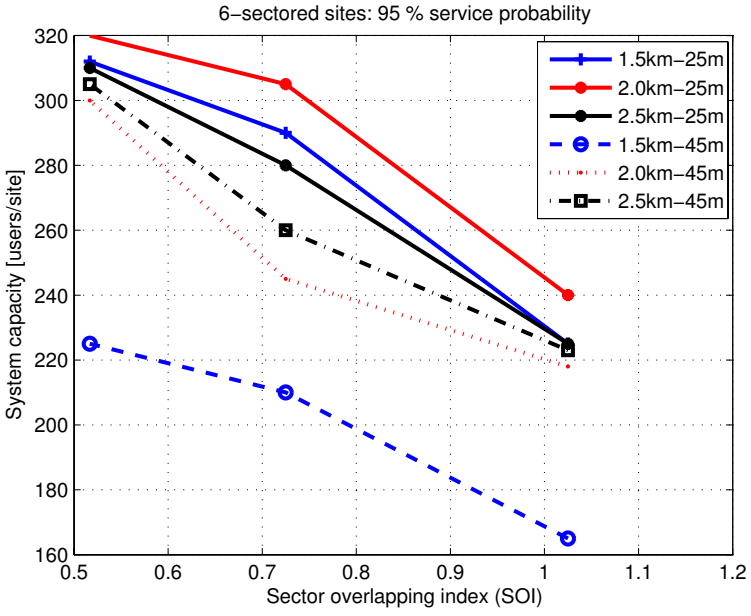


**Figure 3.8** Sector overlap for 6-sectored sites with $33°/6°$ antennas.

6-sectored sites would be even lower than $33^\circ$ (Fig. 3.8).

**Conclusions**

Sectoring obviously improves the system capacity. However, the evolution strategy for sectoring plays an important role for the final sectoring efficiency. For instance, maintaining $65^\circ$ beamwidth also in the 6-sectored configuration results in a capacity gain close to 40% between the 6-sectored and 3-sectored configurations. In contrast, sectoring efficiency can be increased up to 95% if antennas are changed to $33^\circ$ beamwidth (without downtilt). Thus, the achievable sectoring gain in capacity (between 6-sectored $33^\circ$ and 3-sectored $65^\circ$ configuration) can be around 1.8 and 1.95—slightly depending on the network configuration.

Moreover, an optimum $SOI$ seems to locate around 0.5, and seems to be connected with coverage overlap (index). The sensitivity of system capacity with respect to $SOI$ is naturally higher (approximately twice) in a 6-sectored network due to double number of overlap sectors. Hence, further analysis should be performed in order to find an optimum $SOI$ as a function of $COI$.

## 3.4 Antenna Downtilt

Antenna downtilt comprises the final optimization method of radio network topology. With antenna downtilt, the vertical radiation pattern is directed towards the ground in order to control the radiation towards other cells. In general, the impact of antenna downtilt on system capacity is widely known for macrocellular [37, 49, 55–64], [P1], [P5] as well as for microcellular environments [65–67].

With mechanical downtilt (MDT), the antenna element is physically directed towards the ground [59]. Naturally, the areas near the base station experience better signal level due to the fact that the antenna main lobe is more precisely directed towards the intended dominance (serving) area. However, the effective downtilt angle corresponds to the physical one only exactly in the main lobe direction, and decreases as a function of horizontal direction in such a way that the antenna radiation pattern is not downtilted at all in the side lobe direction [59]. Nevertheless, interference towards other cells is reduced mostly in the main lobe direction, which provides capacity enhancements in the downlink in GSM [60] and in WCDMA [56], [P1]. In the uplink, the capacity enhancement is typically smaller, as observed in [P5]. Naturally, higher capacity gain in the downlink can be observed with larger coverage overlap [P1].

Antenna electrical downtilt (EDT) is carried out by adjusting the relative phases of antenna elements of an antenna array in such a way that the radiation pattern can be downtilted uniformly in all horizontal directions [68]. Changing the relative phases of different antenna elements slightly changes the vertical radiation pattern depending on the chosen EDT angle (i.e. depending on the relative phase differences between different antenna elements). By using EDT, the achievable downlink capacity gain is slightly higher than with MDT [P1].

The fundamental differences between MDT and EDT are seen in the horizontal

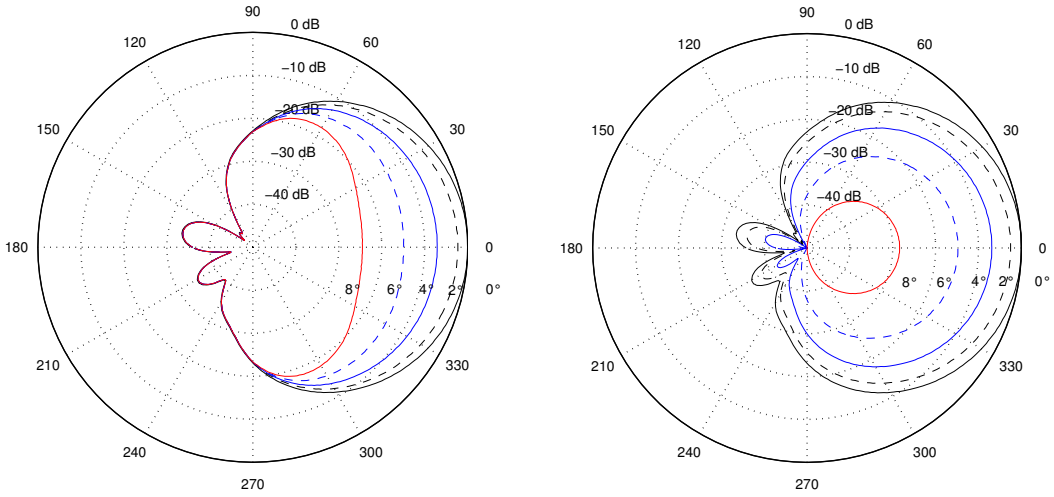


(a) Mechanical downtilt.

(b) Electrical downtilt.

**Figure 3.9** The impact of antenna (a) mechanical and (b) electrical downtilt on the horizontal (azimuthal) radiation pattern in the horizontal plane. Antenna gain is normalized to zero and the scale is in decibels. The 'uptilt' of back lobe direction for mechanical downtilt is not illustrated. [P1]

radiation patterns if antennas are downtilted (Fig. 3.9). The relative widening of the horizontal radiation pattern is illustrated in Fig. 3.9(a) for a horizontally $65°$ and vertically $6°$ wide antenna beam as a function of increasing downtilt angle. The reduction of the antenna gain towards the boresight, e.g. with an $8°$ downtilt angle, is as large as 25 dB, whereas towards a $60°$ angle the reduction is less than 10 dB. In contrast, Fig. 3.9(b) illustrates the behavior of the horizontal radiation pattern for $65°$ and vertically $6°$ with EDT. It reduces radiation efficiently also towards the adjacent sectors, since all directions are downtilted uniformly. However, the coverage in the side lobe direction reduces rapidly as well, which lowers the network performance if antennas are downtilted excessively.

As the downtilt angle increases (with MDT and EDT), the soft handover (SHO) probability in the cell border areas decreases [2, 55]. However, in MDT, the relative widening of the horizontal radiation pattern increases the overlap between adjacent sectors, which makes softer handovers (SfHO) more attractive [56], [P1]. This increase of softer handovers as a function of downtilt angle depends on sector overlap (i.e. sectoring and antenna horizontal beamwidth).

In conclusion, utilization of EDT antennas might become more attractive due to better ability to change the tilt angle remotely or automatically. This is actually the idea in remote-controlled electrical tilt (RET) concept, or, continuously adjustable electrical downtilt (CAEDT). By using a sophisticated control mechanism (or system), tilt angles can be changed remotely even without any site visit [62]. Moreover, the usage of RET facilitates significantly the effort required for antenna downtilt optimization. A simple and automatic algorithm could be deployed in order to further automate the optimization process as in the CAEDT concept [69]. The need for a

common interface for base station equipment to support RET has also been recognized within the 3GPP specification body, which is currently specifying RET concept for the Release 6 [70].

The latest research results have indicated the potential capacity gains that could be achieved by utilizing remote electrical downtilt. In [71], an optimum downtilt angle, which was evaluated based on the minimization of uplink transmit power, was observed to change even with an homogenous traffic distribution according to traffic load. In [72], the idea was extended to include the impact of non-homogeneous traffic distribution. Moreover, with simultaneous usage of RET and pilot power adjustment, capacity gain was achieved: mainly through traffic load balancing. In [73], a method for load balancing with tilt angle control was presented. The tilt angle optimization criterion was based on the minimization of uplink load for a cluster of three cells. Achieved capacity gains were approximately 20-30% with respect to constant, network-wide tilt angle.However, as all these methods were based on the uplink, a downlink assessment would still be required.

In this chapter, the impact of downtilt in WCDMA is covered with system level simulations [P1] and measurements [P4]. Moreover, a feasibility study is provided to assess the need for rapid change of the downtilt angle due to change in traffic conditions [P5].

### 3.4.1 Antenna Downtilt Simulations

#### Optimum Downtilt Angles

The simulation parameters and environment for achieving the following results are described in detail in [P1]. More detailed description of the definition method of optimum downtilt angle (ODA) can be found from [55]. The massive simulation campaign was targeted to solve the impact of

- coverage overlap (site spacing and antenna height)
- antenna vertical radiation pattern (beamwidth)
- downtilt scheme (MDT and EDT)
- sectoring (3-sectored and 6-sectored)
- service type (traffic mix)

on the optimum downtilt angle of a WCDMA antenna in macrocellular suburban environment, and also on the performance of WCDMA network in terms of downlink capacity. The simulation methodology was that all antennas in the network were downtilted by the same amount, and the optimum downtilt angle was then derived as a function of the items listed above. In order to avoid confusion and misunderstandings, [P1] did not propose utilization of the same downtilt angle for each antenna, but it was targeted to find an optimum downtilt angle through an averaging process.

Table 3.4 gathers optimum downtilt angles (ODA) for simulated site and antenna configurations for a macrocellular suburban environment. The variation of optimum

**Table 3.4** Optimum downtilt angles for mechanically and electrically downtilted antennas for all simulated site and antenna configurations. Evaluation of an optimum downtilt angle is based on a simple algorithm that utilizes the simulation results with two different traffic loads. [P1]

| Site spacing | Antenna height | EDT 3-sec 6 | EDT 3-sec 12 | EDT 6-sec 6 | MDT 3-sec 6 | MDT 3-sec 12 | MDT 6-sec 6 |
|---|---|---|---|---|---|---|---|
| 1.5 km | 25 m | 5.1° | 7.3° | 5.4° | 5.7° | 5.9° | 4.9° |
| | 35 m | 6.1° | 9.1° | 6.3° | 7.3° | 8.1° | 5.9° |
| | 45 m | 7.1° | 10.3° | 7.1° | 8.1° | 9.1° | 7.0° |
| 2.0 km | 25 m | 4.3° | 5.6° | 3.8° | 5.1° | 4.3° | 3.8° |
| | 35 m | 5.8° | 7.9° | 5.1° | 6.7° | 7.5° | 4.8° |
| | 45 m | 6.3° | 9.3° | 6.1° | 6.9° | 8.2° | 5.9° |
| 2.5 km | 25 m | 4.5° | 5.2° | 4.6° | 5.1° | 3.4° | 3.7° |
| | 35 m | 5.4° | 7.6° | 5.3° | 6.1° | 4.4° | 4.5° |
| | 45 m | 5.9° | 8.3° | 5.7° | 6.9° | 6.9° | 5.8° |

downtilt angles within the simulated configurations is from 3.4° up to 10.3°. The optimum downtilt angles for the 3-sectored configurations with 6° and 12° vertical antenna beamwidth varies between 4.3°–8.1° and 3.5°–10°, respectively. One reason for lower ODAs for 12° beamwidth is the interference conditions (i.e. lower coverage overlap) that differ due to lower antenna gain. Moreover, wider vertical spread of antenna pattern makes the use of downtilt not so beneficial. For 6-sectored configurations, the observed ODAs (4°–7°) are very close to the values of the corresponding 3-sectored configurations.

### An Empirical Equation for Selection of Downtilt Angle

Based on the simulated optimum downtilt angles, an empirical equation was derived [P1]:

$$\nu_{opt} = 3[ln(h_{bs}) - d_{dom}^{0.8}]log_{10}(\theta_{-3\ dB}^{ver}) \tag{3.3}$$

Eq. (3.3) relates the topological factors such as the base station antenna height[12] ($h_{bs}$ in meters), the intended length of the sector dominance area ($d$ in kilometers), and also the half-power vertical beamwidth ($\theta_{-3dB}$ in degrees). The equation was derived with a simple curve fitting method. It provides a zero mean error with 0.5°

[12]Note that in an undulating environment, $h_{bs}$ has to be proportioned to the effective base station antenna height.

standard deviation with respect to simulated optimum downtilt angles for all simulated scenarios. As the error of (3.3) is rather small, it could be embedded into a radio network planning tool. Thereafter, the tool would automatically provide a suggestion of downtilt angle for a planner based on the information of antenna vertical beamwidth, antenna height (also ground height level could be utilized), and expected dominance area of a particular sector. Hence, it could provide an initial downtilt angle setting for each antenna depending on the sector configuration.

#### Identification of Excessive Downtilt Angles

Another topic addressed in [P1] was the identification of an excessive downtilt angle with two different downtilt schemes. With EDT due to uniform reduction of the horizontal radiation pattern, a too large EDT angle could be identified by larger proportion of mobiles with higher uplink TX (transmit) power (or large uplink TX power before the cell edges). Naturally, depending on the actual power budget and selected services, it can be either uplink or downlink that limits the coverage. In contrast, the increase of SfHO connections due to effective widening of horizontal beamwidth affects most on the downlink capacity degradation with too high MDT angles.

#### Expected Capacity Gains

Tables 3.5 and 3.6 provide the capacity gains and the corresponding maximum DL throughputs with selected network and antenna configurations for EDT and MDT. The downlink capacity gains vary from 0 % up to 60 %, depending heavily on the network configuration [P1].

Generally, the capacity gain becomes larger if the coverage overlap increases, i.e. either the antenna height increases or the site spacing decreases. Considering an urban macrocellular environment, where the network is typically very dense due to requirements of higher coverage probabilities and capacity, the utilization of antenna downtilt is mandatory. An interesting observation in [P1] was the increase of absolute sector capacity as a function of higher antenna position. Geometrically thinking, it is obvious that the achievable capacity gain is higher with higher antenna position. This is due to better ability to aim the antenna beam towards the intended dominance area. However, a higher antenna position requires more precise adjustment of the antenna downtilt angle. Hence, from the radio network planning point of view, placing antennas higher and using larger downtilt angles provides better system capacity. This planning approach might not be applicable for an urban network if the antennas are placed on the top of buildings, since the probability of distant interferers easily increases with higher antenna positions. The achieved isolation between cells with rooftop antenna installation could be lost, and thus in practice the net effect could be close to zero.

#### SHO Probabilities

An example of reduction of soft handover (SHO) probability is shown in Fig. 3.10 for 3-sectored 1.5 km configurations (25 m and 45 m antenna heights) as a function

**Table 3.5** Capacity gains for electrical downtilt. Maximum sector throughput [kbps] in the downlink with optimum downtilt angles and corresponding capacity gains with respect to non-tilted scenario for all simulated network configurations. The maximum capacity values are based on 0.5 average DL load. [P1]

| Site spacing | Antenna height | EDT 3-sec 6 | EDT 3-sec 12 | EDT 6-sec 6 |
|---|---|---|---|---|
| 1.5 km | 25 m | 494 (18.1%) | 472 (2.8%) | 492 (27.5%) |
| | 35 m | 510 (33.5%) | 484 (12.1%) | 504 (43.8%) |
| | 45 m | 526 (48.4%) | 493 (18.7%) | 522 (58.1%) |
| 2.0 km | 25 m | 457 (8.0%) | 440 (1.4%) | 438 (9.4%) |
| | 35 m | 496 (17.8%) | 457 (4.3%) | 468 (22.5%) |
| | 45 m | 499 (27.7%) | 472 (8.0%) | 500 (37.5%) |
| 2.5 km | 25 m | 451 (5.3%) | 423 (0.8%) | 462 (6.3%) |
| | 35 m | 480 (9.9%) | 433 (2.1%) | 482 (16.9%) |
| | 45 m | 488 (20.4%) | 440 (2.6%) | 504 (31.3%) |

**Table 3.6** Capacity gains for mechanical downtilt. [P1]

| Site spacing | Antenna height | MDT 3-sec 6 | MDT 3-sec 12 | MDT 6-sec 6 |
|---|---|---|---|---|
| 1.5 km | 25 m | 489 (17.0%) | 466 (1.6%) | 458 (18.8%) |
| | 35 m | 500 (30.8%) | 475 (9.9%) | 474 (35.3%) |
| | 45 m | 516 (45.6%) | 479 (15.4%) | 480 (45.5%) |
| 2.0 km | 25 m | 459 (8.5%) | 440 (1.4%) | 438 (9.3%) |
| | 35 m | 494 (17.4%) | 453 (3.3%) | 458 (20.0%) |
| | 45 m | 495 (26.8%) | 466 (6.6%) | 471 (29.4%) |
| 2.5 km | 25 m | 451 (5.3%) | 424 (1.1%) | 456 (5.0%) |
| | 35 m | 487 (11.5%) | 433 (2.0%) | 464 (12.5%) |
| | 45 m | 479 (18.3%) | 437 (2.0%) | 463 (20.6%) |

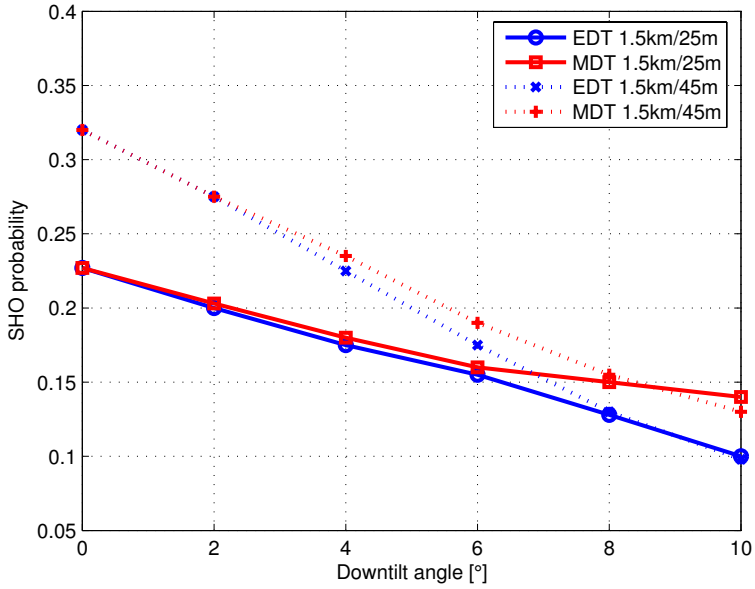


**Figure 3.10** An example of SHO reduction with EDT and MDT downtilt schemes with different antenna heights of 3-sectored sites and antenna vertical beamwidth of 6°.

of EDT and MDT angle. Clearly, EDT is able to reduce the SHO probability more efficiently due to more efficient antenna pattern control. This is partly the reason for higher capacity gains for EDT. Moreover, it was observed that with optimum downtilt angles, SHO probabilities were systematically around 17%, which, on the other hand, indicates a common optimum coverage overlap index for optimum downtilt angles. Naturally, the expected SHO probability with optimum downtilt angle depends on the SHO window setting. Nevertheless, the reduction of SHO connections is one reason for improved system capacity in the downlink due to downtilt.

### Conclusions

The simulation results show the importance of downtilt on the downlink capacity in a WCDMA network. The gain of downtilt is due to the reduction of other-cell interference and SHO probability. The downlink capacity gains with simulated network topologies varied between 0% and 60%. The obtained optimum downtilt angles and the empirical equation provide an initial downtilt angle for suburban WCDMA antennas.

As shown in [P1], the sensitivity of the selection of downtilt angle increases generally as a function of higher antenna position and shorter site spacing, i.e. the more coverage overlap, the higher is the sensitivity. As expected, also the required downtilt angle for vertically wider antenna beamwidth is higher. However, the relation seems not to be linear.

In general, the selection of downtilt angles for EDT and MDT can be the same. However, larger MDT angles should be avoided due to larger sector overlap that introduces an increased amount of SfHO overhead. Moreover, the utilization of EDT provides a slightly better system capacity than MDT, but only with marginal differences. Finally, as shown in [P1], the impact on traffic layer (indoor vs. outdoor users and service type) on the optimum downtilt angle is rather small, and hence its impact of the downtilt angle does not have to be considered.

As the cell orthogonality factor was a constant in the simulations, the impact of downtilt on orthogonality was not assessed. This, however, could be another source of downlink capacity gain. An improvement could be observed due to decreased delay spread values [28,74].

### 3.4.2 Measured Performance of Mechanical Downtilt

This section provides the measurement results of mechanical downtilt [P4]. The measurements were conducted in a network that included different EDT and MDT angles. Afterwards, all MDT angles[13] were removed (i.e. antennas were directed to their boresight), and similar measurements were repeated. The measurements were firstly conducted by measuring a route with two test mobiles, and estimating the downlink average cell capacity with the method described in [P7]. Secondly, in addition to these test mobiles, two static interfering mobiles were placed in order to increase the impact of other-cell interference.

#### Capacity Analysis

Tables 3.7 and 3.8 show the averaged measurement results for downlink throughput and $E_c/N_0$ (per mobile) for both network configurations (denoted as with MDT and without MDT). The average throughput in the MDT configuration without interferers is 336 kbps over the whole measurement route. The corresponding average $E_c/N_0$ over the whole measurement route was $-5.63$ dB. Based on the capacity estimation from the measured $E_c/N_0$ and average throughput values [P7], the average cell capacity within the measurement route would correspond to 880 kbps[14] with 3 dB allowed noise rise (i.e. 0.5 downlink load). Interestingly, without MDT, the measured throughput was higher (402 kbps). However, the average $E_c/N_0$ level was correspondingly lower ($-6.00$ dB). This results in average cell capacity of 820 kbps. In this particular measurement setup, where basically no other-cell interference was present (assuming that the test mobiles located in the same car are most of the time connected to the same cell), the capacity gain from downtilt is not significant (7 %). Note also that the capacity estimates depend strictly on the selected measurement route (e.g. average distance to base station, etc.). Therefore, evaluated average cell capacity is comparable only with exactly the same measurement route. However, as the measurement route was the same for both configurations, the evaluated average

[13]The existing MDT angles in the measured part of the network were significant, so that difference should be observed.

[14]The capacity analysis was performed by assuming the following parameter values in the downlink load equation: bit rate (R) = 384 kbps, service activity (v) = 1, and orthogonality factor ($\alpha$) = 0.7.

**Table 3.7** Measurement results without mechanical downtilt. [P4]

| | | No interferers | With interferers |
|---|---|---|---|
| Test mobiles | Throughput [kbps] | 184/217 | 174/188 |
| | $E_c/N_0$ [dB] | $-5.91/-6.08$ | $-6.78/-6.64$ |
| Interfering mobiles | Throughput [kbps] | — | 201/152 |
| | $E_c/N_0$ [dB] | — | $-7.89/-7.71$ |
| Total throughput [kbps] | | 401 | 722 |

**Table 3.8** Measurement results with mechanical downtilt. [P4]

| | | No interferers | With interferers |
|---|---|---|---|
| Test mobiles | Throughput [kbps] | 201/135 | 204/154 |
| | $E_c/N_0$ [dB] | $-5.63/-5.63$ | $-5.79/-6.20$ |
| Interfering mobiles | Throughput [kbps] | — | 191/199 |
| | $E_c/N_0$ [dB] | — | $-7.35/-5.94$ |
| Total throughput [kbps] | | 336 | 748 |

cell capacities are comparable to each other.

With the presence of interfering (static) mobiles, the configuration with MDT is able to provide on average 748 kbps. Conversely, in the configuration without MDT, the average throughput is 722 kbps. The average $E_c/N_0$ values of all four mobiles were $-6.32$ dB and $-7.25$ dB with and without MDT, respectively. By applying the capacity evaluation method, the corresponding estimates of cell capacities are 1000 kbps and 830 kbps. This difference turns out to be 20 % in the downlink capacity. These results clearly indicate how the impact of MDT becomes more crucial when other-cell interference is present. Moreover, evaluated capacity gain matches rather accurately to the observed outcomes from the simulations in [P1] and [56].

### SHO Probabilities

Table 3.9 shows the mean sizes of active set (AS) and SHO probability within the measurement route (averaged also for both mobiles) as well as for interfering mobiles. Without MDT, the active set size is approximately 1.20 with a SHO probability (including softer handovers) of nearly 20%. Conversely, the mean size of AS with MDT is approximately 1.15, and the corresponding SHO probability around 14%. This implies that over the measurement route, the reduction of SHO probability is around 25%, which corresponds roughly to the earlier understanding based on simulations [56], [P1]. The most visible changes in the mean AS size and in the SHO probabilities due to the removal of MDT angles are observed in the location of inter-

**Table 3.9** Average AS sizes and SHO (including SfHO) probabilities without / with mechanical downtilt. [P4]

| | | No interferers | With interferers |
|---|---|---|---|
| Test mobiles | AS size | 1.22 / 1.15 | 1.20 / 1.16 |
| | SHO probability [%] | 19.9 / 13.5 | 18.2 / 14.0 |
| Interfering mobiles | AS size | — | 1.50 / 1.22 |
| | SHO probability [%] | — | 44.0 / 22.4 |

ferers. In this location, the removal of MDT angles nearly doubles the probability of SHO and more than doubles the mean AS size. Increased coverage overlap due to inadequate downtilt angles is realized as increased SHO probability that consumes more downlink capacity.

### 3.4.3 Possibilities for Utilization of RET

This subsection targets solving the impact of a change in geographical traffic load distribution on the optimum downtilt angle [P5]. In other words, the aim is to solve whether there is need for remote electrical tilting (RET) that reacts to changes of user distribution within a cell by changing the downtilt angle. This approach differs from load balancing which requires the simultaneous monitoring and controlling of several cells (i.e. a cluster of cells). In the following, the analysis is based on simulations where the traffic in each cell was changed similarly. Firstly, the traffic distribution was changed from being homogenous to concentrating closer to the base station, and secondly, to concentrate closer to cell edge. With all traffic distributions, the network was simulated with different downtilt angles from $0^\circ$ to $18^\circ$ with steps of $2^\circ$.

Figs. 3.11-3.13 represent the attained average service probabilities and average cell capacities for simulated downtilt angles with different traffic distributions. Moreover, the service probabilities are provided with different traffic loads (i.e. low, medium and high loads). The simulation results reveal that the range of optimum downtilt angle in the corresponding network topology (1.5 km site spacing and 25 m antenna height) changes from $6^\circ$ to $14^\circ$, if the optimum downtilt angle is defined from service probability (Figs. 3.11(a)-3.13(a)). However, monitoring the situation from the uplink or downlink capacity point of view, the optimum downtilt angle is always between $8^\circ$ and $10^\circ$ (Figs. 3.11(b)-3.13(b)). Moreover, the optimum downtilt angle seems to be almost independent of the traffic load distribution. With the simulated traffic load distributions, the attainable downlink capacity gains vary between 10% and 90%. The corresponding gain in the uplink capacity varies from 5% to 9%.

Using an $8^\circ$ downtilt angle for all simulated traffic distributions would result in a maximum 1% degradation in service probability (due to coverage constraints), and an approximately 5% degradation in downlink capacity in the worst scenario (users close to BS) with respect to optimum downtilt angle. Hence, the simulation

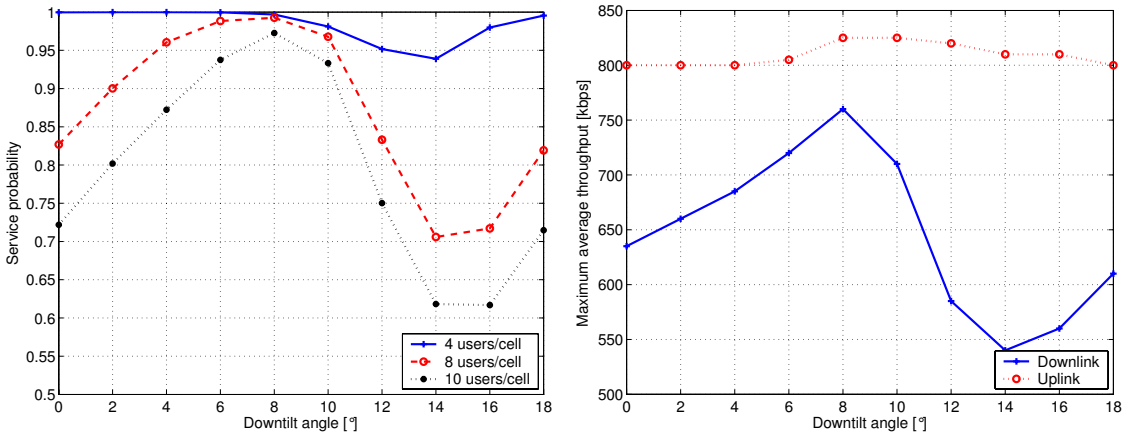


(a) (b)

**Figure 3.11** Simulation results with homogenous traffic distribution. (a) Service probability with different offered traffic loads, and (b) maximum average capacities in downlink and uplink directions. Uplink noise rise threshold for capacity analysis was 3 dB. [P5]

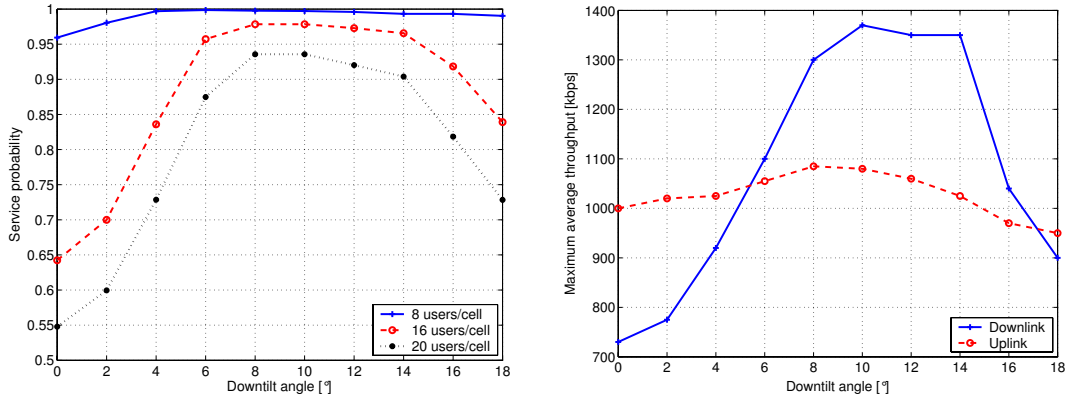


(a) (b)

**Figure 3.12** Simulation results with a user distribution close to base stations. (a) Service probability with different offered traffic loads, and (b) maximum average capacities in downlink and uplink directions. Uplink noise rise threshold for capacity analysis was 4 dB. [P5]

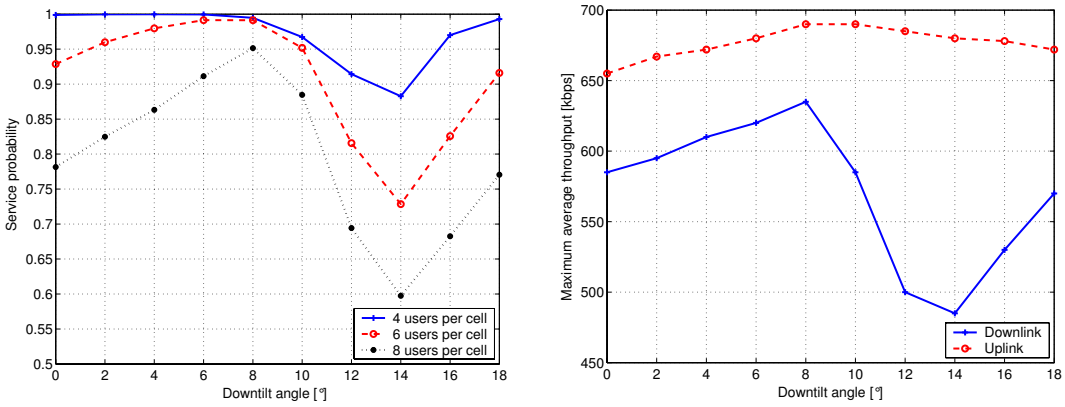


(a) (b)

**Figure 3.13** Simulation results with a user distribution close to cell edge. (a) Service probability with different offered traffic loads, and (b) maximum average capacities in downlink and uplink directions. Uplink noise rise threshold for capacity analysis was 2.5 dB. [P5]

results clearly indicate that geometrical traffic load distribution does not affect the required downtilt angle. However, it has to be noted that this does not exclude the usage of RET (or CAEDT), but proposes to use it only for slow rate adjustment to facilitate changes of tilt angles during network evolution and optimization process, or for load balancing. From a radio network planning point of view, it is strongly recommended to use RET, since the downtilt angles are heavily sector configuration and environment specific. Moreover, by using RET, the final adjustment of tilt angles can be performed on a cell-by-cell basis in order to maximize system capacity and functionality from network topology point of view. Finally, it has to be noted that geographical traffic load variations might have a larger impact, if they changed unequally between adjacent cells.

## 3.5 Suppression of Pilot Polluted Areas

In the WCDMA system, mobiles in the network are able to identify different base station sectors according to their primary common pilot channel (P-CPICH) [3]. P-CPICH is send by all the base station stations; typically with a fixed power. P-CPICH signal is a predefined symbol sequence and it is used as a phase reference for the other downlink common physical channels. Moreover, it is considered as a pure physical channel, since it carries no data. P-CPICH is used for handover decisions, cell selections and reselections. Moreover, secondary-CPICH (S-CPICH) can be used to aid in channel estimation in the context of adaptive antenna solutions [75]. In the following analysis, the impact of S-CPICH is not considered. [2, 3]

*Pilot pollution*[15] is observed in areas in which there are too many P-CPICH signals (different P-CPICH signals or their multipath components) received at the mobile

[15]Fundamentally, pilot pollution is a fraction of the total other cell interference, and not any new source

station's RAKE receiver than it is capable of processing, or none of the received P-CPICH signals is dominant enough [2]. Each cell which is heard by the mobile will practically increase the interference level in the downlink. Thus, hearing unnecessary pilot signals will reduce the received energy per chip over the power density ($E_c/N_0$) from the serving cell; in other words, pilot pollution reduces the quality of an existing connection. In order to avoid pilot polluted areas, the cell dominance areas should be as clear as possible and unnecessary P-CPICH signals should not be heard. However, pilot pollution cannot be totally avoided with traditional radio network planning methods due to the non-homogeneous propagation environment and requirement for coverage overlap. [P6]

**Reduction of Pilot Pollution**

In general, pilot pollution interference can be reduced by optimizing the pilot powers automatically in such a manner that required coverage thresholds are still exceeded. By a simple P-CPICH power controlling method, the air interface performance of the WCDMA network can be slightly enhanced [77, 78]. A simple tuning of P-CPICH power is not enough to increase the system capacity sufficiently, as the interference radiation (or, in other words, the other-to-own cell interference ratio) is not reduced at all, and hence the gain in the system capacity is observed only through different power allocation strategy, not optimization of radio network topology. Thus, tuning of P-CPICH should always be connected with the adjustment of downtilt angles [79]. Implementation of repeaters can also be seen as a method for reducing pilot pollution interference in CDMA-based networks [80], [P10]. Clear dominance areas (meaning smaller amounts of pilot pollution) could also make a SHO process more reliable, as discussed in [81].

There are also different, non-topological methods for reducing pilot pollution. However, note that the received interference of other P-CPICH signals is only a fraction of the total received interference, and hence, the potential gains from these schemes are typically smaller. Ultimately, the best solution would be to use interference cancellation (IC) at the mobile station at the expense of increased complexity and power consumption of the mobile station [9]. In [82], a method is proposed for detecting pilot polluted areas without considering the impact of antenna configuration. In contrast, the method in [83] relies on the implementation of multicarrier technology.

This section provides an outlook to the impact of base station antenna configuration on the level of pilot pollution. Firstly, 3-sectored configuration and different 6-sectored antenna configurations are assessed through simulations [P6], and secondly, measurement results providing a more practical view are shown for a 3-sectored network [P4]. More extensive analysis of the impact of pilot pollution on the SHO algorithm performance is provided in [84].

---

of interference. Hence, minimization of pilot pollution interference is the same as minimization of other cell interference. However, pilot signal cancellation (e.g. [76]) can be performed, since the P-CPICH signal sequences are known, and hence their interference can be mitigated by using interference cancellation techniques.

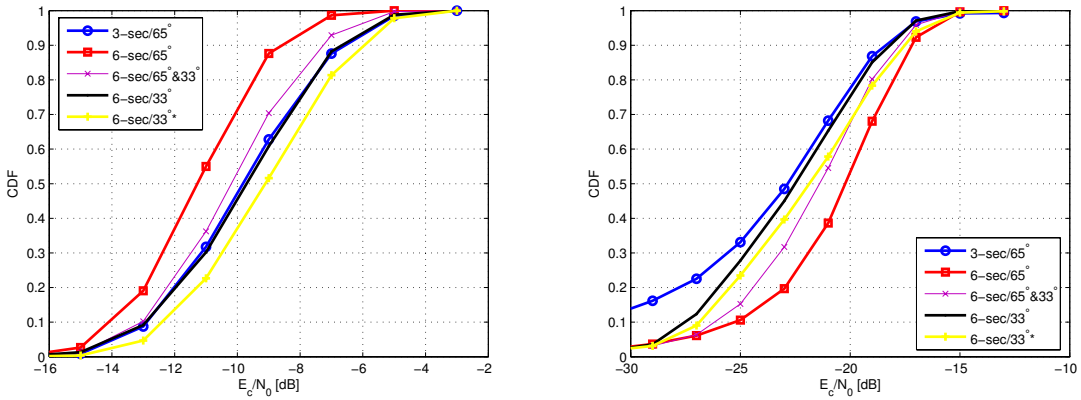


(a) The distribution of dominant P-CPICH $E_c/N_0$. (b) The distribution of the fourth strongest $E_c/N_0$.

**Figure 3.14** CDFs of (a) the dominant (strongest) and (b) the fourth strongest $E_c/N_0$ signals with 3-sectored configuration and different 6-sectored antenna configurations. [P6]

### 3.5.1 Assessment through Simulations

The P-CPICH $E_c/N_0$ statistics were gathered from the simulation conducted with roughly 50 % uplink and downlink loads and without downtilt [P6]. Fig. 3.14(a) shows the cumulative distribution function (CDF) of the level of the dominant $E_c/N_0$ with 3-sectored/$65°$ configuration and different 6-sectored antenna configurations. The 6-sectored configurations consisted of antenna configurations of $65°$ antennas, a hybrid solution with an equal amount of $65°$ and $33°$ antennas, one of $33°$ antennas, and the last one with $33°$* of the antennas of the first tier shifted by $30°$. With the 6-sectored/$33°$* configuration, 65% of the simulation area is covered by $E_c/N_0$ level above $-10$ dB, whereas with the worst configuration (6-sectored/$65°$) the corresponding value is 25%. Moreover, the results indicate that the selection of antenna directions slightly improves the reception level of dominant $E_c/N_0$.

The reception level of the fourth highest $E_c/N_0$ increases when higher order sectoring is applied (Fig 3.14(b)). However, suitable antenna solution can reduce the amount of pilot pollution to the level of lower order sectoring. The 6-sectored/$65°$ results in 50% of areas (or time) with $E_c/N_0$ higher than $-20$ dB. In contrast, by using $33°$ antennas, the corresponding percentage can be reduced to 25%.

The simulation results in [P6] clearly indicate the importance of antenna selection also for reducing the level of pilot pollution in WCDMA networks. However, even with sufficient downtilt and shifted antenna directions, a certain fraction of pilot polluted areas is still obtained in the network due to coverage overlap requirements. The impact of these areas can be reduced by planning those areas where the expected customer density is not so high. Moreover, different network layouts could be utilized in order to reduce the amount of pilot pollution [26, 85].

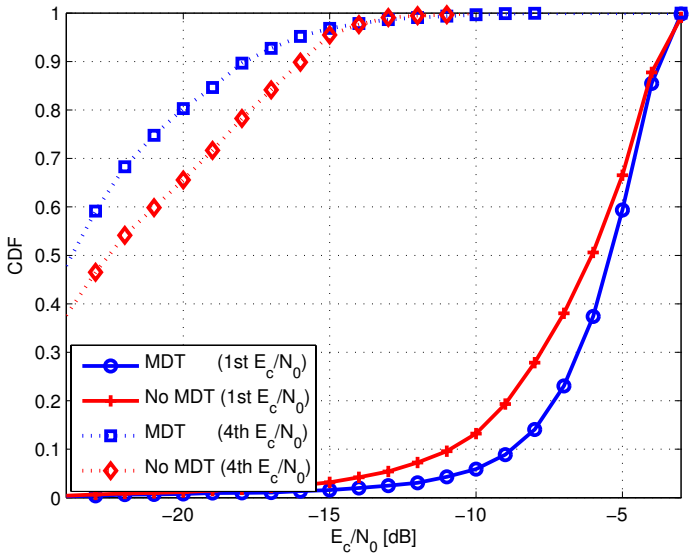


**Figure 3.15** CDF of the dominant and the fourth strongest P-CPICH $E_c/N_0$ with and without MDT. [P4]

### 3.5.2 MDT and Pilot Pollution in Measurements

The amount of pilot pollution in the network was also assessed through measurements [P4]. Fig. 3.15 shows the measured CDF with and without additional MDT angles. In the MDT configuration, the dominance areas (or simply the dominance) are clearer, as the level of the dominating (strongest) $E_c/N_0$ is better over the measurement route as without MDT. Moreover, the level of the fourth pilot is lower with MDT than without it. For example, $-20$ dB threshold exceeds 35% of the measurement time in the configuration without MDT, whereas the corresponding value for the MDT configuration is 20%.

A part of the low $E_c/N_0$ values are caused by so called 'late handovers', where a mobile does not change to the best cell or maintains a low $E_c/N_0$ sector in the active set, even though it should have made a handover to a stronger sector. This phenomenon was caused by the fact that four mobiles (with 384 kbps service request in the downlink) were used in the measurements. These 'late handovers' are caused by capacity limitations and by the resulting actions of admission control (AC). Hence, a part of topology planning also reflects on the functionality of RRM algorithms. Therefore, in an operational network, the network quality and the functionality of RRM algorithms are connected, and naturally the decisions of RRM algorithms depend on, e.g., interference levels defined by the quality of the plan.

**Table 3.10** Absolute P-CPICH coverage for two different thresholds and different deployment strategies for 6-sectored sites. [P2]

| Site type | Thresholds [dBm] | |
|---|---|---|
| | $-75$ | $-84$ |
| 3-sec/$65^\circ$ | 46.1 | 87.9 |
| 6-sec/$65^\circ$ | 61.9 | 91.5 |
| 6-sec/$65^\circ$& $33^\circ$ | 65.7 | 91.6 |
| 6-sec/$33^\circ$ | 64.9 | 90.7 |
| 6-sec/$33^\circ$* | 67.8 | 91.6 |

## 3.6 Topology Planning during Site Evolution

During an evolution from a 3-sectored to a 6-sectored WCDMA site, important topics to be tackled are changes in the coverage (i.e. RF footprint and dominance areas), system capacity, and finally, changes in the SHO and SfHO probabilities [P2]. This section targets providing observations of the changes during site evolution.

### Coverage

Absolute coverage can be improved by using sectoring. Coverage improvements can be explained logically with a higher number of sectors per site. If narrower antennas are utilized at the base station site, then the coverage improvement is also based on higher antenna gain in the main beam direction. The individual coverage areas of sector antennas also define dominance areas of the base station sectors, and hence also affect the locations of SHO areas.

Table 3.10 provides a comparison of the absolute P-CPICH coverage levels with different deployment strategies for 6-sectored sites. The reference 3-sectored network provides $-75$ dBm CPICH coverage for almost half of the network area[16]. All 6-sectored configurations are able to provide over 60% P-CPICH coverage probability. The maximum coverage can be provided with modified $33^\circ$ configuration. Thus, in addition to the low interference levels required for high throughputs in HSDPA (high speed downlink packet access), the absolute level of the coverage has to be high [9]. Therefore, 6-sectored sites might provide a more feasible deployment strategy when HSDPA is enabled.

### Capacity

The system capacity values of different 6-sectored site deployment strategies are shown in Table 3.11 with 98% service probability target. Clearly, the possible ca-

[16]Note that border effect slightly decreases the coverage probability. Also tilting would improve the absolute level of P-CPICH coverage probability.

**Table 3.11** System capacities and sectoring gains with different deployment strategies for 6-sectored sites.

| Site type | System capacity per site [users] | Sectoring gain [%] |
|---|---|---|
| 3-sec/65° | 98 | 0 |
| 6-sec/65° | 152 | 55 |
| 6-sec/65°& 33° | 173 | 77 |
| 6-sec/33° | 185 | 89 |
| 6-sec/33°* | 190 | 94 |

**Table 3.12** SHO and SfHO probabilities with different deployment strategies for 6-sectored sites. $SHO_{ADD}$ window 4 dB.

| Site type | SHO probability [%] | SfHO probability [%] |
|---|---|---|
| 3-sec/65° | 26.7 | 4.2 |
| 6-sec/65° | 23.0 | 22.8 |
| 6-sec/65°& 33° | 23.5 | 10.6 |
| 6-sec/33° | 23.8 | 3.8 |
| 6-sec/33°* | 23.8 | 3.7 |

pacity gain of sectoring is wasted by using 65° antennas (i.e. large sector overlap) at the base station sites. Moreover, by redirecting 33° antennas, an additional capacity gain of 3% can be achieved. This capacity gain corresponds to that achieved in [86].

### SHO and SfHO Probability

SHO and SfHO probability analysis is presented in Table 3.12. The simulations were run with 4 dB $SHO_{ADD}$ window and 33 dBm level of P-CPICH. During site evolution, the SHO probability remains approximately at the same level (or even decreases) when a site is updated to a 6-sectored one. Hence, the results indicate, that in site evolution, no additional capacity on Iub-interface (Node B $\leftrightarrow$ RNC) is needed from a SHO point of view, and only the nominal increase due to higher peak throughput has to be considered. These results also reveal that with 65° antennas in 6-sectored sites (or equivalently, with approximately 1.0 of sector overlap), the expected SfHO probability is higher than 20%. This is naturally the reason for lower system capacity values for sites with a higher degree of sector overlap.

**Downtilt Angles**

The results presented in Table 3.4 indicate that, regarding EDT, the optimum downtilt angles for 3-sectored network ($65°$) are mostly the same as for 6-sectored network ($33°$). If sites are deployed with $65°$ antennas, the situation might be different, as no simulations have been conducted with 6-sectored $65°$ configuration. However, special attention is needed with mechanical downtilt angles. If 3-sectored sites are deployed with high downtilt angles (e.g. $> 7°$), the resulting SfHO probabilities in 6-sectored sites would be higher, if higher MDT angles were configured also for additional sectors. However, the horizontal widening of antenna radiation pattern is highly dependent on the actual shape of the horizontal beam and also on sector overlap, and therefore the problem is also highly site-specific.

# CHAPTER 4

# Verification Methods of Topology

VERIFICATION of the quality of the radio network topology planning can be performed by using radio interface field measurements or system simulations of the actual plan[1]. Measuring the actual radio interface performance provides naturally the most reliable assessment of the quality of the network and its functionality. However, the analysis might not be applicable if the quality parameters are not known. Moreover, achieving statistically reliable measurement results requires several measurement rounds, and even then the achieved measurement results provide the assessment of the network only over the selected measurement route. Hence, the possibility for general conclusions of the network performance through measurements could be rather difficult. The radio interface system simulations provide another extremity of the performance assessment. Simulations are not as time-consuming as radio interface field measurements, but the selection of the simulation methodology (static or dynamic), setting up the network configuration, and other factors might increase the inaccuracy of the simulations.

This chapter provides a quality assessment method for the radio network topology that utilizes averaged measurement results over a cell to establish an estimate of the quality of the cell [P7]. In addition, an example of verification of the reliability of a static planning tool is provided for an urban environment [P8].

## 4.1 Topology Verification through Measurements

For cellular networks, verification of the network plan is very crucial in the network deployment phase. Operators need to be aware of the attainable capacity of the network prior to the commercial release [3]. In addition, a reliable and applicable verification of the changes in radio network topology during the optimization phase is also strongly required. This section introduces a method for mapping the quality of a cell with the aid of the average measured $E_c/N_0$ of a cell into $i_{DL}$ [P7]. Moreover, with a certain estimate of the propagation environment (namely in terms of average orthogonality factor), the average cell throughput can also be estimated with a given traffic mix.

[1]The quality of radio network can be also assessed analytically as discussed in Section 2.2.

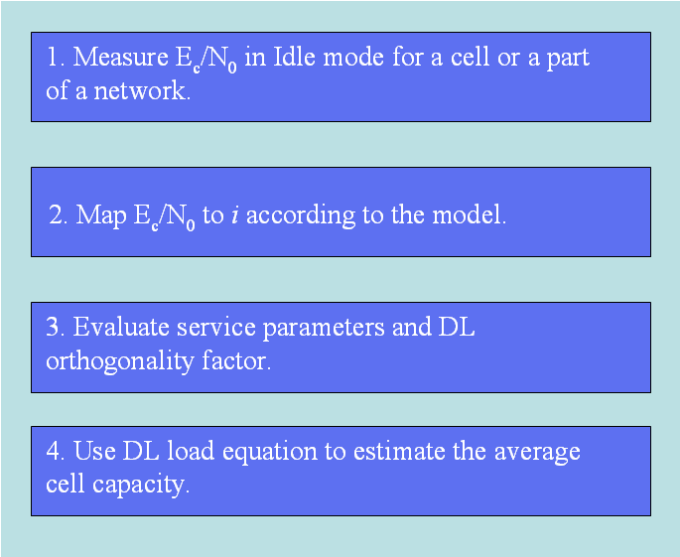


**Figure 4.1** The overall flow of the capacity estimation method. [P7]

### 4.1.1 Air Interface Capacity Estimation Method

The overall flow of the capacity estimation method is depicted in Fig. 4.1. The idea is to use the average measured idle mode $E_c/N_0$ over the cell area to establish an estimate of other-to-own-cell interference ratio ($i_{DL}$). Estimation of $i_{DL}$ is possible in the downlink already in an empty network, since downlink interference is present due to transmission of common channels [3]. The model for mapping $E_c/N_0$ to $i_{DL}$ in [P7] is rather simple and can be interpret in general form as:

$$i_{DL} = \frac{1}{10\log_{10}(\frac{P_{P-CPICH}}{P_{P-CPICH}+P_{CCCH}})} E_c/N_0[dB] - 1 \tag{4.1}$$

where $P_{P-CPICH}$ and $P_{CCCH}$ are the powers allocated for P-CPICH and other common channels (CCCH). For example, provided that the power allocation in a measured cell is equal between P-CPICH and other common channel (CCCH), the reference level $E_c/N_0$ would be $-3$ dB. This corresponds to a scenario without any other cell interference ($i_{DL}$=0) very close to the base station. In contrast, exactly between two cells, if the power allocation of common channels is the same, the reference $E_c/N_0$ is $-6$ dB, and $i_{DL}$=1, and so on. In practice, the most convenient way to determine the power allocation is to measure it very close to base station antenna so that the contribution of other-cell interference and noise is minimal. For a reliable estimation of a cell's $i_{DL}$, the common channel power allocation has to be known (or measured), and during the idle mode measurements, the network has to be empty (without any traffic). However, the mapping method can also be used for loaded cells if the average throughput during the $E_c/N_0$ measurements can be determined [P7]. For certain traffic service parameters and assumption of the orthogonality factor, the cell quality can be defined in terms of average throughput by using the standard load equation [9].

The final cell throughput estimate reflects to an equally loaded scenario and does not take into account the soft capacity. As the method relies on mapping of a cell capacity according to its average $E_c/N_0$, there should actually not be any coverage limitations. In practice, this means that RSCP should preferably be maintained above the level of $-100$ dBm in order to keep the contribution of thermal noise at minimum level. This way, the capacity estimation does not suffer from reductions of $E_c/N_0$ due to coverage restrictions.

### 4.1.2 Performance of Capacity Evaluation Method

Measurement results assessing the performance of idle mode $E_c/N_0$ mapping method are presented here. The presented figures in [P7] were partly erroneous[2], and hence the updated versions of the corresponding figures are presented here.

Figs 4.2-4.5 provide graphs of average $E_c/N_0$ as a function of downlink average throughput for four different cells. In each figure, the first dot (marked as circle), represents the measured average $E_c/N_0$ over the measurement route of a cell in idle mode and in an empty network. Based on this value, $i_{DL}$ is estimated by using the method presented in [P7]. Other parameters used for the load equation are: $E_b/N_0$ = 4 dB, bit rate ($R$) = 384 kbps, chip rate ($C$) = 3.84 Mcps, and activity factor ($v$) = 1. The average orthogonality factor was evaluated for each cell separately depending on the average distance from the base station[3]. The second (square) and the third dot (diamond) represent the measurement results over the very same measurement route, but with one DCH (dedicated channel) connection (384 kbps) and two DCH connections (2 x 384 kbps), respectively.

As seen from Figs 4.2-4.5, all the capacity estimate lines are under the corresponding measured points with load in a cell. This is due to soft capacity. As the initial $E_c/N_0$ measurement was based on constant P-CPICH power from all sectors, for the measurements with one and two DCH connections, some additional power was required from the measured cell. Therefore, the actual $i_{DL}$ was lower in the measured cell, and the measurement points are located over the estimated load. The curves in Figs 4.2-4.5 represent the achievable capacity in an equally loaded scenario and the dots in an unequally loaded one. However, it seems that with lower value of $i_{DL}$ (Cells 1 and 4), the difference between the estimated load curve and measured (biased) points is lower. This makes sense as the potential reduction of $i_{DL}$ is possibly higher for Cells 2 and 3. Without this bias in the 'verification' load points, the cell capacity estimates that are based merely on the idle mode measurements could be rather accurate.

These 'verification' measurements (square and diamond marks) might also be erroneous, and hence contort the assessment. The impact of the selection of bit rate and corresponding activity factor on the error should be rather small as the 'verification' points were based on the actual recorded throughput. However, the two

[2]The average orthogonality over each cell was evaluated based on the average distance of the measurement route, but the orthogonality was calculated as the distance would have been the maximum distance from the base station. This resulted in too high estimates of the orthogonality factor.

[3]The distance information was retrieved from base station coordinates and position of the measurement mobile through a GPS receiver.

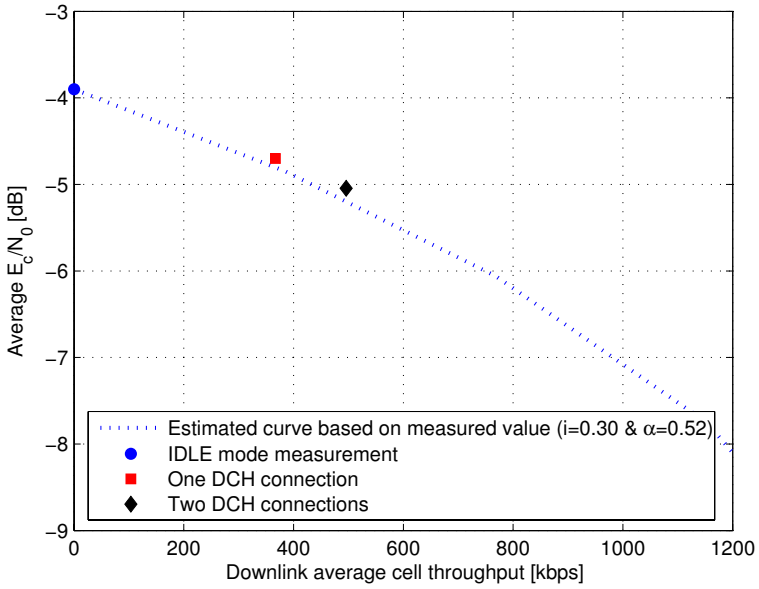


**Figure 4.2** Capacity estimation curves and measurement results for Cell 1.

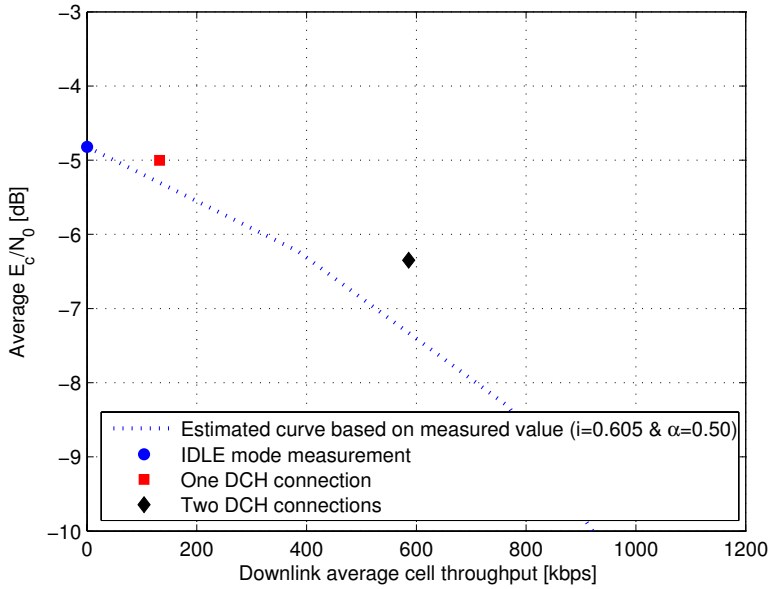


**Figure 4.3** Capacity estimation curves and measurement results for Cell 2.

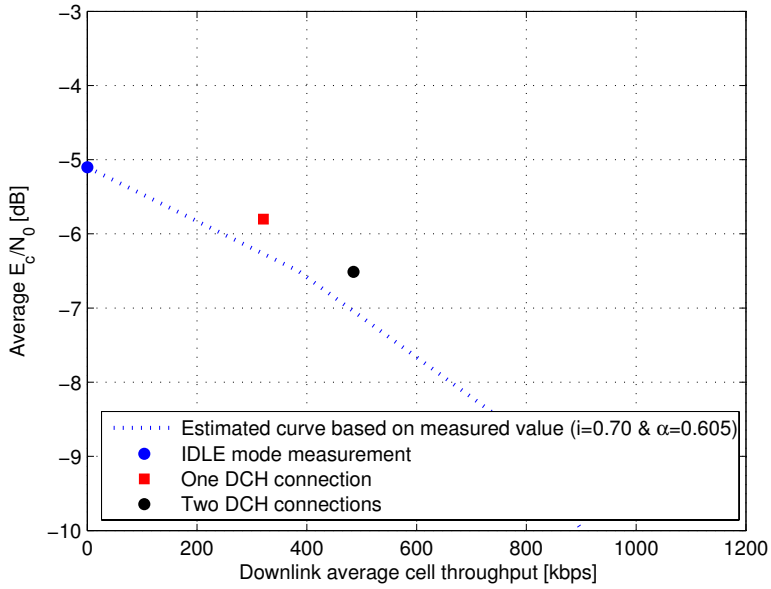


**Figure 4.4** Capacity estimation curves and measurement results for Cell 3.

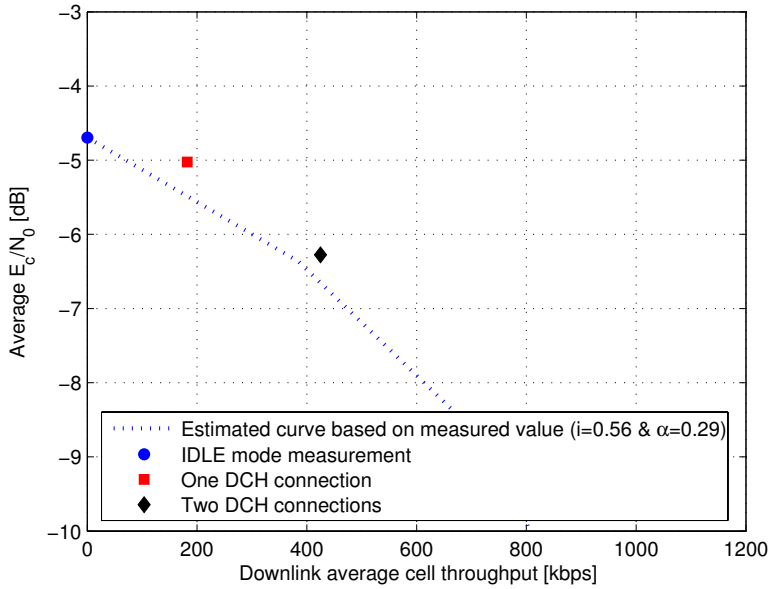


**Figure 4.5** Capacity estimation curves and measurement results for Cell 4.

most crucial estimates concern $E_b/N_0$ and average orthogonality factor. The selection of $E_b/N_0$=4 dB was based on the existing understanding from the literature for 384 kbps service in the downlink (e.g., [9]), and also, on the observation that the measured average SIR target[4] for this particular service was around 4 dB (even though SIR $\neq E_b/N_0$). On top of this, the estimates of the average orthogonality factor were based only on a simple model, the accuracy of which was not assessed here.

**Conclusions**

This section provided an assessment method for radio network quality based on radio interface $E_c/N_0$ measurements. For mapping the quality of the cell, $E_c/N_0$ distribution provides this information: the lower the average $E_c/N_0$ is, the better the quality of a cell (given the same power allocation). For providing cell throughput values, the method requires estimates of the parameters of the load equation, which on the contrary might add offset with respect to absolute cell capacity with a given traffic mix. Moreover, the method is not able to capture the impact of soft capacity. Regarding the verification measurements, there are few possible error sources. Hence, possible improvements for the method could consist of:

- more sophisticated $E_c/N_0$-to-$i_{DL}$ mapping function
- simultaneous measurement of the downlink orthogonality factor
- utilization of scanner measurements (rather than mobile measurements)
- mitigation of the impact of soft capacity

Nevertheless, continuously monitoring the average $E_c/N_0$ levels in the cells provides valuable information regarding the radio network topology. Moreover, the monitoring process itself could be a suitable approach, e.g. for radio network topology optimization based on RET or CAEDT [P7].

## 4.2 Topology Verification through Simulations

This section provides the results of an assessment of the performance of the static planning tool with two different propagation models in an urban WCDMA network [P8]. The capacity analysis is performed for downlink direction.

The importance of coverage predictions of the system capacity estimation has been outlined already in [87]. The simulation results showed mostly the limited dynamics of the COST-231-Hata propagation model against the ray tracing model in a dense urban environment. With the COST-231-Hata model, the capacity was observed to be 15% larger than with the ray tracing model due to underestimation of cell overlap. On the other hand, the performance of the static tool is expected to be similar to the dynamic one, as a static simulator has been observed to provide sufficiently accurate results compared to a dynamic simulator [88].

[4]The average measured SIR target over the measurement route should correspond to actual average SIR, if the downlink power control has been working within its dynamic range.

The performance of the static radio network planning tool [20] was evaluated by using two different propagation models—namely, the extended COST-231-Hata model[5] and a 2D ray tracing model (vertical plane model) [90]. Due to lack of 3D building information, a full 3D ray tracing model was not utilized. Both models were tuned roughly with total number of 3000 samples over distances from 0.3 km to 1.5 km with a dedicated transmission system using CW (continuous wave) measurements. The dynamic range of the measured signal varied from $-60$ dBm down to $-115$ dBm. Both models were tuned in order to provide a standard deviation (STD) less than 7 dB between predicted and measured samples [P8].

The network used in the measurements and simulations could be characterized as an urban environment with an average roof top level at 25 m and the base station antennas at the same level. The proportion of LOS connections (visual LOS) was rather significant over the measurement route. Moreover, the longest distance from/to a base station antenna within the measurement route was roughly 500 m.

**Performance Comparison**

The summary of simulated and measured results together with estimations of the average cell capacity over the measurement route is provided in Tables 4.1 and 4.2 for network configurations without and with MDT[6]. The average cell capacities were evaluated by the method presented in [P7] and in Section 4.1.

The errors in the average downlink cell capacity estimates (based on simulations) are significant for the COST-231-Hata model, but rather moderate for ray tracing. The resulting errors (overestimation) with and without MDT for the COST-231-Hata are almost 70% and around 50%, respectively. Whereas for the ray tracing model, the simulations with and without MDT show errors at the level of 9% and and 15% with respect to measurements. Note that with the selected simulation parameters, the resulting capacities overestimate the measurement-based capacity estimation with both propagation models.

In addition to regular inaccuracies of the static simulator (e.g. selection of simulation parameters) and description of the simulation environment (e.g. accuracy of digital map), there are several possible errors in these capacity estimates. First of all, the selected $E_b/N_0$ is possibly the most important factor. In the simulations, $E_b/N_0$=7 dB[7] was used only for the mobile station having 768 kbps service requirement in the downlink. Already an underestimation of a few decibels the average $E_b/N_0$ could result in high changes in the simulated results. The second simulation parameter -related overestimation could have been caused by selection of the average orthogonality factor. The selected $\alpha$=0.7 might have been overestimated, even through the average distance from the base station was 250 m, and the propagation

[5]See [89] for a description of the extended COST-231-Hata model.

[6]The mechanical downtilt measurements referred to are described in Section 3.4.2 and in [P4]. The difference between $E_c/N_0$ values from the same measurements comes from the fact that here it is averaged from the highest possible $E_c/N_0$ value as it is done in the static simulator rather than from the highest serving $E_c/N_0$.

[7]The selection was based on the literature and also on the fact that the average SIR target over the measurement route was close to 5 dB. From this value, it was estimated that $E_b/N_0 \approx$4 dB, which is 7 dB for two similar connections.

**Table 4.1** The measurement and simulation results for the capacity analysis of static planning tool without MDT over the measurement route.

| Parameter | Unit | Measurements | COST-231-Hata | Ray tracing |
|---|---|---|---|---|
| $E_c/N_0$ | [dB] | −5.50 | −5.48 | −6.69 |
| Observed throughput | [kbps] | 402 | 768 | 768 |
| DL 3 dB capacity | [kbps] | 830 | 1260 | 950 |
| RSSI | [dBm] | −69.8 | −58.3 | −51.3 |
| UL TX power | [dBm] | −20.4 | −24.0 | −29.6 |
| Handover probability | [%] | 19.9 | 17.2 | 29.4 |

**Table 4.2** The measurement and simulation results for the capacity analysis of static planning tool with MDT over the measurement route.

| Parameter | Unit | Measurements | COST-231-Hata | Ray tracing |
|---|---|---|---|---|
| $E_c/N_0$ | [dB] | −5.30 | −4.98 | −6.66 |
| Observed throughput | [kbps] | 336 | 768 | 768 |
| DL 3 dB capacity | [kbps] | 880 | 1475 | 960 |
| RSSI | [dBm] | −63.3 | −60.1 | −51.7 |
| UL TX power | [dBm] | −27.3 | −22.0 | −29.2 |
| SHO probability | [%] | 13.5 | 12.8 | 29.2 |

environment was a combination of macro- and microcellular environment. Possible errors in the service activity factor are compensated by the $E_c/N_0$ capacity estimation method that takes into account only the actual throughput. Moreover, the errors produced by the capacity estimation method itself (and related parameters for the load equation) only produce offset for the absolute capacity estimates as they were the same for simulated and measured values.

Coverage-related indicators, such as RSSI (received signal strength indicator) and UL TX power, are clearly more sensitive for errors in the simulation parameters and environment description. This was expected, since the simulation did not include any link level -related compensation factor of $E_b/N_0$ (as SHO/SfHO gains or impact of speed). Moreover, for example, different UL antenna diversities were modeled simply with 3 dB gain, as in practice these gains are at higher level already at 1800 MHz frequency [91]. Therefore, relatively high errors in the absolute coverage levels were expected. As seen from the results (Table 4.1 and 4.2), the level of RSSI is clearly overestimated in both cases. The RSSI values with the COST-231-Hata are in general overestimated very close to the base station, and in contrast, underestimated at and beyond the SHO area (i.e. low coverage overlap and the resulting high cell capacity). This indicates the unsuitability of the COST-231-Hata propagation model in an urban environment. In contrast, the overestimation with the ray tracing model is even higher. Hence, as a result, the overlap between cells is overestimated, which is indicated by high predicted handover (both SHO and SfHO) probability. In contrast, the estimated handover probability with COST-231-Hata was rather accurate.

**Conclusions**

The complexity and sensitivity of errors in a comparison process of real radio interface field measurements and static simulations can be performed most easily from relative measures (as $E_c/N_0$). However, the results and conclusions presented in this section provide only an initial assessment of the functionality of the static planning tool, and leaves open questions and topics for future research. Nevertheless, the results clearly indicate the inaccuracy of the empirical COST-231-Hata model in an urban environment. With the selected simulation parameters and in this particular measurement setup, the resulting error of the COST-231-Hata model in the downlink capacity was of the order of 50%-70%. Hence, the utilization of deterministic or more accurate physical models is mandatory for WCDMA (and other interference-limited) networks in urban environments, even though the prediction calculation time clearly exceeds the one of simpler empirical models. However, deterministic models also suffer from inaccuracy in the selection of simulation parameters, and also from inadequate description of the propagation environment (i.e. accuracy of the digital map). The static nature of a radio network planning tool affects at a certain level on the absolute level of cell capacities. Hence, a successful modeling of coverage and capacity of a network is a combination of a careful and successful selection of all these parameters.

# CHAPTER 5

# Supplementary Radio Network Concepts

THIS chapter introduces two supplementary radio network concepts that affect radio network topology planning: repeaters and network-based mobile positioning techniques. In general, repeaters improve the signal levels in the network, and hence affect not only the coverage, but also interference conditions in the network. Therefore, they have to be considered as part of radio network topology planning. The second concept that might affect the deployment of radio network topology is network-based location techniques. They have a tendency to utilize a fraction of radio resources for estimating user positions. Hence, optimization of the availability and also accuracy of a network-based location technique might also require modifications in the radio network topology.

## 5.1 Repeaters

One of the most obvious additional network elements which affect radio network topology, are repeaters. In the context of this thesis, a repeater is treated as an analog device that filters and amplifies all signals within its frequency band. In contrast to a digital repeater (decode and amplify), an analog repeater is a simple and easy-to-implement device, since it does not include any intelligence. On the contrary, the most significant drawback of an analog repeater is that it amplifies all signal components at its operational frequency (including noise) [92].

The utilization of repeaters can be divided generally into two parts: usage for coverage extensions (e.g. [93–98]) and for capacity enhancements [99,100], [P9], [P10]. Most of the references consider repeaters for coverage enhancements. Moreover, in a power controlled CDMA network, they have a tendency to decrease the required link power. Thus, they will also contribute to interference levels, and finally, on the system capacity as well. This subsection addresses the impact of repeater deployment in urban, capacity-limited WCDMA network through simulations [P9] and measurements [P10].

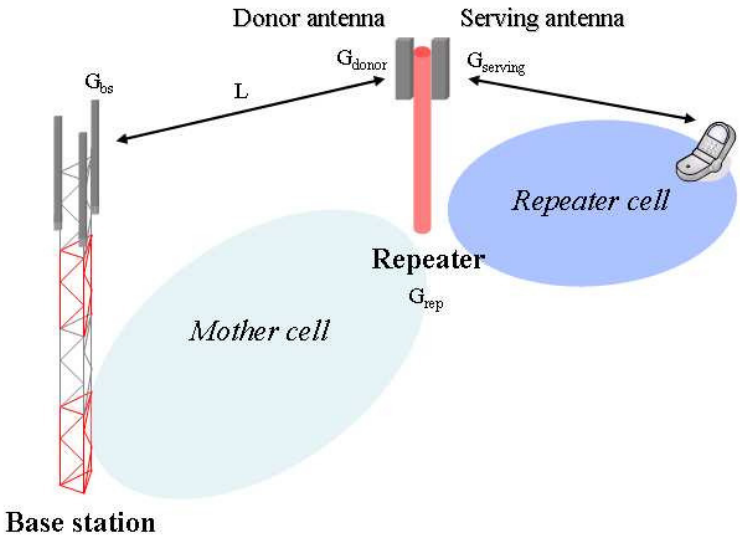


**Figure 5.1** Repeater configuration. [P9]

### 5.1.1 Repeater Configuration

The repeater gain parameter[1] ($G_t$) defines unambiguously the repeater configuration from base station to the repeater serving antenna:

$$G_t = G_{bs} - L + G_{donor} + G_{rep} \qquad \text{[dB]} \tag{5.1}$$

where $G_{bs}$ is the base station antenna gain, $L$ is the path loss (also denoted as coupling loss) between the base station antenna and the repeater donor antenna, $G_{donor}$ is the donor antenna gain, and $G_{rep}$ is the repeater gain (amplification) (Fig. 5.1). The repeater gain parameter provides information on how much the repeater is contributing to the noise increase of the base station [92]. The selection of the location of the repeater, the resulting link loss between base station antenna and repeater donor antenna is thus already defined when a repeater is deployed. Moreover, as the selected donor and serving antennas have typically certain gains, the only tunable parameter remaining is the repeater gain.

### 5.1.2 Assessment through Simulations

The target of the simulations in [P9] was to observe the impact of

- repeater gain (or $G_t$)
- traffic distribution within a repeater cell
- traffic mix

[1]The term repeater loss was originally adopted from [99]. However, here repeater gain parameter is used instead.

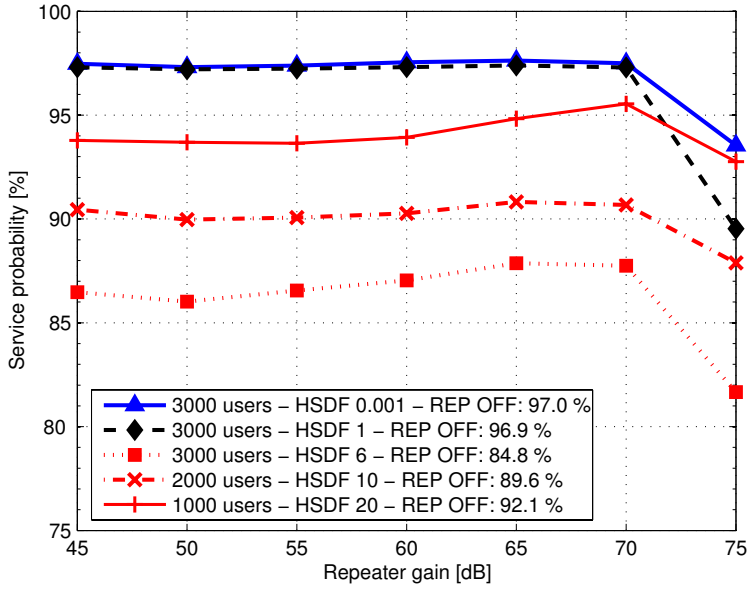


**Figure 5.2** Service probability for different traffic distributions in repeater cells. [P9]

on the service probability, interference levels, and capacity gains with repeaters in a capacity-limited environment. The impact of traffic distribution within a repeater cell is modeled by emphasizing the traffic density in hotspots. Hot spot density factor (HSDF) defines the density of users in a hotspot with respect to user density in all other locations than hotspots [100]. The higher the HSDF, the larger is the proportion of users under the hotspots. Moreover, as the repeaters are located near the hotspots, the gain of the repeater configuration should be higher with higher HSDF.

According to the selected simulation parameters, the conversion between repeater gain and repeater gain parameter is:

$$G_t = G_{rep} - 66 \qquad \text{[dB]} \tag{5.2}$$

Fig. 5.2 provides the simulation results from a network with 6 repeaters in a 19 base station hexagonal grid for different HSDF values [P9]. The service probability values without repeaters are given in the legend for different HSDF values. The impact of repeater on average service probability increases as more users are located in hotspots. Moreover, optimum repeater gain setting that maximizes the service probability over the network is around 65-70 dB (i.e. in terms of $G_t$ between $-1$ and 4 dB). At larger gain settings (such as 75 dB), the average service probability decreases rapidly due to degradation of uplink performance.

Fig. 5.3 provides the achievable capacity gains separately for downlink and uplink directions as a function of repeater gain. Both the downlink and uplink capacity values were based on 0.5 average load of all sectors. As indicated by Fig. 5.3(a), the downlink capacity gain increases with repeater gain. The capacity gain in the downlink is based on the reduction of required BS TX power in mother cells, which

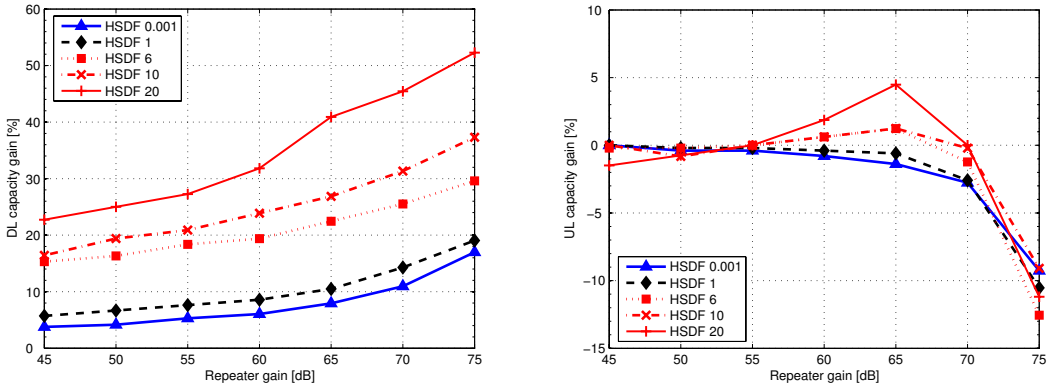


(a) Downlink capacity gain.

(b) Uplink capacity gain.

**Figure 5.3** The system capacity gains in a) downlink and b) uplink for a repeater configured network with respect to configuration without repeaters. [P9]

on the contrary, decrease other-cell interference towards neighboring cells, and so on. However, in the uplink, only a marginal capacity gain can be achieved with the traffic distribution concentrating on the hotspot (Fig. 5.3(b)). Clearly, the inherent increase of the total base station noise figure limits the achievable capacity gain in the uplink. Only with a traffic distribution concentrating on the hotspots is the reduction of uplink path loss (and following reduction of other-cell interference) able to provide a small capacity gain. In other cases, the noise level increase at the mother cells due to repeater deployment overruling the positive impact of repeaters. Moreover, if the repeater gain exceeds 70 dB, the repeater configuration produces only capacity loss in the uplink.

The optimum repeater gain depends on the definition. The optimum repeater gain according to service probability is between 65 dB and 70 dB for the given scenario. However, if some capacity degradation is allowed in the uplink capacity (such as 5%), the optimum repeater gain is between 72 dB and 73 dB, which corresponds to $G_t$ of 6 dB or 7 dB. With these repeater gain settings, the achievable downlink capacity gains are between 7% and 45%. Moreover, as shown in [100], the optimum repeater gain parameter does not depend on the path losses (or equally on the distance) between mother cell antenna and donor antenna. Moreover, the optimum repeater gain parameter does not change remarkably with respect to traffic distribution in mother cells [P9], [100].

### Conclusions

According to the simulations, optimum $G_t$ locates around 5 dB and depends only slightly on the traffic distribution under the repeater cell. Thus, an optimum repeater configuration can be defined by setting $G_t$ close to 5 dB. With this setting, a certain amount of uplink capacity loss has to be tolerated and the attainable downlink capacity gains are around 7% (HSDF 0.001) and 45% (HSDF 20). However, if any

uplink capacity degradation is not allowed, then $G_t$ should be 0 dB, and the resulting downlink capacity gains would be moderately smaller. However, it is highly possible that the optimum $G_t$ depends also on the direction and position of the donor and serving antennas, which makes the repeater deployment case-dependent. Finally, it seems clear that the uplink is the limiting direction in the repeater deployment, and within the simulated repeater gain values, the capacity gain only increases in the downlink.

### 5.1.3 Assessment through Measurements

The performance of repeaters was also assessed through actual field measurements [P10]. In the measurement scenario, a hotspot was generated close to the dominance area edge, and the repeater was placed in a favorable location with respect to the hotspot.

The analysis was performed in the downlink, and it was based on the measured average noise rises (i.e. in practise observed with decrease of $E_c/N_0$) and recorded average throughput. Fig. 5.4 shows the estimated load curves[2] for the mother cell. The reference points, circle and square, represent the measurement results without repeater with a single DCH (dedicated channel) connection and with two DCHs, respectively. The other DCH connection recorded the statistics while moving and the other while staying still close to the dominance area edge. The estimated load curve tries to provide an average cell throughput as it passes the measurement points from the middle. The estimated 3 dB noise rise capacity for the downlink without repeater is 940 kbps.

The reference points, diamond and triangle, represent the measurement results with repeater with a single DCH connection and with two DCHs, respectively. In this scenario, the load curve estimation provides a slightly pessimistic capacity estimate, as it leaves the latter measurement point (2 times DCH) on the right side. Nevertheless, the estimated 3 dB noise rise capacity for the downlink with repeater is 1230 kbps, resulting in a downlink capacity gain of 30% for the mother cell. These capacity estimates reflect a scenario where the additional load for the cell is not concentrating on the dominance area edge.

With a linear estimate of the downlink load curve, the resulting 3 dB noise rise capacity would have been 700 kbps and 1800 kbps without and with a repeater, respectively. Note that these capacity estimates reflect a scenario where the additional traffic load would be placed on the same location as the hotspot mobile (i.e. on the cell edge). Hence, the capacity gain would have been over 150%. As the capacity gain produced by the repeater depends heavily on the location of the additional mobile (i.e. the second DCH connection), it can be expected that in the measurements, the achievable capacity gain in the mother cell varies between 30% and 150% depending on the location of traffic.

[2]The load curves are based on standard downlink load equation with the following parameters: $E_b/N_0$ = 4 dB, bit rate (R) = 384 kbps, chip rate (C) = 3.84 Mcps, activity factor (v) = 1, and orthogonality ($\alpha$) = 0.7.

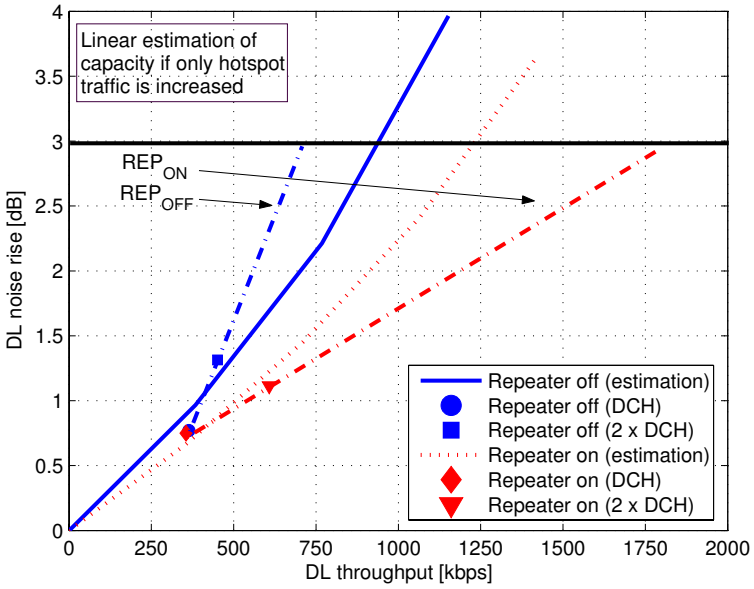


**Figure 5.4** Capacity analysis from measurements. [P10]

### Conclusions

The measurement results related to repeaters in a capacity-limited environment revealed their positive impact on the downlink capacity. However, the corresponding assessment should be fully applied with several different repeater gain settings in order to compare simulation and measurements directly. Although the capacity estimates provided here are not any absolute values, the direction of the measurement results and analysis strongly verifies the direction that was observed with the simulations. However, these measurements were only scratch of the surface, and thus, a deeper analysis and more comprehensive measurements should be conducted in order to fully understand the impact of repeaters in a WCDMA network. For example, the impact of the direction of serving and donor antennas as well as location of repeater should be more comprehensively analyzed.

## 5.2 Mobile Positioning Techniques

The applications and services for *mobile positioning* are still waiting for their breakthrough. However, the research in the area starts to be mature, and most of the research has concentrated or is concentrating on inexpensive solutions, which provide high accuracy with minimized complexity. In general, the methods intended for mobile positioning can be either mobile-based, radio network -based, satellite-based, or a combination of these. The influence of purely mobile- and satellite-based methods on the radio network functionality is extremely minor. However, radio network -based mobile positioning methods affect at a certain level the radio network

functionality because they require usage of radio resources for performing positioning estimates. All technical solutions for mobile positioning naturally differ in the sense of providing *complexity*, *availability*, and *accuracy*. The complexity of a positioning method can be implemented either on the mobile (mobile-based methods) or on the network (network-based methods), or it can be a combination of these (hybrid). Naturally, as the power consumption of the mobile station is one of the top concerns of mobile communications, network-based methods have become more attractive during the past decade. The complexity logically increases the availability and the accuracy of positioning methods. The availability and estimated accuracy level of certain positioning methods is partly defined by the radio network topology. For example, the accuracy of a simple cell identification (cell ID) method is based on a fixed geographical mapping point, and is therefore mostly defined by applied sectoring and site density.

Three location methods have been included in the Third Generation Partnership Project (3GPP) for the nearest releases of UMTS network: cell ID, Observed Time Difference of Arrival (OTDOA) with Idle Period Downlink (IPDL) enhancement, and Assisted Global Positioning System (AGPS) [101]. On top of this, many mobile positioning methods have been designed and proposed for future releases, which mainly consists of availability enhancements to OTDOA (time alignment IPDL (TA-IPDL) [102], positioning elements IPDL (PE-IPDL) [103,104], and Cumulative Virtual Blanking (CVB) [105]). Other radio network -based approaches for position estimation include angle of arrival (AOA) [104, 106, 107], Cell ID + round trip time (RTT) [P11], Enhanced cell global ID (E-CGI), AOA+RTT [108], and OTDOA+AOA [109]. Satellite-based methods utilizing GALILEO data (Assisted GALILEO) or a combination of GPS and GALILEO data (AGPS + Assisted GALILEO) are also under investigation [110].

The target in this chapter is to ascertain the impact of radio network topology on the accuracy and availability of simple cell ID positioning and with its possible enhancements. These enhancements consist of a standardized time-based round trip time (RTT) measurement, which increases the accuracy of simple cell ID, and of a forced soft handover (FSHO) algorithm, which tends to improve the availability of cell ID+RTT.

### 5.2.1 Theoretical Accuracy of cell ID+RTT

The simplest mobile positioning method included in the 3GPP, cell ID, is typically implemented as a network-based method, and thus it does not require any changes to the terminals. The accuracy of cell ID positioning depends mostly on the site density and sectoring scheme. However, since the accuracy of simple cell ID can be increased if a mobile is either in SfHO or SHO, the impact of SHO-related parameters (such as P-CPICH power setting and SHO window sizes[3]) should be known as well [P11].

RTT consists of the time difference between beginning of the transmission of a downlink dedicated physical channel (DPCH) frame and the beginning of the recep-

[3]SHO window here means generally the sizes of add, drop, and replace thresholds in a SHO algorithm [111].

**Table 5.1** Theoretical inaccuracies (in meters) of cell ID+RTT for different areas with different radio network topologies. [P11]

| Scenario | Type of area | Site spacing | | |
|---|---|---|---|---|
| | | 0.75 km | 1.0 km | 1.5 km |
| 3-sectored/65° | Single | 240 | 320 | 480 |
| | SfHO | 22 | 29 | 44 |
| | SHO | 16-99 | 16-99 | 16-99 |
| 6-sectored/65° | Single | 65 | 87 | 131 |
| | SfHO | 32 | 44 | 65 |
| | SHO | 16-99 | 16-99 | 16-99 |
| 6-sectored/33° | Single | 90 | 120 | 180 |
| | SfHO | 8 | 11 | 16 |
| | SHO | 16-99 | 16-99 | 16-99 |

tion of the corresponding uplink frame. Therefore, it is sufficient to establish only a radio bearer signalling connection (i.e. dedicated physical control channel (DPCCH) in uplink and DPCH in downlink) with a 3.4 kbps bit rate for performing an RTT measurement. On top on this, the accuracy of time-based RTT measurement (as any time-based measurement) can be significantly improved by performing multiple RTT measurements from geometrically different locations [112].

The derivation of the accuracy under a single cell area, in SfHO, and in a two-way SHO is provided in [P11]. The accuracy under a single cell area naturally depends on the sectoring scheme and site density. The accuracy in SfHO area is typically better due to smaller outspread angle. However, typically the highest accuracy is achieved in SHO. Table 5.1 provides theoretical accuracies of cell ID+RTT for 3-sectored sites with $65°$ horizontal antenna beamwidth and for 6-sectored sites with $65°$ and $33°$ antennas. The accuracies are calculated presuming that the mobile is located in the middle of the cell range[4], and that the geographical mapping point of the cell ID locates in the middle of the sector. Moreover, the precision of RTT measurement is assumed to be 5 m (1/16 oversampling), and without any multipath errors. The outspread angles of SfHO were $10°$, $20°$, and $5°$ for 3-sectored/$65°$, 6-sectored/$65°$, and 6-sectored/$33°$ configurations, respectively [113,114].

The accuracies are considerably smaller in a single cell area for 6-sectored sites than for 3-sectored sites. Moreover, by using larger antenna beamwidth, the resulting outspread angle of single cell ID is smaller at the cost of slightly poorer accuracy at the SfHO (softer handover) area. These theoretical accuracies clearly illustrate that radio network topology (sectoring and antenna beamwidth) clearly have an impact on the expected accuracy of the cell ID+RTT. However, these accuracies do not include the harmful impact of multipath propagation on time-based RTT measure-

[4]Assuming hexagonal cell structure, cell range corresponds to 2/3 of the site spacing with 3-sectored sites and 1/2 of the site spacing with 6-sectored sites.

**Table 5.2** Availability (in percentages) of different accuracy areas for different SHO window sizes and with different radio network topologies with 1.0 km site spacing. [P11]

| Scenario | SHO window | Type of area | | |
|---|---|---|---|---|
| | | Single | SfHO | SHO |
| 3-sectored/65° | 3 dB | 75.9 | 3.1 | 21.0 |
| | 4 dB | 68.3 | 4.7 | 27.0 |
| | 5 dB | 62.6 | 5.2 | 32.2 |
| 6-sectored/65° | 3 dB | 46.5 | 28.4 | 25.1 |
| | 4 dB | 31.0 | 36.6 | 32.4 |
| | 5 dB | 19.1 | 42.9 | 38.0 |
| 6-sectored/33° | 3 dB | 73.3 | 2.1 | 24.6 |
| | 4 dB | 66.6 | 2.7 | 30.7 |
| | 5 dB | 60.1 | 6.4 | 36.5 |

ment, which occurs in practice. Moreover, the oversampling factor 1/16 is an optimistic assumption, and for example without any oversampling, the resolution of RTT measurement would be roughly 80 m. Nevertheless, the differences between different radio network topologies should stay the same. In practice, also the accuracy in SHO is expected to be higher than in SfHO due to geometry.

Because the resulting single cell, SfHO and SHO areas are different with different radio network topologies, so the availability of these accuracies also changes. Table 5.2 shows an example of the expected availabilities of different accuracy areas with different SHO window sizes. These availability values are based on system level simulations with 19 sites. Clearly, the best availability of better accuracy SfHO and SHO areas is achieved with 6-sectored/65° configuration as the percentual amount of these areas exceeds 80%. The corresponding value with 3-sectored/65° and 6-sectored/33° is around 40%. However, the cost of wider antenna beamwidth and larger (possibly too large) SHO window size is reduced downlink capacity. Furthermore, the availability of SfHO and SHO areas can be slightly increased with higher P-CPICH power, which, however, reduces the available capacity for DCH channels.

The final accuracy values for different topologies are derived based on simulations. Fig. 5.5 shows the CDF of the expected accuracies for different network topologies. The results are based on SHO window of 5 dB and site spacing of 1.0 km. The better single cell ID accuracy with higher order sectoring and the higher availability of SfHO areas with wider antenna beamwidth can be clearly seen in the final accuracy values.

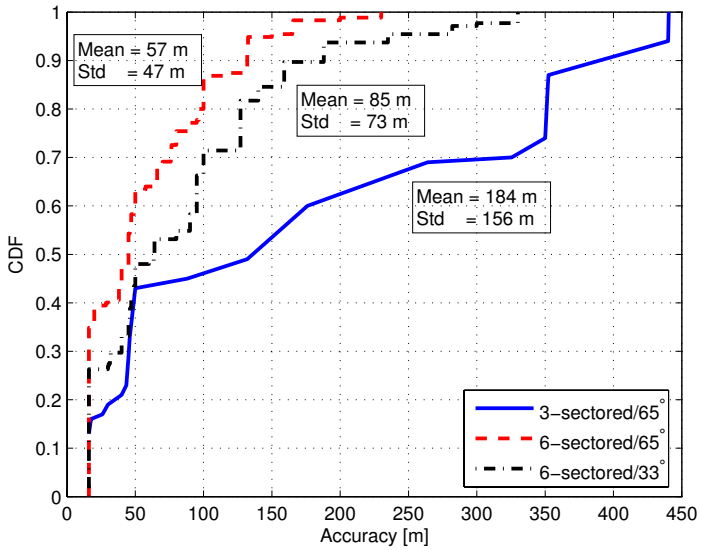


**Figure 5.5** Theoretical maximum inaccuracies for different radio network topologies. [P11]

### 5.2.2 Forced SHO algorithm

Performing a time-based measurement from several different geographical locations simultaneously increases the accuracy of the position estimate considerably [112]. In a cellular mobile communication system, this can be performed by conducting corresponding time-based range measurements from several different base stations.

For GSM, the so-called forced handovers that support the cell ID+timing advance (TA) location method were analyzed in [115–118]. However, in GSM, the fundamental problem is the lack of SHO and poorer resolution of TA. In WCDMA, the availability of SHO can be increased by the so-called forced SHO (FSHO) algorithm [P12]. The FSHO algorithm increases temporally the SHO window for a mobile being located (i.e. for the duration of RTT measurements). Then, by performing RTT measurement from base station sectors in the active set, the reliability of the positioning estimate can be increased. On top of this, multiple RTT measurements can be performed for a single sector to minimize the impact of multipath propagation.

Fig. 5.6 shows the visibility of the third strongest P-CPICH $E_c/N_0$. The distributions are based on simulations of 19 base station hexagonal grids with two different site spacings: 1.0 km and 1.5 km. As the RTT measurement requires only a control channel connection (i.e. 3.4 kbps), the required $E_c/N_0$ for sufficient BER can be rather low, and values as low as $-23$ dB could still be enough for sufficient quality [9]. As indicated by the results, with 6-sectored/$65^\circ$ configuration, the resulting visibility of the third pilot is around 90%, whereas with the other simulated configuration is it at the level of 70%. Hence, the availability of FSHO algorithm is also expected to be higher with 6-sectored/$65^\circ$. Note that these distributions do not separate pilot signals from different sites, but only from different sectors. Hence, in practice, the

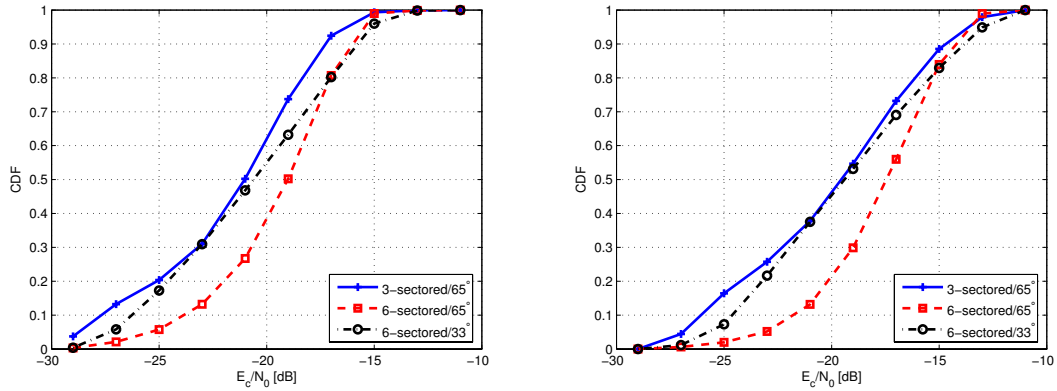


(a) 1.0 km site spacing

(b) 1.5 km site spacing

**Figure 5.6** Visibility of the $3^{rd}$ strongest P-CPICH $E_c/N_0$. [P12]

visibility of three pilots from different sites is lower. On the other hand, the probability of observing three pilots from the same site is rather low, and moreover, it could happen most certainly close to the base station, where the accuracy of RTT is expected always to be rather sufficient.

The most significant drawback of the FSHO algorithm is interference peaks produced by the mobiles being forced to SHO. However, as there should not be more than one simultaneous FSHO attempt per cell, the interference peaks are averaged over time. Thus, their impact on system capacity should be rather small as shown in [119].

### 5.2.3 Trade-off between Optimum Topology and Availability of Cell ID+RTT

The results yield for a compromise if we want radio network topology and the performance of cell ID+RTT should be optimized. Naturally, higher order sectoring increases the accuracy of cell ID+RTT. Moreover, the availability of SfHO areas is on a higher level with 6-sectored/$65°$ configuration. This also affects the expectable accuracy, which is obviously better with $65°$ antennas. The drawback of $65°$ antennas deployment is approximately 30-35% poorer radio network capacity compared to $33°$ antennas. On top of this, the proportion of pilot polluted areas is higher with wider antenna beamwidths. Note also that availability and the resulting accuracies have been evaluated with non-optimized radio network topology being used (e.g. without downtilt).

To increase the accuracy of cell ID+RTT, all mobiles in the network should be in SHO. However, this would lead to very poor downlink performance in WCDMA as it would require large SHO windows. Thus, the idea of forced soft handover was introduced in which SHO parameters are changed only for the mobile that is located. Moreover, the FSHO algorithm requires that at least three P-CPICH signals from different base station sectors have to be heard. Clearly, in an interference-limited

WCDMA network, the visibility of at least three P-CPICH signals simultaneously all over the network is not possible. However, $65^\circ$ antennas provide better visibility for the third P-CPICH signal than $33^\circ$ antennas. Visibility of the fourth P-CPICH signals is an unwanted situation, since it causes pilot pollution. Therefore, also the amount of pilot pollution areas can be minimized through antenna configuration by using narrow antennas. However, the visibility results were also derived based on non-optimized radio network topology, and hence, in an optimized network, the availability of FSHO would be at a lower level. It is up to an operator's deployment strategy as to which one of these approaches – enhanced radio network capacity or availability of cell ID+RTT mobile positioning method – it is willing to satisfy.

# CHAPTER 6

# Conclusions

## 6.1 Concluding Summary

Detailed optimization of radio network topology planning for WCDMA is clearly needed to be able to provide high system capacity with minimum network deployment costs.

In the first part of the thesis, different radio network topologies and their impact on network coverage and system capacity were addressed. An empirical approach for estimating an optimum coverage overlap index was presented. According to evaluations, the maximum sector throughput was achieved typically with $COI \approx 0.5$, which can be realized only by antenna downtilt. From an academic point of view, the results indicate that the network topology optimization should be as follows: maximize the antenna height and use correspondingly higher downtilt angles. From a more practical point of view, the site density for a planning area should be minimized according to coverage or capacity requirements in order to minimize the network deployment costs and the required number of base stations. For a capacity-limited network, deployment of new sites is allowed only if coverage overlap can be maintained at a reasonable level. Otherwise, the system capacity will degrade.

A small random deviation of site location (less than 1/4 of the site spacing) from the hexagonal grid was shown to have a negligible impact on the system performance in a real propagation environment (i.e. when the information of the digital map is taken into account), and when high indoor coverage thresholds are required (1.5 km site spacing). However, if high indoor coverage probabilities are not required, i.e. the cells are not overlap significantly, a random deviation in base station location becomes more and more crucial as with 3.0 km site spacing. Hence, in urban and suburban environments with higher coverage overlap due to the required indoor coverage, the requirements for site location selection can be loosened, as non-hexagonality does not deteriorate network performance. In addition, the simulation results indicate that WCDMA network performance is robust for random antenna direction deviation under different traffic scenarios.

Regarding sector overlap with different sectoring schemes, it was found that $SOI \approx 0.5$ provides the optimum with moderate coverage overlap schemes. However, for high overlap schemes (as in very dense networks), narrower antennas should be used in order to avoid high other cell interference levels. The sensitivity of system capacity with respect to $SOI$ is naturally higher (approximately twice) in 6-sectored network due to the double number of overlapping sectors. However, further analy-

sis should be performed in order to find an optimum $SOI$ as a function of $COI$.

For different antenna downtilt schemes, the downlink capacity gains with simulated network topologies varied between 0% and 60% with optimum downtilt angles between $3.4^\circ$ and $10.3^\circ$. For uplink direction, capacity gains are typically significantly lower. The obtained optimum downtilt angles and the derived empirical equation provide an initial downtilt angle for suburban WCDMA antennas. Moreover, the impact of antenna downtilt was also verified with radio interface measurements. The measurements indicated also the reduction of pilot polluted areas due to antenna downtilt. In addition, it was shown that utilization of an algorithm that adjusts antenna downtilt angles based on the traffic distribution in a cell seems not to be worth deploying. Finally, regarding site evolution, it was concluded that downtilt angles in 6-sectored sites can be almost the same as in 3-sectored sites.

In the second part of the thesis, two different assessment methods for radio network topology were shown. A method based on radio interface measurements was introduced and partly verified. On the other hand, the performance of a static radio network planning tool was evaluated for urban WCDMA networks. A comparison between simulations and measurements showed the limited accuracy of the COST-231-Hata propagation model, as the inaccuracy of the downlink capacity estimate exceeded 50%. Therefore, it was suggested that ray tracing models should be used for urban radio network planning.

The third part covered an analysis of repeater deployment and a network-based mobile positioning technique called cell ID+RTT. The results clearly indicate that repeater deployment should be considered as a part of the topology planning as it heavily affects network coverage and system capacity. Moreover, it clearly seems that there is a tradeoff between maximization of radio network capacity and accuracy and availability of cell ID+RTT positioning (without or with FSHO algorithm) method.

## 6.2 Future Work

The ideas related to coverage and sector overlap modeling are at the moment quite immature, and would hence require more attention. These parameters could be optimized and possibly implemented in planning or optimization tools to provide suggestions of the optimum overlap between cells. However, for that purpose, the model should be more general and not only applicable for WCDMA networks.

Regarding site location deviations, the ultimate target would be to have a planning guideline between the coverage overlap and the maximum allowable site location deviation. Again, this information would be useful during the planning process.

Most of the simulation results in this thesis concentrated for a suburban or light urban macrocellular environment, and hence, an interesting question is: what happens in dense urban or in microcellular environment? For example, how the antenna downtilt angles should be set in case of roof-top installations when the most strongest signal component in non-LOS situations becomes typically from over roof-top diffraction. In general, the impact of practical and different site locations for antenna deployment as roof-top, mast, and pole installations should be studied to

find optimum solutions from the coverage and capacity point of view per site basis. Moreover, the studies related to evaluation of the applicability of CAEDT with practical user distributions, not only with moving hot-spots, would be needed in a real network.

Related to verification techniques of the radio network topology, different models and methods could be developed, and furthermore, their utilization during the radio network optimization should be considered. In addition, the example study performed for the planning tool verification should be also extended to cover more suburban environments and also rural environments for possible implementation of lower frequency CDMA technologies as CDMA450 [120] or WCDMA900 [121]. Moreover, the possible utilization of the COST-231-Walfisch-Ikegami to model the propagation in urban environment should be considered also.

Part of the work introduced here of the repeaters and mobile positioning techniques have already been continued within the Radio Network Group. However, especially repeaters seem to create an attractive approach to cover the so-called coverage dead-spots in otherwise capacity-limited environment by taking advantage, e.g. from indoor distributed antenna (DAS) implementations. Moreover, the tendency of using even higher frequencies for cellular systems (e.g. [122]) will make the absolute coverage area from a single antenna smaller and smaller, and hence creating a need for intelligent repeater solutions.

The above mentioned points are mostly related to current evolution and direction of cellular networks. However, the evolution of cellular networks is continuous and hence the attention regarding the radio network topology should be also directed towards the future systems. For example, the next system released by the 3GPP will be based on orthogonal frequency division multiple access (OFDMA) technique [123], and hence, the impact of this new radio interface technology on the radio network topology planning should be studied. Another aspect related directly to different antenna configurations is multiple input multiple output (MIMO) systems where several antennas are used for transmission and reception. Hence, from the radio network topology point of view, one interesting question is that how much antenna positions or configurations affect the correlation of different antenna elements, which heavily impacts the achievable capacity, in a MIMO system.

# CHAPTER 7

# Summary of Publications

## 7.1 Overview of Publications and Thesis Results

Basic radio network topology studies were conducted in [P1]-[P6]. The reference simulations of coverage overlap were provided in [P1]. However, all the required analyses were performed in this thesis only, and have not been published elsewhere. The approach for modeling coverage overlap with a single parameter seems to be valid, even though more research is needed on that topic. Nevertheless, the results showed the importance of optimum coverage overlap a from system capacity point of view.

The impact of non-hexagonal site locations and non-uniform antenna directions on the system level performance was assessed in [P2]. The results indicate that the performance of WCDMA network is rather robust for moderate changes on hexagonal site locations, and also on small changes of nominal antenna directions. In [P2], some site evolution strategies were also presented, but the analysis was slightly extended in the frame of the thesis.

The importance of the selection of antenna beamwidth for different sectoring schemes was studied in [P3]. For this thesis, the number of simulation scenarios was increased to cover also different degrees of overlap. As a result, it was observed that optimum sector overlap depends on coverage overlap.

Publication [P1] presented the results of simulation campaign regarding optimum downtilt angles for a suburban WCDMA network. The results indicated that downtilt is of great importance, and especially in dense networks. The measurements of the impact of the mechanical antenna downtilt were provided in [P4], which verified the capacity gain of downtilt also in practice. Moreover, [P5] emphasized the impact of different geographical user distributions on the optimum downtilt angle. The results indicated that usage of rapidly changing downtilt angle is not worth deploying in a cellular WCDMA network.

Verification studies on the radio network topology were provided in [P7]-[P8]. A method for verifying the quality of a network plan was introduced in [P7]. Although a simple model, the $E_c/N_0$ mapping method seems to be rather accurate for verifying the quality of the radio plan, and, moreover, extremely applicable for immediate use. Publication [P8] provided an initial assessment of the functionality and reliability of the static WCDMA radio network planning tool with two different propagation models. The results clearly indicate insufficient accuracy of the COST-231-Hata propagation model, whereas certain problems might also be observed with

ray tracing models. However, the performance assessment was only performed only in an urban environment.

The impact of repeaters was simulated and measured in [P9] and [P10]. The assessment was carried out in a capacity-limited network, not in a coverage-limited one as is typical in the context of repeaters. The results clearly indicate the potential capacity gain of a repeater deployment.

Finally, [P11] and [P12] provide an accuracy assessment of cell ID+RTT with and without forced SHO for a WCDMA network. Clearly, the radio network topology partly defines the availability and attainable accuracy. Moreover, both of these performance indicators can be maximized with an non-optimum radio network topology configuration from the capacity point of view.

## 7.2 Author's Contribution to the Publications

All the research work for this thesis was performed at the Institute of Communications Engineering, Tampere University of Technology, as part of larger research project, "Advanced Techniques for Mobile Positioning".

The performance assessments and the analyzes of [P1]-[P10] were carried out by the author. For [P11]-[P12], Jakub Borkowski (M.Sc.) carried out all the analyses, and the author's contribution was in the radio network performance analysis. Naturally, all publications were supported and guided by the thesis supervisor Prof. Jukka Lempiäinen. Moreover, it goes without saying that numerous informal discussions between the author, supervisor, and all co-authors have contributed considerably to the reported results as well as to the general research directions.

The initial idea for coverage overlap index was originally introduced by the author. Furthermore, the analysis for coverage overlap index in this thesis was solely carried out by the author. Regarding the simulations in [P1], they were performed together with Tero Isotalo (Tech. Stud.). Moreover, Tero Isotalo helped significantly with the tools required for the result analysis. However, the majority of the performance analyzes and the writing work was performed by the author.

In [P3], all the system level simulations and performance analyses were performed by the author. The writing was done together by the author and Prof. Jukka Lempiäinen.

The measurements and simulations in [P4] and [P8] were conducted together with Jakub Borkowski. However, the analysis tool of the measurement results, the performance analyzes, and the writing were done solely by the author.

For [P5], [P2], and [P6], the simulation methodology was realized by the author. Moreover, all the simulations, performance analyzes, and writing were performed by the author. However, in [P6], Tero Isotalo carried out most of the work required for the analysis tool.

The author came up with the idea of the $E_c/N_0$ mapping method in [P7]. Jakub Borkowski initiated the writing work, but all the measurements, analyzes and also most of the writing was carried out by the author.

For [P9], the author performed part of the system analyzes and most of the writing work. The simulator development was performed by Panu Lähdekorpi (M. Sc.),

who also carried out all the simulations. The repeater measurements in [P10] were carried out by the author and Jakub Borkowski. The author also contributed to the results analyzes and to the final appearance of the paper.

For [P11] and [P12], the authors' contribution was significantly smaller as the majority of the work was carried out by Jakub Borkowski. Most of the contribution of the author was in the simulations and simulation analyzes. Moreover, numerous informal discussions took place between Jakub Borkowski and the author.

# APPENDIX A

# Statistical Analysis of the Simulation Results

The statistical reliability of any experimental results means that the probability of a pure chance should be extremely small, and that in the considered physical phenomenon no such result exists. For constant system parameters, the capacity of the system, as classified by the simulator via simulating a number of different realizations of the user distributions (snapshots), will vary for different sets of analyzed snapshots. In this thesis, the system capacity is defined as the number of served users over the total number of users in the system (i.e. the number of served users with a given service probability target) when averaged over $Y$ snapshots. If the system does not provide an acceptable service to a requesting user, this user will be considered to be in *outage* (i.e. service probability = 1−outage).

Let $x$ be the random variable that counts the total number of users that incur outage from the overall set of users requesting service ($N$). Under the previous assumptions, it can be stated that $x$ follows a binomial probability density function whose mean is [124]

$$\mu_x = E\{x\} = N \cdot p \tag{A.1}$$

where $p$ is the outage probability. Moreover, the variance of $x$ equals

$$\sigma_x^2 = N \cdot p \cdot (1-p) \tag{A.2}$$

The standard deviation (relative to the mean) of the variable that counts the total number of users that incur outage during one snapshot equals to

$$\frac{\sigma_x}{\mu_x} = \sqrt{\frac{1-p}{N \cdot p}} \tag{A.3}$$

On the other hand, from statistics it is known that the estimator

$$\widehat{X}_Y = \frac{1}{Y}(X_1 + ... + X_Y) \tag{A.4}$$

for the mean of the normal distributed random variables $X_1$ to $X_Y$ with mean $\mu$ and variance $\sigma^2$ has the same mean value $\mu$ and variance [124]

$$\sigma_Y^2 = \frac{\sigma^2}{Y} \tag{A.5}$$

Therefore, the standard deviation over all snapshots $\sigma_Y$ decreases with $\sqrt{Y}$ and can be given as

$$\sigma_Y = \sqrt{\frac{1-p}{N \cdot p}} \cdot \frac{1}{\sqrt{Y}} \tag{A.6}$$

The simulations carried out in this thesis considered service probability targets of 95% or 98%. For example, for the results in Table 3.3 (3-sectored/$65^\circ$ with 1.5 km/25 m and 3-sectored/$90^\circ$ with 1.5 km/45 m), the standard deviation over all snapshots (Y=10000) relative to the mean is 0.078% and 0.097% with a 95% service probability target. On the other hand, for different simulations in Table 3.11, the service probability target was 98%. Given the number of snapshots of 2000 and the system capacity of 98 users per site (altogether 19 sites), the standard deviation relative to the mean is 0.36%. Hence, the statistical reliability of the Monte Carlo simulations with several thousands of snapshot can be considered statistically reliable. Note that this analysis takes into account only the statistical reliability of the snapshots, and does not anyhow address the amount of systematic error in the simulations caused by the propagation model, digital map, or the algorithms of the static planning tool.

# Bibliography


[1] GSM World, *http://www.gsmworld.com/*, referred 26.2.2006.

[2] J. Lempiäinen and M. Manninen, Eds., *UMTS Radio Network Planning, Optimization and QoS Management*. Kluwer Academic Publishers, 2003.

[3] J. Laiho, A. Wacker, and T. Novosad, Eds., *Radio Network Planning and Optimisation for UMTS*. John Wiley & Sons Ltd, 2002.

[4] T. Ojanperä and R. Prasad, *Wideband CDMA for Third Generation Mobile Communications*. Artech House, 1998.

[5] J. Laiho and A. Wacker, "Radio network planning process and methods for WCDMA," *Annals of Telecommunications*, vol. 56, no. 5-6, pp. 317–331, 2001.

[6] S. Dehghan, D. Lister, R. Owen, and P. Jones, "W-CDMA capacity and planning issues," *Annals of Telecommunications*, vol. 12, pp. 101–118, 2000.

[7] P. R. Gould, "Radio planning for third generation networks in urban areas," in *Proc. of IEE 3rd International Conference on 3G Mobile Communication Technologies*, Oct. 2002, pp. 64–68.

[8] J. Lempiäinen and M. Manninen, *Radio Interface SystemPlanning for GSM/GPRS/UMTS*. Kluwer Academic Publishers, 2001.

[9] H. Holma and A. Toskala, *WCDMA for UMTS*. 3rd ed., John Wiley & Sons Ltd, 2004.

[10] C. Braithwaise and M. Scott, Eds., *UMTS Network Planning and Development: Design and Implementation of the 3G CDMA Infrastructure*. Elseview Newses, 2004.

[11] J. Niemelä, *Impact of Base Station and Antenna Configuration on Capacity in WCDMA Cellular Networks*, M.Sc. Thesis, Tampere University of Technology, 2003.

[12] 3GPP Technical Specification, *Spreading and Modulation (FDD)*, 3GPP TS 25.213, version 3.9.0, Release 99.

[13] B. Schroder, B. Liesenfeld, A. Weller, K. Leibnitz, D. Staehle, and P. Tran-Gia, "An analytical approach for determining coverage probabilities in large UMTS networks," in *Proc. IEEE 54th Vehicular Technology Conference*, vol. 3, Oct. 2001, pp. 1750–1754.

[14] D. Staehle, K. Leibnitz, K. Heck, B. Schroder, A. Weller, and P. Tran-Gia, "Approximating the othercell interference distribution in inhomogeneous UMTS networks," in *Proc. IEEE 55th Vehicular Technology Conference*, vol. 4, May 2002, pp. 1640–1644.

[15] K. Sipilä, Z. Honkasalo, J. Laiho-Steffens, and A. Wacker, "Estimation of capacity and required transmission power of WCDMA downlink based on a downlink pole equation," in *Proc. IEEE 51st Vehicular Technology Conference*, vol. 2, 2000, pp. 1002–1005.

[16] J. Laiho, "Radio network planning and optimisation for WCDMA," Ph.D. dissertation, Helsinki University of Technology, 2002.

[17] R. Hoppe, G. Wlfle, H. Buddendick, and F. Landstorfer, "Fast planning of efficient WCDMA radio networks," in *Proc. IEEE 54th Semiannual Vehicular Technology Conference*, vol. 4, Oct. 2001, pp. 2721–2725.

[18] U. Turke, M. Koonert, R. Schelb, and C. Gorg, "HSDPA performance analysis in UMTS radio network planning simulations," in *Proc. IEEE 59th Vehicular Technology Conference*, vol. 5, May 2004, pp. 2555–2559.

[19] P. Ameigeiras, J. Wigard, and P. Mogensen, "Performance of packet scheduling methods with different degree of fairness in HSDPA," in *Proc. IEEE 60th Vehicular Technology Conference*, vol. 2, 2004, pp. 860–864.

[20] *Nokia NetAct Planner ver. 4.2*, Radio Network Planning tool.

[21] A. Niininen, *Appendix A: Integrated network planning tool: Nokia NetAct Planner*, Fundamentals of Cellular Network Planning and Optimisation: 2G/2.5G/3G... Evolution to 4G by A. R. Mishra, John Wiley Sons Ltd., 2004.

[22] M. Wallace and R. Walton, "CDMA radio network planning," in *Proc. Third Annual International Conference on Universal Personal Communications*, 1994, pp. 62–67.

[23] H. Stellakis and A. Giordano, "CDMA radio planning and network simulation," in *Proc. IEEE Seventh IEEE International Symposium on Personal, Indoor and Mobile Radio Communications*, Oct. 1998, pp. 1160–1162.

[24] M. Metsälä, *Geospatial raster analyses in mobile phone network planning*, Licentiate's Thesis, Helsinki University of Technology, 2001.

[25] S. Asari, P. Ho, A. Jalan, and N. Velayudhan, "Performance analysis of the forward link in a power controlled CDMA network," in *Proc. 47th IEEE Vehicular Technology Conference*, vol. 3, May 1997, pp. 2118–2122.

[26] J. Itkonen, B. P. Tuzson, and J. Lempiäinen, "A novel network layout for CDMA cellular networks with optimal base station antenna height and downtilt," in *Proc. 63rd IEEE Vehicular Technology Conference*, 2006.

[27] W. C. Y. Lee, *Mobile Communication Engineering*. McGraw-Hill, 1997.

[28] E. Benner and A. B. Sesay, "Effects of antenna height, antenna gain, and pattern downtilting for cellular mobile radio," *IEEE Trans. Vehicular Technology*, vol. 45, no. 2, pp. 217–224, May 1996.

[29] T. C. Tozer and D. Grace, "High-altitude platforms for wireless communications," *Electronics & Communications Engineering Journal*, vol. 13, pp. 127–137, June 2001.

[30] D. Avagina, F. Dovis, A. Ghiglione, and P. Mulassano, "Wireless networks based on high-altitude platforms for the provision of integrated navigation/communication services," *Electronics & Communications Engineering Journal*, vol. 40, pp. 119–125, Feb. 2002.

[31] C. M. H. Noblet, R. H. Owen, C. Saraiva, and N. Wahid, "Assessing the effects of GSM cell location re-use for UMTS network," in *Proc. Second International Conference on 3G Mobile Communication Technologies*, 2001, pp. 82–86.

[32] T. X. Brown, "Cellular performance bounds via shotgun cellular systems," *IEEE Journal on Selected Areas in Communications*, vol. 18, no. 11, pp. 2443–2455, 2000.

[33] W. C. Y. Lee, *Mobile Communication Design Fundamentals*. John Wiley & Sons, Inc., 1993.

[34] L. Wang, K. Chawla, and L. J. Greenstein, "Performance studies of narrow-beam trisector cellular systems," in *Proc. 48th IEEE Vehicular Technology Conference*, vol. 2, 1998, pp. 724–730.

[35] A. G. Spilling and A. R. Nix, "Aspects of self-organisation in cellular networks," in *The Ninth International Symposium on Personal, Indoor and Mobile Radio Communications*, vol. 2, 1998, pp. 628–686.

[36] V. M. Jovanovic and J. Gazzola, "Capacity of present narrowband cellular systems: Interference-limited or blocking-limited?" *IEEE Personal Communications*, vol. 4, pp. 42–51, 1997.

[37] M. J. Nawrocki and T. W. Wieckowski, "Optimal site and antenna location for umts - output results of 3g network simulation software," in *14th International Conference on Microwaves*, vol. 3, May 2002, pp. 890–893.

[38] K. S. Gilhousen, I. Jacobs, R. Padovani, A. J. Viterbi, L. A. Weaver, Jr., and C. E. Wheatley, "On the capacity of a cellular CDMA system," *IEEE Trans. Vehicular Technology*, vol. 40, no. 2, pp. 303–312, May 1991.

[39] G. K. Chan, "Effects of sectorization on the spectrum efficiency of cellular radio systems," *IEEE Trans. Vehicular Technology*, vol. 41, no. 3, pp. 217–225, May 1991.

[40] T. W. Wong and V. K. Prabhu, "Optimum sectorization for CDMA 1900 base stations," in *Proc. IEEE 47th Vehicular Technology Conference*, vol. 2, 1997, pp. 1177–1181.

[41] P. Newson and M. R. Heath, "The capacity of a spread spectrum CDMA system for cellular mobile radio with consideration of system imperfections," *IEEE Journal on Selected Areas in Communications*, vol. 12, no. 4, pp. 673–684, May 1994.

[42] S. Wang and I. Wang, "Effects of soft handoff, frequency reuse and non-ideal antenna sectorization on CDMA system capacity," in *Proc. IEEE 43rd Vehicular Technology Conference*, 1993, pp. 850–854.

[43] M. G. Jansen and R. Prasad, "Capacity, throughput, and delay analysis of a cellular DS CDMA system with imperfect power control and imperfect sectorization," *IEEE Trans. Vehicular Technology*, vol. 44, no. 1, pp. 67–75, Feb. 1995.

[44] X. Yang, S. G. Niri, and R. Tafazolli, "Sectorization gain in CDMA cellular systems," in *Proc. of IEE 1st International Conference on 3G Mobile Communication Technologies*, 2000, pp. 70–75.

[45] C. Lee and R. Steele, "Effect of soft and softer handoffs on CDMA system capacity," *IEEE Trans. Vehicular Technology*, vol. 47, no. 3, pp. 830–841, Aug. 1998.

[46] G. Wibisono and R. Darsilo, "The effect of imperfect power control and sectorization on the capacity of CDMA system with variable spreading gain," in *Proc. Pacific Rim Conference on Communications, Computers and Signal Processing*, vol. 1, 2001, pp. 31–34.

[47] B. C. V. Johansson and S. Stefansson, "Optimizing antenna parameters for sectorized W-CDMA networks," in *Proc. IEEE 52nd Vehicular Technology Conference*, vol. 4, 2000, pp. 1524–1531.

[48] A. Wacker, J. Laiho-Steffens, K.Sipilä, and K. Heiska, "The impact of the base station sectorisation on WCDMA radio network performance," in *Proc. 50th IEEE Vehicular Technology Conference*, 1999, pp. 2611–2615.

[49] J. Laiho-Steffens, A. Wacker, and P. Aikio, "The impact of the radio network planning and site configuration on the WCDMA network capacity and quality of service," in *Proc. IEEE 51st Vehicular Technology Conference*, vol. 2, 2000, pp. 1006–1010.

[50] T. I. Song, D. J. Kim, and C. H. Cheon, "Optimization of sectored antenna beam patterns for CDMA2000 systems," in *Proc. of IEE 3rd International Conference on 3G Mobile Communication Technologies*, 2002, pp. 482–432.

[51] L. Chunjian, *Efficient Antenna Patterns for Three-Sector WCDMA Systems*, M.Sc. Thesis, Chalmers University of Technology, 2003.

[52] W. L. Stutzman and G. A. Thiele, *Antenna Theory and Design (2nd Ed.)*, 1998.

[53] P. Monogioudis, K. Conner, D. Das, S. Gollamudi, J. A. C. Lee, A. L. Moustakas, S. Nagaraj, A. M. Rao, R. A. Soni, and Y. Yuan, "Intelligent antenna solutions for UMTS: algorithms and simulation results," *IEEE Communications Magazine*, vol. 42, pp. 28–39, Oct. 2004.

[54] M. Elsey, E. Farrell, and C. Johnson, "Matching WCDMA site configuration with coverage and capacity requirements," in *Proc. of IEE 2nd International Conference on 3G Mobile Communication Technologies*, 2001, pp. 73–77.

[55] T. Isotalo, J. Niemelä, and J. Lempiäinen, "Electrical antenna downtilt in UMTS network," in *Proc. 5th European Wireless Conference*, Barcelona, Spain, 2004, pp. 265–271.

[56] J. Niemelä and J. Lempiäinen, "Impact of mechanical antenna downtilt on performance of WCDMA cellular network," in *Proc. IEEE 59th Vehicular Technology Conference*, 2004, pp. 2091–2095.

[57] I. Forkel, A. Kemper, R. Pabst, and R. Hermans, "The effect of electrical and mechanical antenna down-tilting in UMTS networks," in *Proc. IEE 3rd International Conference on 3G Mobile Communication Technologies*, 2002, pp. 86–90.

[58] S. Bundy, "Antenna downtilt effects on CDMA cell-site capacity," in *IEEE Radio and Wireless Conference*, 1999, pp. 99–102.

[59] D. J. Y. Lee and C. Xu, "Mechanical antenna downtilt and its impact on system design," in *Proc. IEEE 47th Vehicular Technology Conference*, vol. 2, 1997, pp. 447–451.

[60] L. Zordan, N. Rutazihana, and N. Engelhart, "Capacity enhancement of cellular mobile network using a dynamic electrical down-tilting antenna system," in *Proc. IEEE 50th Vehicular Technology Conference*, vol. 3, 1999, pp. 1915–1918.

[61] M. J. Nawrocki and T. W. Wieckowski, "Optimal site and antenna location for UMTS – output results of 3g network simulation software," in *Proc. IEEE 14th Microwaves, Radar and Wireless Communications*, vol. 3, 2002, pp. 890–893.

[62] A. Wacker, K. Sipilä, and A. Kuurne, "Automated and remotely optimization of antenna subsystem based on radio network performance," in *Proc. IEEE 5th Symposium on Wireless Personal Multimedia Communications*, vol. 2, 2002, pp. 752–756.

[63] J. Wu and D. Yuan, "Antenna downtilt performance in urban environments," in *Proc. IEEE Military Communications Conference*, vol. 3, Sept. 1996, pp. 739–774.

[64] P. Herhold, W. Rave, and G. Fettweis, "Joint deployment of macro- and microcells in UTRAN FDD networks," in *Proc. 4th European Wireless Conference*, 2002, pp. 128–134.

[65] Y. K. H. Cho and D. K. Sung, "Protection against cochannel interference from neighboring cells using downtilting of antenna beams," in *Proc. IEEE 53rd Vehicular Technology Conference*, vol. 3, 2001, pp. 1553–1557.

[66] J. Wu, J. Chung, and C. Wen, "Hot-spot traffic relief with a tilted antenna in CDMA cellular networks," *IEEE Trans. Vehicular Technology*, vol. 47, pp. 1–9, Feb. 1998.

[67] D. H. Kim, D. D. Lee, H. J. Kim, and K. C. Whang, "Capacity analysis of macro/microcellular CDMA with power ratio control and tilted antennas," *IEEE Trans. Vehicular Technology*, vol. 49, pp. 34–42, Jan. 2000.

[68] G. Wilson, "Electrical downtilt through beam-steering versus mechanical downtilt," in *Proc. IEEE 42nd Vehicular Technology Conference*, vol. 1, Denver, USA, 1992, pp. 1–4.

[69] W. C. Drach, *Using continuously adjustable electrical down-tilt (CAEDT) antennas to optimize wireless networks*, RFS World: Detailed White Papers, available [online]: http://www.rfsworld.com.

[70] 3GPP Technical Specification, *UTRAN Iuant interface: Remore Electrical Tilting (RET) antennas application part (RETAP) signalling*, 3GPP TS 25.463, version 6.0.0, Release 6.

[71] M. Garcia-Lozano and S. Ruiz, "Effects of downtilting on RRM parameters," in *Proc. IEEE 15th Personal, Indoor, and Mobile Radio Communications*, vol. 3, 2004, pp. 2166–2170.

[72] ——, "UMTS optimum cell load balancing for inhomogenous traffic patterns," in *Proc. IEEE 60th Vehicular Technology Conference*, vol. 2, Sept. 2004, pp. 909–913.

[73] M. Pettersen, L. E. Braten, and A. G. Spilling, "Automatic antenna tilt control for capacity enhancement in UMTS FDD," in *Proc. IEEE 60th Vehicular Technology Conference*, vol. 1, Sept. 2004, pp. 280–284.

[74] P. Soma, L. C. Ong, and Y. W. M. Chia, "Effects of down tilt antenna on the multipath propgation characteristics in the presence of an imperfect obstacle," in *Proc. IEEE Asia Pacific Microwave Conference*, vol. 3, Dec. 1999, pp. 610–613.

[75] 3GPP Technical Report, *Beamforming Enhancements*, 3GPP TR 25.877, version 1.0.0, Release 5.

[76] J. S. Sadowsky, D. Yellin, S. Moshavi, and Y. Perets, "Capacity gains from pilot cancellation in CDMA networks," in *Proc. IEEE Wireless Communications and Networking*, vol. 2, Mar. 2003, pp. 902–906.

[77] K. Valkealahti, A. Höglund, J. Parkkinen, and A. Hämäläinen, "WCDMA common pilot power control for load and coverage balancing," in *Proc. 13th IEEE Int. Symp. Personal, Indoor, and Mobile Radio Communications*, vol. 3, 2002, pp. 1412–1416.

[78] R. T. Love, K. A. Beshir, D. Schaeffer, and R. S. Nikides, "A pilot optimization technique for CDMA cellular systems," in *Proc. IEEE 50th Vehicular Technology Conference*, vol. 4, May 1999, pp. 2238–2242.

[79] I. Siomina, "P-CPICH power and antenna tilt optimization in UMTS networks," in *Proc. Advanced Industrial Conference on Telecommunications / Service Assurance with Partial and Intermittent Resources Conference / E-Learning on Telecommunications Workshop*, 2005, pp. 268–273.

[80] F. Sapienza and S. Kim, "Dominant pilot recovery in IS-95 CDMA systems using repeaters," *IEICE Trans. Communications*, vol. 82, no. 1, pp. 34–42, Jan. 1999.

[81] J. Leino, M. Kolehmainen, and T. Ristaniemi, "On the effect of pilot cancellation in WCDMA network," in *Proc. IEEE 55th Vehicular Technology Conference*, vol. 2, May 2002, pp. 611–614.

[82] M. M. El-Said, A. Kumar, and A. S. Elmaghraby, "Pilot pollution interference reduction using multi-carrier interferometry," in *Proc. 8th IEEE International Symposium on Computers and Communication*, June 2003, pp. 919–1328.

[83] ——, "Sensory system for early detection of pilot pollution interference in UMTS networks," in *Proc. 10th International Conference on Telecommunicatios*, vol. 2, June 2003, pp. 1323–1328.

[84] T. Isotalo, J. Niemelä, J. Borkowski, and J. Lempiäinen, "Impact of pilot pollution on SHO performance," in *Proc. 8th IEEE International Symposium on Wireless Personal Multimedia Communications*, 2006.

[85] J. Itkonen, N. Rahmani, and J. Lempiäinen, "A novel network topology for CDMA networks based on modified hexagonal grid," in *Proc. IEE 6th International Conference on 3G and Beyond*, Nov. 2005.

[86] T. Baumgartner, "Smart antenna strategies for the UMTS FDD downlink," Ph.D. dissertation, Technische Universität Wien, 2003.

[87] M. Coinchon, A. Salovaara, and J. Wagen, "The impact of propagation predictions on urban umts planning," in *International Zurich Seminar on Broadband Communications*, Feb. 2002, pp. 32–1–32–6.

[88] J. Laiho, A. Wacker, T. Novosad, and A. Hämäläinen, "Verification of WCDMA radio network planning prediction methods with fully dynamic network simulator," in *Proc. IEEE 54th Semiannual Vehicular Technology Conference*, vol. 1, Oct. 2001, pp. 526–530.

[89] W. Backman, *Error correction of predicted signal levels in mobile communications*, M.Sc. Thesis, Helsinki University of Technology, 2003.

[90] Siradel, *Volcano ray-tracing model*, www.siradel.com.

[91] J. Lempiäinen, "Assessment of diversity techniques in a microcellular radio propagation channel," Ph.D. dissertation, Helsinki University of Technology, 1999.

[92] Qualcomm, *Repeaters for Indoor Coverage in CDMA Networks*, Qualcomm white paper, April, 2003.

[93] W. C. Y. Lee and D. J. Y. Lee, "The impact of repeaters on CDMA system performance," in *Proc. 53rd IEEE Vehicular Techonology Conference*, vol. 3, May 2000, pp. 1763–1767.

[94] S. Park, W. W. Kim, and B. Kwon, "An analysis of effect of wireless network by a repeater in CDMA system," in *Proc. 51st IEEE Vehicular Techonology Conference*, vol. 4, May 2001, pp. 2781–2785.

[95] H. Jeon, Y. Jung, B. Kwon, and J. Ihm, "Analysis on coverage and capacity in adoption of repeater systems in CDMA2000," in *Proc. International Zurich Seminar on Broadband Communications*, Feb. 2002, pp. 33–1–33–6.

[96] W. Choi, B. Y. Cho, and T. W. Ban, "Automatic on-off switching repeater for DS/CDMA reverse link capacity improvement," *IEEE Communications Letters*, vol. 5, p. 2001, 138–141.

[97] M. R. Bavafa and H. H. Xia, "Repeaters for CDMA systems," in *Proc. IEEE 48th Vehicular Technology Conference*, vol. 2, May 1998, pp. 1161–1165.

[98] P. Herhold, W. Rave, and G. Fettweis, "Relaying in cdma networks: Pathloss reduction and transmit power savings," in *Proc. 62nd IEEE Vehicular Technology Conference*, vol. 3, 2003, pp. 2047–2051.

[99] M. Rahman and P. Ernström, "Repeaters for hot-spot capacity in DS-CDMA," *IEEE Trans. Vehicular Technology*, vol. 53, p. 2004, May 626–633.

[100] P. Lähdekorpi, J. Niemelä, J. Borkowski, and J. Lempiäinen, "WCDMA network performance in variable repeater hotspot traffic cases," in *Proc. 6th IEE International Conference on 3G and Beyond*, Nov. 2005.

[101] 3GPP Technical Specification, *UMTS: UE positioning in Universal Terrestrial Radio Access Network (UTRAN)*, 3GPP TS 25.305, version 5.5.0 , Release 5.

[102] B. Ludden and L. Lopes, "Cellular based location technologies for UMTS: A comparison between IPDL and TA-IPDL," in *Proc. 51st IEEE Vehicular Technology Conference*, vol. 2, May 2000, pp. 1348–1353.

[103] W. Y. Park, W. R. Lee, S. H. Kong, and W. C. Lee, "High resolution time delay estimation technique for position location," in *Proc. International Technical Conference on Circuits/Systems*, May 2003, pp. 1610–1614.

[104] 3GPP Technical Report, *Technical Specification Group Radio Access Network; UE positioning enhancements*, 3GPP TR 25.847, version 4.0.0 , Release 4.

[105] P. J. Duffett-Smith and M. D. Macnaughtan, "Precise UE positioning in UMTS using cumulative virtual blanking," in *Proc. Third International Conference on 3G Mobile Communication Technologies*, Oct. 2002, pp. 335–339.

[106] T. Rappaport, J. Reed, and B. Woerner, "Position location using wireless communications on highways of the future," *IEEE Communication Magazine*, vol. 34, pp. 33–41, Oct. 1996.

[107] S. Sakagami, S. Aoyama, K. Kuboi, S. Shirota, and A. Akeyama, "Vehicle position estimates by multibeam antennas in multipath environments," *IEEE Trans. Vehicular Technology*, vol. 41, no. 1, pp. 63–68, Feb. 1992.

[108] 3GPP Technical Specification, *UMTS; Physical Layer Measurements (FDD)*, 3GPP TS 25.215, version 5.3.0 , Release 5.

[109] N. Thomas, D. Cruickshank, and D. Laurenson, "Performance of a TDOA-AOA hybrid mobile location system," in *Proc. First International Conference on 3G Mobile Communication Technologies*, Oct. 2000, pp. 216–220.

[110] 3GPP Technical Report, *Study into applicability of Galileo in Location Services (LCS)*, 3GPP TR 23.835, version 1.0.0 , Release 6.

[111] 3GPP Technical Specification, *Physical layer procedures (FDD)*, 3GPP TS 25.214, version 3.9.0 Release 1999.

[112] J. Syrjärinne, "Studies of modern techniques for personal positioning," Ph.D. dissertation, Tampere University of Technology, 2001.

[113] J. Niemelä and J. Borkowski, "Topology planning considerations for capacity and location techniques in WCDMA radio networks," in *Proc. 10th Eunice Summer School Tampere*, June 2004, pp. 1–8.

[114] J. Borkowski, J. Niemelä, and J. Lempiäinen, "Location techniques for UMTS radio networks," in *Proc. Mobile Venue Conference*, May 2004.

[115] J. H. Reed, K. J. Krizman, B. D. Woerner, and T. S. Rappaport, "An overview of the challenges and progress in meeting the E-911 requirements for location servce," *IEEE Communications Magazine*, vol. 36, pp. 30–37, Apr. 1998.

[116] C. Drane, M. Macnaughtan, and C. Scott, "Positioning GSM telephones," *IEEE Communications Magazine*, vol. 36, pp. 46–54, Apr. 1998.

[117] M. Pettersen, R. Eckhoff, P. H. Lehne, T. A. Worren, and E. Melby, "An experimental evaluation of network-based methods for mobile station positioning," in *Proc. IEEE 13th International Symposium on Personal, Indoor, and Mobile Radio Communications*, vol. 5, Sept. 2002, pp. 2287–2291.

[118] M. I. Silventoinen and T. Rantalainen, "Mobile station emergency locating in GSM," in *Proc. IEEE International Conference on Personal Communications*, Feb. 1996, pp. 232–238.

[119] J. Borkowski and J. Lempiäinen, "Practical network-based techniques for mobile positioning in UMTS," *EURASIP Journal on Applied Signal Processing*, 2006 accepted for publication.

[120] CDMA450 - CDMA Development Group, *http://www.cdg.org/technology/3g*, referred 29.8.2006.

[121] 3GPP Technical Report, *UMTS 900 MHz Work Item*, 3GPP TR 25.816, version 7.0.0, Release 7.

[122] ——, *UMTS 2.6 GHz (FDD) Work Item Technical Report*, 3GPP TR 25.810, version 7.0.0 , Release 7.

[123] ——, *Requirements for Evolved UTRA (E-UTRA) and Evolved UTRAN (E-UTRAN)*, 3GPP TR 25.913, version 7.3.0, Release 7.

[124] S. M. Kay, *Fundamentals of Statistical Signal Processing - Estimation Theory*. Prentice Hall, 1993.

# Publications

Tampereen teknillinen yliopisto
PL 527
33101 Tampere

Tampere University of Technology
P.O. Box 527
FIN-33101 Tampere, Finland